

Diss.ETH No. 16511

**Identification and characterization of *soldat8*, a suppressor
of the cell death program activated by singlet oxygen in
Arabidopsis seedlings**

A dissertation submitted to the
SWISS FEDERAL INSTITUTE OF TECHNOLOGY ZURICH
for the degree of
DOCTOR OF SCIENCES

presented by

NÚRIA SÁNCHEZ COLL

M.Sc. in Biology, University of Barcelona
born December 14, 1978
in Barcelona, Spain

Accepted on the recommendation of
Prof. Dr. K. Apel, examiner
Prof. Dr. N. Amrhein, co-examiner

March 2006

Contents

SUMMARY	4
ZUSAMMENFASSUNG	5
ABBREVIATIONS	6
1. INTRODUCTION	8
1.1 Stress in plants	8
1.2 Oxidative cell damage	8
1.2.1 Defence mechanisms against ROS	10
1.2.2 Mode of action of ROS in biological systems	10
1.3 ROS as signalling molecules	11
1.3.1 Signalling role of ROS	12
1.4 Photo-oxidative stress and singlet oxygen signalling	14
1.4.1 Singlet oxygen formation	14
1.4.2 Mode of action of singlet oxygen	15
1.4.3 Singlet oxygen signalling	16
1.4.5 The <i>flu</i> system	17
1.4.6 <i>flu</i> suppressor screen	19
1.5 Goals	20
2. MATERIALS AND METHODS	21
2.1 Chemicals	21
2.2 Primers	21
2.3 Growth of Arabidopsis	26
2.3.1 Growth on agar	26
2.3.2 Growth on soil	26
2.4 DNA techniques	27
2.4.1 Isolation of genomic DNA	27
2.4.2 Isolation of plasmid DNA from <i>E.coli</i>	27
2.4.3 Polymerase chain reaction (PCR)	27
2.4.4 Purification of PCR products	27
2.4 RNA techniques	28
2.5.1 Isolation of total RNA	28
2.5.2 Reverse transcription	28

2.5.3	Real-time PCR	29
2.5.4	Chloroplast macroarray.....	30
2.6	Protein techniques	32
2.6.1	Isolation of total proteins	32
2.6.2	Separation of proteins by SDS-PAGE	33
2.6.3	Western analysis	33
2.7	Mapping of the second-site mutation	34
2.7.1	Crude mapping	34
2.7.2	Fine mapping and sequencing	35
2.8	Complementation assay	35
2.8.1	Ligation of <i>SOLDAT8</i> genomic sequence into plasmid DNA	35
2.8.2	Transformation techniques	37
2.9	<i>In vivo</i> measurements of photosynthetic activity	40
2.9.1	Principles of chlorophyll a fluorescence measurements	40
2.9.2	Light-induced changes in the PSI redox state	42
2.10	Other techniques	44
2.10.1	Microscope techniques	44
2.10.2	The protoplast assay	44
2.10.3	Pchl _a detection by HPLC	44
3.	RESULTS	46
3.1	Characterization of the <i>soldat8/flu</i> mutant	46
3.1.1	Generation of second-site mutants	46
3.1.2	The phenotype of mature <i>soldat8/flu</i> plants	46
3.1.3	The phenotype of <i>soldat8/flu</i> seedlings.....	47
3.2	Mapping of the <i>soldat8</i> locus	51
3.2.1	Establishment of a mapping population	52
3.2.2	Crude mapping	52
3.2.3	Fine mapping	54
3.2.4	Sequencing	55
3.3	Complementation	56
3.4	Characterization of the <i>soldat8</i> mutant	58
3.4.1	Identification of the <i>soldat8</i> mutant	58
3.4.2	The <i>soldat8</i> phenotype	60
3.4.3	Analysis of the gene expression in the <i>soldat8</i> mutant	62
3.4.4	Analysis of the protein content in the <i>soldat8</i> mutant	69

3.4.5	<i>In vivo</i> measurements of photosynthetic activity	70
3.4.6	The effect of high light stress	74
4.	DISCUSSION	79
4.1	Oxidative stress signalling	79
4.2	Generation of singlet oxygen results in the activation of different stress responses in the <i>flu</i> system	80
4.3	A mutation in <i>SOLDAT8</i> suppresses cell death in <i>flu</i> seedlings	81
4.4	The <i>SOLDAT8</i> locus encodes a chloroplast sigma factor, <i>SIG6</i>	82
4.5	Involvement of <i>SIG6</i> in the recognition of the plastid-encoded polymerase of young cotyledons	83
4.5.1	The nuclear-encoded plastid sigma factors	83
4.5.2	Characterization of <i>SIG6</i>	85
4.6	Enhanced tolerance of photo-oxidative stress in <i>soldat8</i> seedlings	90
4.7	Conclusions and future prospects	91
	REFERENCES	93
	ACKNOWLEDGEMENTS	103
	CURRICULUM VITAE	104

Summary

The conditional *fluorescent* (*flu*) mutant of *Arabidopsis* overaccumulates protochlorophyllide (Pchl_{ide}) in the dark. This photosensitizer can transfer light energy to molecular oxygen giving rise to singlet oxygen, a nonradical reactive oxygen species (ROS). Immediately after reillumination *flu* starts to generate singlet oxygen in the plastids. This ROS activates a genetically determined stress response program resulting in the death of seedlings and the inhibition of growth of mature *flu* plants. Second-site mutants were identified, which are able to abrogate either one or both stress responses of the *flu* mutant. These mutants were classified as two different groups. The singlet oxygen-linked death activator (*soldat*) mutants constitute one of these groups. Seedlings of the *soldat/flu* mutant are able to survive after a dark-to-light shift, even though they accumulate similar levels of Pchl_{ide} as *flu*. However, the growth inhibition of mature *flu* plants is not suppressed by the *soldat* mutations. In the present work the *soldat8/flu* double mutant was characterized. A map-based cloning approach revealed that the mutated locus in *soldat8* encodes the chloroplast sigma factor SIG6. *soldat8/flu* plants complemented with a wt copy of the *SIG6* gene restored the original *flu* phenotype.

Sigma factors confer promoter specificity to the plastid-encoded RNA polymerase during chloroplast gene transcription in response to developmental and environmental cues. SIG6 acts as a major general sigma factor in chloroplasts during early seedling development in the light. The *soldat8* mutant exhibits a cotyledon-specific pale-green phenotype and chloroplast development is significantly delayed. In a very early stage of development, the mutant suffers from light stress under normal light conditions and contains reduced amounts of D1 protein. However, *soldat8* mutant seedlings show an enhanced tolerance of photoinhibitory conditions (high light + cold) when compared to wt. Taken together the results suggest that in *soldat8* light exposure triggers acclimatory adjustments at the cotyledon stage, which could increase the tolerance of unfavorable situations. High light and the *flu* mutation may lead to the production of singlet oxygen and the activation of a genetically controlled cell death response. The *soldat8* mutant is able to escape this singlet oxygen-mediated cell death during early seedling development.

Zusammenfassung

Die konditionale fluoreszierende Arabidopsis-Mutante (*flu*) akkumuliert im Dunkeln freies Protochlorophyllid (Pchlid) in Plastiden. Pchlid kann als Photosensitizer Lichtenergie auf molekularen Sauerstoff übertragen, wobei Singulett Sauerstoff produziert wird, eine nicht-radikale, reaktive Sauerstoffspezies. Unmittelbar nach Belichtung der *flu* Mutante beginnt die Freisetzung von Singulett-Sauerstoff, durch den anschließend ein genetisch determiniertes Stress-Programm aktiviert wird, welches zum Zelltod bei Keimlingen und zur Wachstumshemmung bei vollentwickelten *flu* Pflanzen führt. „Second-site“-Mutanten wurden identifiziert, welche fähig sind, eine oder beide Stressreaktionen der *flu* Mutante zu unterdrücken. Diese Mutanten wurden in unterschiedliche Klassen eingeteilt. Der singlet oxxygen-linked death activator (*soldat*) bezeichnet eine dieser Klassen. Eine der *soldat* Mutanten, *soldat8*, wurde in der vorliegenden Arbeit einer detaillierten genetischen und physiologischen Analyse unterzogen. Keimlinge der *soldat8/flu* Mutante können einen Wechsel von Dunkelheit zu Licht überleben, obwohl sie ähnliche Mengen an Pchlid wie *flu* akkumulieren. Die Wachstumshemmung der adulten *flu* Pflanzen während eines Licht-Dunkel-Wechsels wird dagegen durch die *soldat8* Mutation nicht unterdrückt. Mittels kartierungsbasierter Klonierung konnte gezeigt werden, dass der mutierte Locus von *soldat8* den chloroplastidären Sigmafaktor SIG6 kodiert. Die Wildtyp-Kopie des *SIG6*-Genes konnte, nachdem sie in die *soldat8/flu* Mutante eingeführt worden war, die Mutation komplementieren und den elterlichen *flu* Phänotyp wiederherstellen.

Sigmafaktoren vermitteln bei der Transkription der Plastidengene die Promotorspezifität der Plastiden-kodierten RNA-Polymerase. SIG6 ist ein essentieller Sigmafaktor, der in den Chloroplasten vor allem während der frühen Keimlingsentwicklung im Licht benötigt wird. Die *soldat8* Mutante zeigt einen Keimblatt-spezifischen hellgrünen Phänotyp mit einer verzögerten Chloroplastenentwicklung. In einem sehr frühen Stadium der Entwicklung leidet *soldat8* bei normalen Lichtbedingungen unter Lichtstress und weist verringerte Mengen des D1-Proteins auf. Trotz dieser gesteigerten Licht-Empfindlichkeit zeigen *soldat8* Keimlinge gegenüber starkem Licht/Kaltstress eine höhere Stresstoleranz als Wildtyp Keimlinge.

Diese erhöhte Stresstoleranz konnte auf die frühzeitige Aktivierung einer Akklimation der Mutante zurückgeführt werden, die in der frühen Keimlingsentwicklungsphase konstitutiv unter Lichtstress leidet. Zu der gekoppelten *soldat8/flu* Doppelmutante scheint durch diese vorgezogene Akklimation das Ausmaß der durch Singulett-Sauerstoff-Freisetzung ausgelösten Stressantworten der *flu*-Mutante stark unterdrückt zu werden.

Abbreviations

approx.	approximately
bp	base pair
Chl	chlorophyll
CAPS	cleaved amplified polymorphic sequence
Col	<i>Columbia</i>
cDNA	complementary DNA
DCMU	3-(3', 4' - dichlorophenyl) - 1,1 - dimethylurea
dCTP	Deoxycytidine 5'-triphosphate
dNTP	deoxyribonucleotide triphosphate
DMSO	dimethylsulfoxide
DTT	dithiothreitol
EDTA	ethylenediaminetetraacetic acid
ERF	ethylene responsive factor
<i>E.coli</i>	<i>Escherichia coli</i>
EX	EXECUTER
HPLC	high performance liquid chromatography
HR	hypersensitive response
INDEL	insertions/deletions
Ler	<i>Landsberg</i>
LB	Luria-Bertrani
mRNA	messenger RNA
MS	Murashige & Skoog
POR	NADPH-protochlorophyllide oxidoreductase
NCBI	National center for biotechnology information
NEP	nuclear-encoded RNA polymerase
NMD	nonsense-mediated mRNA decay
NPQ	non-photochemical quenching
OD	optical density
ORF	open reading frame
PAGE	Poly acrylamide gel electrophoresis
pCam	pCambia
PCD	programmed cell death
Pchl _{ide}	protochlorophyllide
PCR	polymerase chain reaction

PEP	plastid-encoded RNA polymerase
PSI	photosystem I
PSII	photosystem II
qP	photochemical quenching
ROS	reactive oxygen species
rpm	revolutions per minute
rpu	relative Pchl _a units
RT-PCR	reverse transcriptase-PCR
rRNA	ribosomal RNA
RT	room temperature
SAR	systemic acquired resistance
SDS	sodium dodecyl sulfate
SIG	sigma
SSLP	simple sequence length polymorphism
SNP	single-nucleotide polymorphisms
SOLDAT	singlet oxygen-linked death activator
TAIR	The Arabidopsis information resource
tRNA	transfer RNA
<i>vs</i>	<i>versus</i>
v/v	volume/volume
w/v	weight/volume
wt	wild type

1 Introduction

1.1 Stress in plants

Land plants are sessile organisms in a continuously changing environment. They need to cope with abiotic stress factors like cold, heat, drought, strong light and salt without being able to escape to a more favorable biotope. Additionally, the plant must deal with biotic stress factors, such as pathogens and herbivores as well as with competition from other plants. To meet these demands, plants have evolved a wide range of survival strategies, underlined by a very robust signalling apparatus. Far from being passive entities, plants subsist as dynamic and highly sensitive organisms actively competing for limited resources through phenotypic plasticity.

Multiple signalling pathways control the stress responses of plants (Glazebrook, 2001; Knight and Knight, 2001). Signal transduction pathways leading to stress responses begin with the perception of the stress factor by the plant followed by the generation of second messengers, transient secondary signals inside the cell that greatly amplify the original signal. For example, increased levels of cytosolic free calcium act as second messenger in most abiotic stress responses (Knight and Knight, 2001). This results in the activation or inactivation of enzymes or regulatory proteins. Protein kinases and phosphatases are usually involved in protein phosphorylation cascades, that typically lead to changes in gene expression, driven by specific transcription factors. Several transcription factors that participate in the expression of stress-related genes in plants have been identified in the past years. Some belong to large gene families, that in some cases are unique to plants, like ethylene-responsive-element binding factors (ERF), basic-domain leucine-zipper (bZIP) and WRKY proteins (Singh et al., 2002). The products of the stress-related genes are often involved in the synthesis of plant hormones, like ethylene, salicylic acid or jasmonic acid. These regulatory molecules modify gene expression for finally shaping the plant in response to the environment and can act as systemic signalling molecules, carrying the information to distant parts of the plants.

Stress signalling pathways constitute a network where specificity and cross-talk occur at different levels to produce a complex stress response in the plant (Knight and Knight, 2001; Singh et al., 2002).

1.2 Oxidative cell damage

Molecular oxygen (O_2) has been one of the paradox of life since its release to the atmosphere approximately 2.7 billion ago by O_2 -evolving organisms: it is necessary for aerobic life but at the

same time it is responsible for the formation of reactive oxygen species (ROS). In contrast to O_2 , these derivatives of oxygen are highly reactive and toxic for the cell (Mittler, 2002). ROS have been implicated in many diseases and degenerative processes, first in animals (Marx, 1985). The relevance of ROS and oxidative stress was discovered late probably because of the difficulty in detecting and tracing oxygen molecules, the multitude of forms and intermediates of oxygen, their high reactivity and the velocity of the reactions involved.

Production of ROS follows almost every environmental change that triggers a stress response in plants. Environmental stress has a significant impact on crops, reducing their yield to about 25% of its potential (Boyer, 1982). Therefore, understanding the general principles and mode of action of ROS is an essential issue since its production may result in economic losses.

The major source of ROS production in plant cells are the organelles with a highly oxidizing metabolic activity or an intense rate of electron flow, namely chloroplasts, mitochondria and peroxisomes.

Activation of oxygen to generate reactive intermediates can occur by two different mechanisms: energy transfer or electron transfer reactions. In the first case, if sufficient energy is absorbed to reverse the spin of one of the unpaired electrons of O_2 , it will form the singlet state (1O_2). The uptake of one, two or three electrons by O_2 leads to the formation of superoxide radical (O_2^-), hydrogen peroxide (H_2O_2) or the hydroxyl radical (HO^\bullet) respectively.

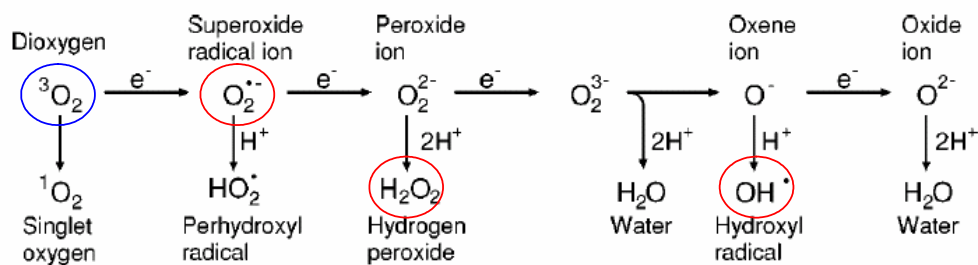


Fig. 1-1: Formation of ROS in cells. Atmospheric oxygen in its ground state is marked in blue and the most commonly produced ROS in red. Modified from Apel and Hirt, 2004.

ROS are produced continuously as inevitable byproducts of reactions involving oxygen, like oxygenic photosynthesis or respiration. Under normal growth conditions, a finely tuned network of scavenging mechanisms keeps the levels of ROS in cells low (Alscher et al., 1997). However, nearly every environmental stress can unsettle the balance between ROS production and ROS scavenging, resulting in a marked increase of the ROS level (Malan et al., 1990; Prasad et al., 1994; Tsugane et al., 1999; Polle, 2001).

Metabolic pathways enhanced during abiotic stress constitute an additional source of ROS, like the glycolate oxidase reaction in peroxisomes during photorespiration (Noctor et al., 2002). Furthermore, new ROS-producing sources have been identified in recent years, which participate in the so-called oxidative burst: a rapid and transient massive production of ROS. This mechanism is triggered as a response to certain environmental changes and involves the activation of enzymes like NADPH oxidases, cell-wall-bound peroxidases and amine oxidases (Doke, 1983; Allan and Fluhr, 1997; Schopfer et al., 2001; Bolwell et al., 2002).

1.2.1 Defence mechanisms against ROS

To avoid oxidative stress, the steady-state level of ROS in cells has to be tightly regulated. Plants have evolved numerous mechanisms that protect them against an excess of ROS. Enzymes like superoxide dismutase, ascorbate peroxidase and catalase are the main scavengers in plants; (Bowler et al., 1992; Willekens et al., 1997). These enzymes are under strong regulation, since the balance between them is critical to maintain the levels of ROS in the cells low (Rizhsky et al., 2002).

A second scavenging system, consisting of antioxidative molecules, includes glutathion, ascorbate (vitamin C), α -tocopherol (vitamin E), carotenoids, flavonoids and alkaloids. Chloroplasts and other cell organelles contain high concentrations of glutathion and ascorbate, which are essential redox buffers for the cell to fight against oxidative stress (Noctor and Foyer, 1998). A proper balance between them seems to be a crucial factor for their function (Asada, 1999; Foyer and Noctor, 2000).

1.2.2 Mode of action of ROS in biological systems

All ROS are extremely reactive and they can interact with nearly all biological molecules (Dat et al., 2000). Peroxidation of lipids is perhaps the most devastating harm for the cell, because when affecting the plasma membrane it can lead to cell leakage (Zimmermann and Zentgraf, 2005). Intracellular membranes can also be damaged by ROS, finally resulting in the impairment of essential cellular processes like respiration or photosynthesis. ROS are also responsible for the bleaching of leaves, caused by the oxidation of pigments (Dat et al., 2001).

Typically, different ROS have different degrees of reactivity and can react with different molecular targets. HO^\bullet is the most reactive among them, being potentially able to oxidize any biological molecule. There exists no enzymatic mechanism to eliminate it, and the massive impairments caused to cell components by an excess of HO^\bullet production often results in cell

death (Vranova et al., 2002). O_2^- can oxidize specific amino acids, affecting the activity of certain enzymes. It is less reactive than HO^* because it cannot cross biological membranes (Knox and Dodge, 1985) and it is rapidly transformed into H_2O_2 by superoxide dismutase. H_2O_2 has particular features that make it of special interest: it has a relative long half life compared to other ROS, it is a diffusible molecule, thus being able to move away from the site of production, and it is moderately reactive. It can inactivate enzymes by modifying their thiol groups (Charles and Halliwell, 1980).

1.3 ROS as signalling molecules

Traditionally, increases in ROS concentration triggered by adverse environmental conditions have been regarded as an inevitable consequence of stress leading to oxidative damage. However, several recent studies have revealed that ROS also function as regulators in several essential biological processes including responses to both biotic and abiotic stress, programmed cell death, hormone signalling, growth and morphogenesis (reviewed in Vranova et al., 2002; Laloi et al., 2004). During the course of evolution photosynthetic organisms have developed numerous protective mechanisms to detoxify ROS within the cell (Ledford and Niyogi, 2005). It has been suggested that the signalling role of ROS in plants appeared as a consequence of the high degree of control that suppresses ROS cytotoxicity in the cells (Mittler et al., 2004). Cell death usually occurs when the amounts of ROS produced exceed the scavenger capacity of the cell. Sublethal ROS concentrations can act as a signal that triggers different stress responses to unfavorable conditions, preparing the plant for further stress.

The first indications of a signalling role for ROS emerged in the field of pathogen-defence responses. Catalase was found to be a salicylic acid (SA)-binding protein and H_2O_2 appeared to be a component in the signaling transduction pathway triggered by SA and leading to pathogenesis-related (PR-1) gene induction (Chen et al., 1993). Since then it has become evident that changes in the concentration of ROS affect the expression of a large number of genes (Neill et al., 2002; Mittler et al., 2004). This gene network includes ROS-scavenging and ROS-producing proteins and seems to be involved in managing the levels of ROS with a signalling purpose as well as for protection against oxidative damage (Mittler et al., 2004).

To understand how ROS are sensed and transduced into signals that regulate gene expression has been an intensively studied issue during the last years. Up to now some components belonging to the ROS signalling network have been identified. Plants seem to have evolved

different strategies to transmit the signal from the site of ROS production to the nucleus, that ultimately results in changes in gene expression.

Three different modes of action have been proposed to describe the signalling transduction pathway triggered by ROS (Apel and Hirt, 2004): first, ROS might interact directly as a second messenger, with *e.g.* a transcription factor, that would be involved in gene regulation. As a second option, ROS might generate oxidation products that act as signalling molecules, as it is the case for oxylipins derived from lipid peroxidation. The third possibility is based on the recently discovered regulatory role exerted by the redox status of chloroplasts (Pfannschmidt, 2003). A higher production of ROS in the chloroplast may have an indirect role, activating scavenging mechanisms that ultimately lead to a shift in the redox balance of the organelle, known to be responsible for the modulation of gene expression and enzyme activity.

1.3.1 Signalling role of ROS

Plant defence

ROS seem to orchestrate the response of plants to a pathogen attack. They act both locally, at the site of infection and systemically, transferring the signal that will activate a defence response into distal parts of the plant. They have been involved in cross-linking of cell wall proteins at the site of attempted ingress by a pathogen (Bradley et al., 1992; Lamb and Dixon, 1997), which constitutes a first barrier to avoid pathogen invasion. Also locally, they can induce the hypersensitive response. The hypersensitive response (HR) is an efficient and active defence response of plants against a broad range of pathogens. HR is triggered by the interaction between plant resistance genes and pathogen avirulence gene products (Martin et al., 2003; Rathjen and Moffett, 2003). One of the most rapid events during HR is the oxidative burst, which results in the accumulation of ROS at the site of invasion, mainly O_2^- and H_2O_2 (Apostol et al., 1989; Hammond-Kosack and Jones, 1996; Grant and Loake, 2000). This rapid oxidative burst results in localized PCD activation at the site of pathogen challenge, limiting the spread of the pathogen. H_2O_2 and nitric oxide (NO) are the main regulators triggering cell death during pathogen attack (Delledonne et al., 2001; Neill et al., 2002; Wendehenne et al., 2004).

Whereas infection by a virulent pathogen results in a single transient oxidative burst leading to PCD, the production of ROS in response to an avirulent pathogen is biphasic, with a sustained second oxidative burst (Levine et al., 1994). This second rise in ROS occurs in distant parts of the plant and activates additional defence processes throughout the plant, leading to systemic acquired resistance (SAR) to a subsequent attack (Alvarez et al., 1998).

Furthermore, the activities of ascorbate peroxidase and catalase are suppressed during the defence of plants against pathogen attack by salicylic acid and NO (Klessig et al., 2000). Indeed, the activation of PCD during this response requires suppression of ROS-detoxifying mechanisms and production of NO (Mittler et al., 1999; Delledonne et al., 2001).

Abiotic stress

Plants have developed a variety of mechanisms to tolerate abiotic stress. Mild, non-lethal stress conditions trigger acclimatory processes in the plant. These reversible physiological changes help to maintain the functioning of the organism under changing environmental conditions and enhance the ability of plants to cope with future harsh conditions. ROS are key components for the activation of acclimation of plants to a number of stresses (Prasad et al., 1994; Karpinski et al., 1999), and most abiotic stress responses involve the accumulation of ROS (Dat et al., 2000).

A common feature of plant defence responses against biotic and abiotic stresses is the apoplastic oxidative burst leading to cell death, which does not only occur after pathogen attack but it is also responsible for the PCD observed during the ozone (O₃)-induced stress response (Overmyer et al., 2003). However, in contrast to biotic stress, abiotic stress responses involve an induction of ROS-scavenging enzymes, thus avoiding cytotoxicity caused by high levels of ROS (Mittler, 2002).

The signalling cascades triggered by ROS interact with a number of different signalling pathways, involving cross talk and the regulatory role of hormones (Overmyer et al., 2003; Apel and Hirt, 2004). The specific stress response shown by the plant may originate from the integration of different information derived from this vast signalling network, different variables may overlap, for instance the nature of the stress factor, the chemical identity of a given ROS and the intracellular site of its production (Laloi et al., 2004).

Most of the components of the ROS network are not known yet (Mittler et al., 2004). Very few cases prove the existence of selective ROS signatures, where a single ROS is responsible for the activation of a given signalling pathway (Jabs et al., 1996; Leisinger et al., 2001; op den Camp et al., 2003). Most of the attention has been drawn to the signalling role of the long-lived H₂O₂ (Dat et al., 2000), whereas other ROS that are more difficult to trace have been ignored.

1.4 Photo-oxidative stress and singlet oxygen signalling

Little is known about the highly reactive singlet oxygen ($^1\text{O}_2$), which is of particular concern to photosynthetic organisms. Singlet oxygen is an excited state molecule produced when a photosensitizer absorbs light energy and transfers it to ground-state oxygen. Since the main photosensitizers in plants are chlorophylls and their precursors, singlet oxygen is of special relevance to the chloroplast, which contains the photosynthetic apparatus, embedded in the thylakoid membranes. Almost any environmental change affects this highly organized system, optimized for light harvesting. The photosynthetic apparatus is a major site of damage under photo-oxidative stress conditions since it involves the combination of an oxygen-rich environment and the formation of highly reactive intermediates (Karpinski et al., 2003; Ledford and Niyogi, 2005).

Only a small portion of the total energy absorbed under full sunlight is finally used for CO_2 fixation (Asada, 1999). The excess of energy absorbed causes a permanent handicap for plants, because the energy that can not be used for photosynthetic metabolism is a potential source of photo-oxidative damage for plants, often evidenced as chlorosis or bleaching of leaves (Karpinski et al., 1999; Karpinska et al., 2000; Kulheim et al., 2002).

1.4.1 Singlet oxygen formation

Singlet oxygen is produced in the antenna and reaction centers of the photosynthetic apparatus, where chlorophyll (Chl) is the main light-absorbing pigment. After absorbing light energy, Chl rapidly becomes an unstable, excited, singlet-state molecule ($^1\text{Chl}^*$) (Fig. 2-2). During photosynthesis, the excitation energy from $^1\text{Chl}^*$ is converted into an electrochemical potential via charge separation. Alternatively, energy can be released as heat or fluorescence.

Unfavorable conditions can disturb the balance between light harvesting and light-driven electron transport. In this case $^1\text{Chl}^*$ may be converted to a lower excitation triplet-state molecule ($^3\text{Chl}^*$), which arises when an electron changes spontaneously the spin. The lifetime of the $^3\text{Chl}^*$ is greater than that of $^1\text{Chl}^*$ and it can react with molecular oxygen ($^3\text{O}_2$) to form singlet oxygen (Macpherson et al., 1993).

There is general agreement that singlet oxygen is generated even in the absence of environmental stress. In the reaction center of PSII, singlet oxygen is continuously produced during illumination. It has been suggested that α -tocopherols are specifically involved in the maintenance of the PSII function by scavenging singlet oxygen produced by the reaction center (Trebst et al., 2002; Havaux et al., 2005). However, tocopherol may not be the only singlet

oxygen scavenger in the reaction center. Even under low light intensities rapid turnover of D1 protein occurs (Keren et al., 1995), which indicates that this active form of oxygen reacts also with D1 protein. Controlled degradation of D1 could serve as a safety valve to quench singlet oxygen in the reaction center of PSII (Kruk et al., 2005).

Besides collecting the light energy for photosynthesis, the antenna system of PSII is essential for the dissipation of excess excitation energy during illumination (Horton and Ruban, 2005). Carotenoids are very abundant in the antenna and act as the main scavengers of $^3\text{Chl}^*$ and singlet oxygen.

However, under conditions that limit CO_2 in the chloroplast, like high light intensities or drought, singlet oxygen generation is enhanced (Krieger-Liszkay, 2005). Indeed, singlet oxygen has been detected in higher amounts in leaves exposed to high light (Hideg et al., 1998; Fryer et al., 2002). To avoid or respond to photo-oxidative stress, plants have developed numerous photoprotective mechanisms (Niyogi, 2000). In the antenna system, constitutive mechanisms as carotenoids are complemented by specific photoprotective processes activated exclusively under high levels of illumination (Horton and Ruban, 2005). Nevertheless, under circumstances where singlet oxygen generation is favored, the scavenging capacity of the chloroplast can be exceeded, resulting in photo-oxidative stress. In the PSII reaction center an excess of excitation energy results in photoinhibition, when the rate of D1 damage exceeds its rate of repair (Aro et al., 1993).

1.4.2 Mode of action of singlet oxygen

Even though the exact half-life of singlet oxygen *in vivo* is difficult to determine (Ledford and Niyogi, 2005), there is general agreement that because of its short lifetime singlet oxygen can only diffuse over very short distances before reacting with other singlet state molecules (Moan, 1990).

Ground state triplet oxygen forms a biradical because its outer electrons are unpaired and have parallel spins (Fig. 1-2). If triplet oxygen absorbs sufficient energy to reverse the spin direction of one of its unpaired electrons, it will form the singlet state in which the two electrons have opposite spins. This activation overcomes the spin restriction and singlet oxygen can afterwards participate in reactions involving the transfer of two electrons. Since paired electrons are common in organic molecules, singlet oxygen is very reactive towards them.

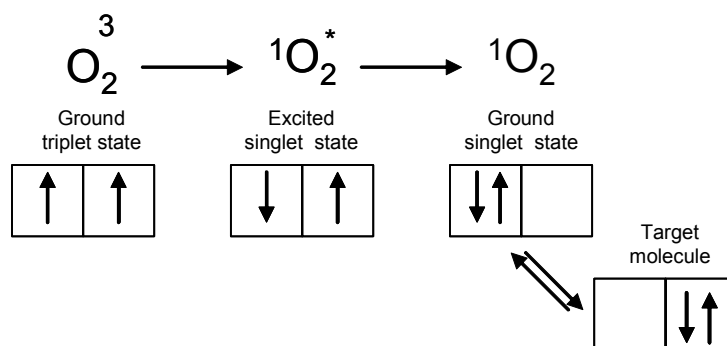


Fig. 1-2: Electronic states of organic molecules: triplet (${}^3\text{O}_2$) and singlet (${}^1\text{O}_2$) states. In the singlet state all electrons in the molecule are spin-paired, whereas in the triplet state one set of electron spins is unpaired. Electrons are shown as vertical arrows.

This reactive oxygen form has been shown to modify lipids (Girotti and Kriska, 2004), nucleic acids (Martinez et al., 2003) and proteins (Davies, 2003). Furthermore, it has been suggested to play a key role in photoinhibition (reviewed in Aro et al., 1993). Large amounts of singlet oxygen are produced in nonfunctional PSII of cyanobacteria (Nishiyama et al., 2004). In *Chlamydomonas*, singlet oxygen is responsible for the light-induced loss of PSII activity and degradation of D1 (Trebst et al., 2002), and in higher plants there is also some evidence that, singlet oxygen contributes to PSII-photodamage processes (Mishra and Ghanotakis, 1994) and can even participate in the inhibition of D1 repair under strong photo-oxidative stress (Nishiyama et al., 2004).

1.4.3 Singlet oxygen signalling

Consistent with what has been shown previously for other ROS, also singlet oxygen may act as a mediator of stress responses. In animals the mode of action of singlet oxygen is well established, especially in the apoptotic process induced by UV-A light and during photodynamic therapy (Kochevar, 2004). Photochemically generated singlet oxygen was shown to regulate gene expression in cell cultures (Ryter and Tyrrell, 1998).

The difficulty of studying responses to singlet oxygen in plants is that under conditions which trigger generation of this ROS also $\text{O}_2^{\cdot -}$ and H_2O_2 are produced (Foyer and Noctor, 2000). Moreover, the onset of stress responses triggered during singlet oxygen-induced photo-oxidative damage, may obscure the specific signalling role of singlet oxygen.

Experimentally it is possible to induce the formation of singlet oxygen through application of photosensitizers like Rose Bengal or methylene blue. Unfortunately such photosensitizing dyes do not colocalize with Chl, therefore they do not provide precise information about how the

stress response after the release of singlet oxygen in the chloroplasts occurs. Inhibitors of photosynthetic electron transport such as the herbicides 3-(3,4-dichlorophenyl)-1,1-dimethylurea (DCMU) or bromoxynil induce singlet oxygen formation in the chloroplast (Krieger-Liszky and Rutherford, 1998; Fufezan et al., 2002). Similarly, inhibitors of Chl biosynthesis promote the accumulation of Chl precursors that are potent photosensitizers and are present in the chloroplasts. Leisinger et al. (2001) have shown the specific induction of the glutathione peroxidase gene in *Chlamydomonas* cells that overaccumulate protoporphyrin IX. In the same work, treatment with neutral red, methylene blue and Rose Bengal also resulted in the overexpression of this protein.

1.4.5 The *flu* system

The conditional *flu* mutant was isolated during an EMS-mutagenesis screen to identify plants which overaccumulate the chlorophyll precursor protochlorophyllide (Pchlde) in the dark (Meskauskiene et al., 2001). It was termed *flu* (*fluorescent*) because etiolated mutant seedlings emit red Pchlde fluorescence when exposed to blue light (Fig1-3 a). Pchlde can act as a potent photosensitizer (Boo et al., 2000), which upon illumination gives rise to singlet oxygen in the plastid. *flu* has provided an exceptional opportunity to study stress responses triggered by the release of singlet oxygen in a non-invasive, manner.

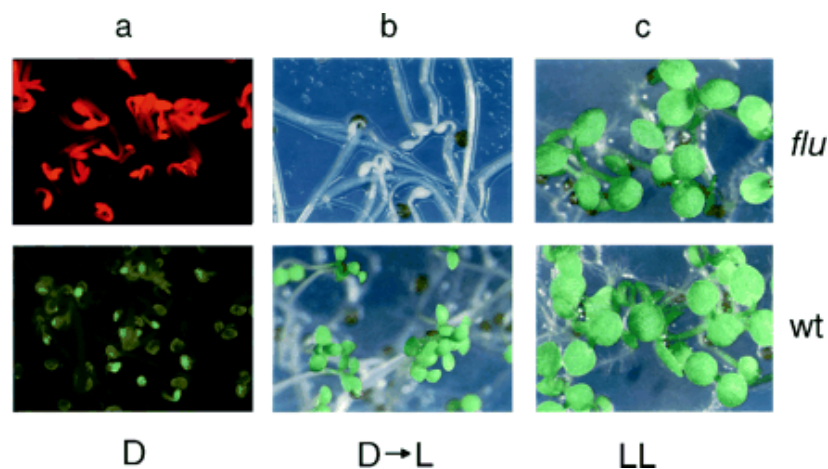


Fig. 1-3: Phenotype of the conditional *flu* mutant. (a) *flu* and wt seedlings were grown in the dark and fluorescence was recorded after exposure to blue light. (b) Etiolated seedlings were transferred to white light for 12. (c) Seedlings were grown under permissive continuous light. From Meskauskiene et al., 2001.

In the dark, the Chl synthesis pathway leads only to the formation of Pchlde. Once a critical level of Pchlde has been reached, aminolevulinic acid (ALA) synthesis is inhibited by a metabolic feedback control (Fig. 1-4). The *flu* mutant is defective in this mechanism, and cannot

restrict the accumulation of Pchl_{ide} in the dark (Meskauskiene et al., 2001). Furthermore, a direct interaction of FLU with glutamyl-tRNA reductase has revealed that FLU is a key negative regulator of Chl biosynthesis (Meskauskiene and Apel, 2002; Goslings et al., 2004).

The reduction of Pchl to chlorophyllide, catalyzed by the ternary photoactive complex Pchl_{ide}-NADPH-NADPH⁻ protochlorophyllide oxidoreductase (POR), is the last step in the Chl biosynthesis pathway, and it is light dependent (Apel et al., 1980). In *flu*, Pchl_{ide} overaccumulates in its free form, because the amounts of Pchl_{ide} produced in the mutant exceed the capacity of the POR enzyme to bind these pigment molecules (op den Camp et al., 2003).

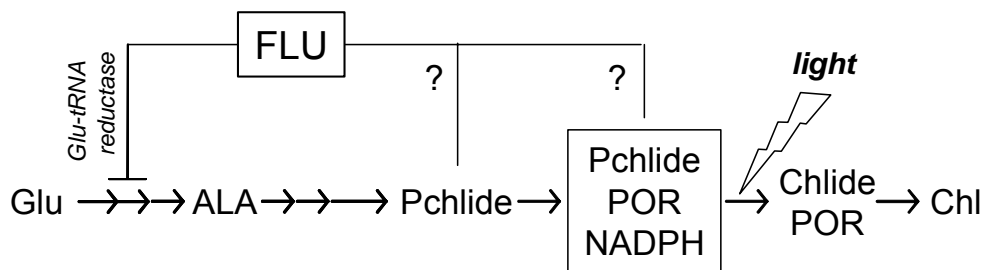


Fig. 1-4: FLU-Dependent Regulation of Pchl_{ide} Synthesis in Arabidopsis. (A) FLU is a membrane-bound plastid protein that mediates the feedback control of chlorophyll synthesis. It has been shown to interact with Glu-tRNA reductase, the enzyme catalyzing the first step in the tetrapyrrole biosynthesis pathway (Meskauskiene et al., 2001). The precise effector upstream of FLU feedback inhibition is not yet known as indicated by the question marks. ALA, -aminolevulinic acid; Chlide, chlorophyllide. Adapted from op den Camp et al., 2003.

After shifting *flu* plants from the dark to the light, free Pchl_{ide} leads to the formation of singlet oxygen in the chloroplast (op den Camp et al., 2003). As shown in Fig. 1-3 (B), etiolated *flu* seedlings rapidly collapse after transferring them to the light. In contrast, when grown under continuous light, *flu* plants develop like wt (Fig. 1-3 C). Therefore the *flu* mutant offers the possibility to study the impact of singlet oxygen on the life cycle of Arabidopsis. Plants can be initially grown under continuous light and at a given developmental stage they can be transferred to the dark. After reillumination seedlings collapse and die whereas mature plants stop growing and develop necrotic lesions (op den Camp et al., 2003). During the past recent years efforts have been made to characterize the stress responses triggered in the *flu* mutant after a dark-to-light shift.

1.4.6 *flu* supressor screen

Chemical mutagenesis of *flu* seeds was used to identify second-site mutants that no longer show the singlet oxygen-mediated stress responses. Two different groups of second-site mutants were identified that abrogate either one or both of the two stress responses of the *flu* mutant (Fig. 1-5) but still overaccumulate Pchl_a. They genetically define signaling pathways activated by singlet oxygen in *flu* and demonstrate that seedling lethality and growth inhibition do not result from mere physicochemical damage caused by oxidative stress. The isolation of such mutants supports the idea of a specific signalling role of singlet oxygen.

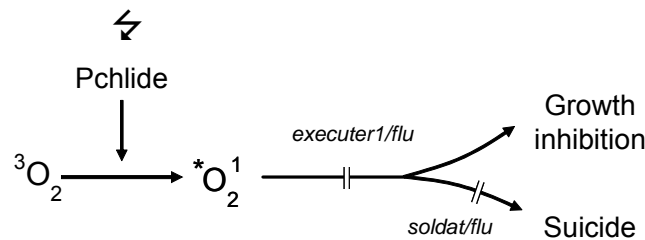


Fig. 1-5: The genetically controlled pathway triggered after the release of singlet oxygen in *flu*. Two different types of second-site mutants of *flu* were identified that helped defining this signalling pathway. The EX1 protein may participate in the transmission of the signal triggered by singlet oxygen before the branching point that defines the two different stress responses. *soldat/flu* mutants are only able to block the suicide program in the seedling stage, but in mature plants the mutation has no effect on the *flu* phenotype. Modified from Wagner et al., 2004.

In the *executer1/flu* double mutant (*ex1/flu*), both the growth inhibition of mature plants and seedling cell death are suppressed, even though the mutant generates similar amounts of singlet oxygen as *flu* after a dark-to-light shift (Wagner et al., 2004), demonstrating that inactivation of a single gene is sufficient to prevent singlet oxygen-activated pathways in *flu*. The *EXECUTER1* gene (*EX1*) may define a branch point from which the two stress responses diverge. Inactivation of EX1 also prevents death in wt treated with DCMU and grown under high light (Wagner et al., 2004). It mimics photoinhibition by inhibiting PSII at the level of the secondary quinone electron acceptor of PSII, Q_B , and inhibiting forward electron transport. Charge recombination in PSII favors the formation of $^3\text{Chl}^*$ that reacts with ground-state triplet oxygen to form singlet oxygen.

Intriguingly, singlet oxygen-mediated changes in gene expression are also present in *ex1/flu*, even though the set of stress-related genes is induced to a lower extent than in *flu* (Wagner et al., 2004). This observation suggests that the EX1-mediated pathway may not be the only pathway activated after the release of singlet oxygen in plants.

1.5 Goals

A second group of mutants was identified in the *flu*-suppressor screen, named Singlet Oxygen-Linked Death ActivaTor (*soldat*). Mutations in *SOLDAT* genes specifically affect the Singlet Oxygen-mediated Suicide (SOS) program in the *flu* background: seedlings do not collapse after reillumination. Mature *soldat/flu* plants, however, behave like *flu*: they stop growing and develop necrotic lesions. Eighteen different *soldat/flu* mutants were identified. The mapping and characterization of one of the mutated genes, *soldat8*, was the goal of this work. Identification of this gene should allow a deeper understanding of how the singlet oxygen-mediated signaling occurs and how it affects the cell death program.

2 Material and Methods

2.1 Chemicals

Unless mentioned otherwise, chemicals used in this work were purchased from Sigma-Aldrich Chemie GmbH (Buchs, Switzerland).

2.2 Primers

All primers were synthesized by Microsynth (Balgach, Switzerland). Lyophilized primers were dissolved in water to a final concentration of 1 μ M (stock solution).

Table 2-1: List of primers and markers

a) Markers used for crude mapping		
Name	Forward primer sequence	Reverse primer sequence
AlwNI	CGGCGCAGGATTTTACTATG	CTGAGAGCACCTTAC
AthBio2b	TGACCTCCTCTCCATGGAG	TTAACAGAAACCCAAA
CEREON1	GGAACCATATTGCCACCA	ACCGGAACCGGTTTACTT
CEREON2	TGATTTGGTGGTGGCAGT	AACCCTCGTAATATAACCCTCA
CEREON3	TGCACAATGGGACTTTGA	ACTGATTCTCCGGTCACG
F12L6	CATCTGCTGCAACTCTGTCC	GAAACACAAAATTTGGCAAGGA
F13K3	CAAACACCCAAAGTTGCTCA	GAAAGGAGAGATGAAGCTGGAA
F13M22	TAGGCTCCTCCGAGCAATTA	GATTCGCATCTCGGACATTT
F13M22(Psil)	GCCATTTGTTGTGTGACAAT	TGCTGGTCATTTGCCATAAA
F13P17	CAAGCACGACGGAGGTTTAT	TGGTCTTCACATCGATCTTTT
F16M14(1)	GCAAGGAATATGTTGAAGACTAAAA	TCAAACTTGTAAGAAGGCAAA
F16M14(2)	AAAACAATGATGAAATCAGTTATGGA	GAATTTACATTTTTCTCTTTCTATCA
F18A8	GAGCTGGTATTTCTCTAATTTAC	GGAGACGCTAATGGTCGACG
F19I13(2)	GAGTCTTGCTTAAGGGTAGTTATG	CAGAGGGACTTGACGAAAGAG
F19I3	GAAATTCACCACAAGAGTTGAAG	CAATGTTGGAGATCCATCTGTTG
F3G5	AAGCCCAATTTGGAGTAGCC	CGTGAGTTCAAGACGGGTAAA

Material and methods

nga361	ACATATCAATATATTAAGTAGC	AAAGAGATGAGAATTTGGAC
T19C21	GCCAGTCTTTCCAATGCCTA	TGAATGCCTTTGCTCACAGT
T1J8	CCTTGCCAACATTTTGGATT	TTTCGCGATTTCTTCTTCGT
T1J8 (2)	GCTTTGAAGCTGTTCCCTCTC	CAGAACCAAACAGACCCTAAA
T1J8 (3)	CGGGCTGTCCATGAACAT	CCGGTTTTTGGTCTGTATTC
T1J8 (MunI)	TTTCCCTTCTGTTGACTTC	CAATCTCCATAACCACAGCA
T1J8 (SacI)	ATCTCAAGACAAAGGCCAAG	CAGGCATAGAACCGAAAGAT
T1J8(4)	ACGAAAAAGCAAACATTATAAGA	ACTTGCTTTTATTTTCGTCAAC
T1J8(5)	CACAACGAATCTGGACCAT	GGGAACGTGAGGAGATATGA
T1J8(ApoI)	TGTTGTTGAACCAGATTTTCAG	AACAATTTCAATTCGCGATA
T1J8(CaiI)	CGGTTGTCTCTGCCTTTG	CAATCTTCCGACCACCA
T1J8(HindIII)	AAAGGGTGGCATTGCTT	CCATCCGTCCATAAACCA
T1J8(HphI)	GTTCCCGATCGTGTCAAT	CATTGTGCAGCATCCATC
T1J8(MnII)	AGGCCAAGGAAGGAGAAG	GACCCATTTGTTTGTTTTACC
T1J8(MnII2)	CCACTGGCTACGGGACTA	AATTCCGATTGGCTGACA
T1J8(MspI)	ACATCACTGCGTCTCGTTT	AGTTTCTATGCCGGAGAGG
T1J8(NlaIII)	AAAAAGCCACGGAGTTATTG	CAATGTGGAAGTGGTTGCT
T1J8(NlaIII2)	TGGTGAGCAAGCACTGAG	AACCAACGCGTTACCAAC
T1J8(StyI)	ACAGCCCACAAGTAGCAGA	GCTTTGTGATGTGGTTGC
T1J8(TruI1)	CGGAGGAGGAGGAACGTA	TGGCAAATAACATTACCAAA
T1J8(TruI12)	CCGTGTACCATGGATCAGT	CATTGTGCAGCATCCATC
T1J8(TseI)	GTTCCCGATCGTGTCAAT	CCAGTTGACGAGGAAGGA
T20F21	TCTTCCCCAAATTTCTGTTC	CGTTTTGGCTAAAATCACAAA
T26J13	TCCTACCTTTGTCTGAGCAATTC	CTCTGCGATGGCTTTCTTTT
T28M21	ATCGAAATCCCTGACTGTC	GGGAAACAATCTCCGTACA
T2N18	CAGAGCTAGGGTCGTCTAGTGT	GATCCCATCATTTTCGTTGA
T2N18 (2)	CGGATATACTTGCTTTTATTTTCGT	GGGGACTTATTTTGGGAAT
T2N18 (3)	GGGCTGCATCTTCAGCTATC	TGGGACTTTGAAGGAGCATC
T2N18 (4)	TCTTTGAGGCTTTGAATGGT	ATTAGGTGTTGCGGATTTGT
T2N18(TruI1)	CCGTAATCTGGCAAAGC	GGGGAGCGATAAAGAGTGA
T2N18(TruI1.2)	CATGGGAGGTGCATCAAG	TCACATATTTTCTTCCTTTTCG

T32F12	TGAATCCGGAGGCAGACTAT	GCGGTTCTTGCTGGTTAGTT
T3G21	CTCGTGTCGTGCGTAGC	AAGCCAAGCAAACGCATC
T4C15 (1)	CTTGGATTCAGCNCATTCTA	ACTCTAGTTATCTGCATATG
T4C15 (2)	CGAACTCAGCTTTCAACTC	GATTTGAGGTTACTCCTTAAATC
T4C15 (3)	TACTTCACGGCCTCATATTT	TCGTGATTTGAGGTTACTCC
T7F6	CTTTGATTCCCCAAAGTTGAA	ACATCAGTTTCTCCGGATGC
VE017	GAGCAATCCAGTAGAGGATA	CTTGAAGCTTAAATCTCAGC

b) Primers used for fine mapping (sequencing)

Name	Forward primer sequence	Reverse primer sequence
1.1	AGACGCTTCGGTAACGAGAA	GTGAGCTCCTTCTCCACTCG
1.2	TGTCGAGGAATCAGAGGAAGA	TTTTCTTCGGCTTAGCGTGT
2.1	TAACACCAACAACAACCTCACGA	TCTTACTTTCTCACTAATGGCGTCT
2.2	CAGATGTTGTCTTCGCCATT	TCATAACGGCGAACATTGTG
2.3	GCTCTCTTGCTTTGGTACGG	AGTGGCGAATAATGCAGGTT
2.4	GGTTTTACGACCCGAACTCA	CAACATCGCTCTTGCTATCG
2.5	GAGGATTGCAGCTGTCTGGT	AAGGGAGCCACAAATGACAG
2.6	AGAAGCTGGCCTTCAAGGAT	TAGCTATGGCTTCACCAGCA
2.7	GTTTCTCGGGAGACCTGGA	ATGTGTTTCCTTATGGCTTTCA
2.8	CCTAGCTCTTGTGGGTCCAA	CTAAGCATCATCTTCCTTAACCCCTA
3.1	ACGAAGAAGAAATCGCGAAA	GTGCTCGTGTCGTTGCCTA
4.1	AAAATGGGTAGATGTCCGACT	CGCAACTCTGTGAATACCAAA
4.2	CGCAACTCGATGCAGATTTA	CAACAAAATTTTCGGGTTCCA
5.1	CATCATTGTGGGGAGCATT	GACAGAAGCGTAGGTTTACTGATAA
6.1	CAAGAATGGGAGAGGTCCAA	TCTGAATACATCCTTCGCAATG
6.2	TTTGTTGTTTACAGAGCGTGGT	TTCTTATATTTACAGTTTAACCCCAT
7.1	GGAAGTTGAAATCAAAGCATGA	TAGCATTGCAGCATTGGTGT
7.2	TTGATGCCAAGAACCCAAAG	TCTTTCTGCGGTCTTTCAGC
7.3	GGACTTGCCAGGGAGAAAAT	AGCTTGGCAGAAAACCTGCAT
7.4	GCTCAGCTGGTGATGTTTCT	CTCTAGATCTTGCGGGACGA

7.5	TGAACGAGGTCAACATGCTC	CCACCAACTGTGAAGGCTCT
7.6	AATCGTTTCGCAAATCCAC	GGACCCCATGCTTTAGCTTT
8.1	GGAGAGAGCAAAGTCGAGGA	TTGCTTTAACCCCTGGTACG
8.2	TTTGTGGTAGATAATCGTAAAGACG	TGGATAACACAACAAAGGCAAA
8.3	TTGGGTTTTACGTCCGGATA	TTTTTCATTGTTTAGTTTGATGGA
9.1	TGAGTTTGCCCAAATGTCTG	AGCATGTACCATCCGTCCA
9.2	ATGGACGGATGGTACATGCT	CCTTCCTCTACAAGGCCTGA
9.3	GTGTCCACGGTTAGCAGAT	TGGGTATCTGCTTCATATTTTTCA
10.1	CATTCGTGGAAGCAAAAACA	TTGCTGTTCAAATTTCTCATCTTC
10.2	GGAGAGGAGGCAGTTTGATG	CAGCTCAGCTTCTTCTTTAGCA
10.3	GATGATGCGCTTCAGCTCT	CGGTAAACGGATTGTTCTGG
10.4	AATCCGGATGCAGATTCG	TCTCCATGAGCTAGACAAGCAA
11.1	TCGACGAATTCGGAGATGAT	ATCAAAAGCCTAATTTTACTAATGGTG
12.1	GGCTACTGACACTGAGATGAGG	GCTTCACGTCGAAGTGCTC
12.2	ACTTCGACGTGAAGCACTTG	TAAGCCGTTGTTTTCCAACC

c) Chloroplast primers

Name	Forward primer sequence	Reverse primer sequence
accD	GGATGAAGACATGGTCTCTGCGG	ACCAAACTAGCTGTCACTCCACC
atpF	GCCGGGAGTTTCGGATTTAATACC	CACGCGAACTTATCCGCTTCCG
atpI	TTTCCAGGTCCATGCCAAGTTC	TTCGTTGGTGCTGCTAACTCCC
clpP	GCCTATTGGCGTTCCAAAAGTACC	CCTAGCGTGAGGGAATGCTATACG
matK	CTGGCAACAAAGGATACGCCGC	CCGTCCAGTTGCTTTACTAATGGG
ndhB	TAGCTGCTTCAGCTTCAGCCAC	TAGTGGAGGAAGACCTCCTAGG
ndhC	ATCTCCAATTAGGAAGGGGCCG	TCCAATGCTCCTTTTCGCCATGC
ndhI	TGGTCAACAAACCCTACGAGCTG	ACTGACATTGGTAAACGACCCAAAGC
ndhJ	GCGGGCTGGTTCATAGATCGTTG	GATCCGTTTCAGTCGTGGATGGC
psaA	ACCACGCCCGCTGAATAGAAAC	TTGTGATGGGCCGGGAAGAG
psaB	CGAGGTGGTACTTGTGATATTTCCGC	CAATTCCTGCCAATAACCACGCC
psaJ	CATATCTTTCCGTAGCACCG	TAATAAACCTGCTAACGAACCG

psbA	AAGGGAGCCGCCGAATACAC	TGGCTATACAACGGCGGTCC
psbD	CTATGGGCTTTTGTGCTCTCCAC	CATGAATAGCGCATAGCAGAGCC
psbK	TTTAGTCGCCAAATTGCCAGAGG	AAAACCTTACAGCGGCTTGCCAAAC
rbcl	CTAGAGGATCTGCGAATCCCTCC	CTAGTATTTGCGGTGAATCCCCC
rpl20	AGCTCGGAGGCGTAGAACAAAAC	TACCCCCATTTGCGTAATTACGGC
rpoB1	CCCTCACGCATGAATGTAGGACAG	AACGGCCTCTAAGGGGTTGTTG
rpoB2	ACGTATTCGCTCTGTAGCGGATC	CGTGTCAATGGGACAAATACGCC
rpoC1	TTCTTCCTCCCGAGTTGAGACC	GTGAAGTCCAACGACAATCACCG
rpoC2.1	CGGTGATATAACCCAAGGTCTTCC	TCTTCTAAAGCACGCCCCGTTT
rpoC2.2	ATAGAAAGGCAGGATGCCCGTG	ATAGAAAGGCAGGATGCCCGTG
rrn16S	TAAGCATCGGCTAACTCTGTGCC	TACAGCACTGCACGGGTCGATAC
rrn23S	TGTGGTTAGGGGTGAAATGCCAC	ATCGCTTAGCCCCGTTTCATCTTC
rrn4S	ACGAGCCGTTTATCATTACGATAGGTGTC	CCGGTCTGTTAGGATGCCTCAG
trnE	CCCCATCGTCTAGTGGTTCAG	GGGAAGTCGAATCCCCGCTG
ycf2.1	CTAACTGGAGTTCGCGGTGGTG	ACCCAGCTCCTTGTGTTTGCAG
ycf2.2	TCCCAGGTAAGATCGGTTCAGG	AAGCGCCTTGCACTTCTAATAGGC

d) Other primers used

Name	Primer sequence	Reverse primer sequence
AAA	TGAGCATCCAGCTACGTTTG	TCGCTGCGATCATTGTAGAC
actin	GTGTGTCTCACACTGTGC	CAGATCCTTCTGATATCC
ERF5	ACAGAGGAGTAAGACAAAGACC	ACGTCAGCATAACATCG
ERF6	CCTCGACGAATTGTCTCCG	GCCAAACCCGAGTTCCACG
pCam	TCTACCATGAGCCCAGAAC	TCAAATCTCGGTGACGGGC

Name	Primer sequence
Prom(EcoRI).F	CCGGAATCCCGAATTCGTCGATTTTGT
cDNA(BamHI).R	CGCGGATCCACCAATATCTCCATGA
wt SIG6.R	GCGAATCTGCATCCGGATTG

mut SIG6.R	GCGAATCTGCATCCGGATTA
10.3(F)	GATGATGCGCTTCAGCTCT
flu-ID (flu).F	CCAAGGGAAGTATAGGGAAGT
flu-ID (wt).F	CCAAGGGAAGTATAGGGAAGC
flu-ID.R	GGCAATTGGCACTTAAGATGGC

2.3 Growth of Arabidopsis

All experiments were performed with *Arabidopsis thaliana* plants ecotypes *Landsberg erecta* (Ler) and *Columbia* (Col).

2.3.1 Growth on agar

Seeds were surface-sterilized by resuspending them in bleach solution (50% (v/v) sodium hypochlorite, 0.01% (w/v) Triton X-100). After 10 min the seeds were washed 4 times in sterile water.

Sterilized seeds were plated on MS-agar plates. MS medium (Murashige and Skoog, 1962) was prepared with 2.5 g/l of MS including vitamins and MES buffer (Duchefa, Haarlem, Netherlands), 0.8% (w/v) agar (Sigma[®], St. Louis, USA) and supplemented with 5 g/l of sucrose. After adjusting the pH to 5.7 the medium was autoclaved and pored into 90 mm Ø petri dishes (~30 ml/plate).

Sown seeds were vernalized at 4°C for 7 days in the dark and then transferred to continuous light (80-100 µmol photons m⁻² s⁻¹, Philips Master TDL 36W, Philips Electronics N.V., Eindhoven, Netherlands and Sylvania Gro Lux F36W SLI Lichtsysteme GmbH, Erlangen, Germany) and controlled temperature (21°C) and humidity (65%). In case the settings of the experiment required other conditions, the specific treatment is mentioned.

2.3.2 Growth on soil

Seeds were sown on common rich soil (85% peat, 10% sand and 5% perlite) with low soluble fertilizer and after 10 days singled out in separate pots containing Klasmann Substrate No.2 (Klasmann-Deilmann GmbH, Geeste-Gross Hesepe, Germany), which contains 100% peat and soluble compound fertilizer. The plants were grown under continuous light until the rosette leaf stage and after bolting they were either transferred to long-day condition (16 h light/8 h dark) to test the growth inhibition or kept in continuous light for transformation and/or seed collection.

2.4 DNA techniques

2.4.1 Isolation of genomic DNA

One cauline leaf was frozen in liquid nitrogen and 500 µl of Shorty buffer were added (0.2 M Tris-HCl pH 9.0; 0.4 M LiCl; 25 mM EDTA pH 8; 1% (w/v) SDS) and ground with an electric micropestle. After centrifugation 5 min at top speed and room temperature (RT), the supernatant was transferred to a fresh Eppendorf tube containing 350 µl of isopropanol. After centrifugation 10 min at top speed and RT, the supernatant was discarded. The pellet was air-dried and dissolved in 400 µl of TE buffer (0.01 M Tris-HCl pH 8; 1 mM EDTA) by shaking at RT for 30 min. DNA was stored at -20°C.

2.4.2 Isolation of plasmid DNA from *E.coli*

The DNA was obtained from an overnight 3 ml *E.coli* liquid LB culture using a QIAprep® Spin Miniprep Kit (Qiagen GmbH, Hilden, Germany). Four ml were used for the isolation, according to protocol provided by the manufacturer, yielding 50 µl of DNA (100-200 ng DNA/µl).

2.4.3 Polymerase Chain Reaction (PCR)

This *in vitro* technique allows the fast amplification of a specific DNA fragment. The PCR mix was prepared by adding to an Eppendorf tube 2 µl of DNA solution, 2 µl of BioTherm™ Mix Buffer, 1.5 units of BioTherm™ DNA Polymerase (Genecraft GmbH, Lüdinghausen, Germany), 25 pmol dNTP (Fermentas GmbH, St. Leon-Rot, Germany), 20 pmol specific forward and reverse primers and water to a final volume of 20 µl.

The reaction was performed in an iCycler Thermocycler (Bio-Rad AG, Reinach, Switzerland) using the following program: 5 min initial denaturation at 94°C; 45 cycles including: 15 s denaturation at 94°C, 30 s annealing at 55-60°C (temperature depending on the melting temperature of the primers) and elongation at 72°C (time depending on length of the DNA fragment, 1 Kb/min); 10 min final elongation at 72°C. The samples were run on an agarose gel or stored at 4°C.

2.4.4 Purification of PCR products

In order to purify PCR products (≥ 200 bp) Quantum Prep® PCR Kleen Spin Columns (Bio-Rad AG, Reinach, Switzerland) were used. The yield obtained ranged between 90-150 ng/µl. To

assess the quantity and quality of the purified DNA, OD₂₆₀ and OD₂₈₀ were measured and the sample was loaded on an 1% agarose DNA gel.

2.5 RNA techniques

2.5.1 Isolation of total RNA

Seedlings grown on agar plates were frozen in liquid nitrogen and ground to a fine powder with mortar and pestle. 50-100 mg of powder were transferred to a 2 ml Eppendorf tube and 1 ml of TRIzol[®] Reagent (Invitrogen AG, Basel, Switzerland) was added. The tubes were centrifuged at 11,400 rpm 15 min at 4°C (Eppendorf 5402) and the supernatants were transferred to a new tube. Chloroform was added (300 µl) and vortex was applied for 15 s. The samples were centrifuged again at 11,400 rpm for 15 min at 4°C and the aqueous phase was transferred to a new tube. After the addition of 750 µl of isopropanol the samples were incubated 10 min at RT and centrifuged at 11,400 rpm for 10 min at 4°C. After washing the pellet with 1 ml of 75% ethanol, the samples were centrifuged at 9,000 rpm for 5 min at 4°C. The pellet was air-dried and dissolved in 150 µl of RNase-free water with a pipette tip. To increase the solubility, the samples were incubated for 5 min at 55°C. For quantification, 100 µl of a 1:100 dilution from each sample were placed in a quartz cuvette and OD₂₆₀ and OD₂₈₀ were measured in a spectrophotometer (DU[®]640 Beckman Coulter, USA). The concentration was calculated according to Sambrook et al (1989). To assess the quality of RNA, an aliquot containing 2 µg was loaded on a 2% agarose gel. The RNA was stored at -80°C.

2.5.2 Reverse transcription

cDNA can be synthesized from RNA by means of reverse transcription. The cDNA is then amplified using standard PCR protocols.

DNase treatment

DNase treatment was performed in order to eliminate the remaining genomic DNA. For each 3 µg of RNA 1 unit of RQ1 RNase-Free DNase and 1 µl of RQ1 RNase-Free DNase 10x Reaction Buffer (Promega, Madison, USA) were mixed and water was added to a final volume of 10 µl. The reaction was incubated for 1h at 37°C and afterwards the enzyme was inactivated by adding 1 µl of a stop solution and incubating it at 65°C for 10 min.

cDNA synthesis

To synthesize the cDNA from the RNA samples, the SuperScript™ II Reverse Transcriptase system (Invitrogen AG, Basel, Switzerland) was used. Half a µg of Random Primers (Invitrogen AG, Basel, Switzerland) and 1 µl of 10 mM dNTP Mix were added to the RNA samples. After incubation at 65°C for 5 min, the samples were allowed to cool down at RT for 10 min. To perform the synthesis, 4 µl of 5 x First-Strand Buffer, 2 µl of 0.1 M DTT, 40 units of RNaseOUT™ Recombinant Ribonuclease Inhibitor and 200 units of SuperScript™ II Reverse Transcriptase were added to the tubes. The contents were mixed gently and the samples incubated at 42°C for 50 min. The reaction was stopped by heating at 70°C for 15 min. After dilution with 80 µl of water the samples could be used for PCR.

2.5.3 Real-Time PCR

Real-time PCR was used to quantify gene expression. In contrast to the traditional PCR, this method detects the amount of template during the early phases of the reaction. This provides more specific, sensitive and reproducible results than other forms of quantitative/semi-quantitative PCR that detect the amount of final amplified product at the end-point. Data are collected during the course of the reaction, avoiding post-PCR processing.

The equipment used was ABI Prism® 7700 Sequence Detection System together with SYBR®Green PCR Master Mix (Applied Biosystems, Foster City, USA). This mix contains the dye SYBR Green, which emits fluorescence after it binds to a double-stranded DNA. A sequence detector reads the changes in fluorescence emission, which are a direct consequence of DNA amplification during PCR.

Samples containing cDNA, specific primers and PCR master mix were prepared according to the manufacturer's instructions and adjusted to a final volume of 25 µl. A standard PCR program was used and the relative mRNA abundance was calculated using the comparative ΔCt method. The ΔCt value is determined by normalizing the Ct of the gene tested (Ct_t) with the Ct of an endogenous control (Ct_e):

$$\Delta Ct = Ct_t - Ct_e$$

Subsequently, the following formula can be used which provides the normalized relative transcript abundance per sample:

$$1/2^{\Delta Ct}$$

As an endogenous control we used *ACTIN2*, At3g18780. The efficiencies of the probes and the control used were comparable.

Different samples (for example mutant vs. wt) were compared using the formula:

$$2^{(\Delta Ct \text{ wt} - \Delta Ct \text{ mutant})}$$

, which allowed us to determine fold changes in transcript abundance between them.

2.5.4 Chloroplast macroarray*

Preparation of the chloroplast macroarray filters

A total of 94 genes of the plastome of Arabidopsis (photosynthetic genes, ribosomal RNAs and tRNAs) were amplified by PCR using 94 gene-specific primer pairs. Genomic DNA of wt (Col) was used as a template. These genes were amplified using a standard PCR protocol with the following conditions: 30 cycles including 20 s denaturation at 94 °C, 1 min annealing at 60°C and 1 min elongation at 72 °C. PCR products were purified with the QIAquick PCR Purification Kit (Qiagen, Hilden, Germany). The size and quality of all PCR products were checked on a 1.2% agarose gel by electrophoresis. The purified PCR products (>400 bp) were diluted into three different concentrations (30.0, 7.5 and 1.87 ng/μl, respectively). The 94 probes were spotted onto the 11.9 cm x 7.8 cm positively charged nylon membrane (Hybond™-N+ Amersham Pharmacia Biotech, Freiburg, Germany) by using a 96-pin tool (0.4 mm pins with a BioGrid spotting Device-Roboter (BioRobotics, UK)). Each probe was spotted 20 times in order to get final DNA quantities of 1.25, 5 or 20 ng per sample on the different spots. Three different concentrations of one gene were spotted in duplicate onto the filters. The spotted membranes were denaturated in 1.5 M NaCl, 0.5M NaOH and afterwards neutralized in 0.5 M Tris-HCl pH 7.2, 1 M NaCl. The filters were subsequently cross-linked using 120 mJ of UV light (302 nm) (Stratalinker UV crosslinker 1800, Stratagene, La Jolla, USA) and dried.

* The experiments using chloroplast macroarrays and subsequent data analysis were performed in the group of Dr. J.Meurer at the at the Botanical Institute of the Ludwig-Maximilians University of Munich.

Table 2-2: List of chloroplastic genes spotted onto the filters

A) Photosynthetic genes			B) rRNAs		C) tRNAs
<u>accD</u>	<u>ndhK</u>	<u>psbI</u>	<u>rpl12</u>	<u>rps7</u>	<u>trnA</u>
<u>atpA</u>	<u>petA</u>	<u>psbJ</u>	<u>rpl14</u>	<u>rps8</u>	<u>trnE</u>
<u>atpB</u>	<u>petB</u>	<u>psbK</u>	<u>rpl16</u>	<u>rrn16S</u>	<u>trnF</u>
<u>atpE</u>	<u>petD</u>	<u>psbL</u>	<u>rpl20</u>	<u>rrn23S</u>	<u>trnI</u>
<u>atpF</u>	<u>petG</u>	<u>psbM</u>	<u>rpl22</u>	<u>rrn4.5S</u>	<u>trnI</u>
<u>atpH</u>	<u>petL</u>	<u>psbN</u>	<u>rpl23</u>	<u>rrn5S</u>	<u>trnI</u>
<u>atpI</u>	<u>petN</u>	<u>psbT</u>	<u>rpl32</u>		<u>trnK</u>
<u>cemA</u>	<u>psaA</u>	<u>psbZ</u>	<u>rpl33</u>		<u>trnL</u>
<u>clpP</u>	<u>psaB</u>	<u>rbcL</u>	<u>rpl36</u>		<u>trnP</u>
<u>matK</u>	<u>psaC</u>	<u>rpoA</u>	<u>rps11</u>		<u>trnR</u>
<u>ndhA</u>	<u>psaI</u>	<u>rpoB</u>	<u>rps12</u>		<u>trnV</u>
<u>ndhB</u>	<u>psaJ</u>	<u>rpoC1</u>	<u>rps14</u>		
<u>ndhC</u>	<u>psbA</u>	<u>rpoC2</u>	<u>rps15</u>		
<u>ndhD</u>	<u>psbB</u>	<u>ycf1</u>	<u>rps16</u>		
<u>ndhE</u>	<u>psbC</u>	<u>ycf15</u>	<u>rps18</u>		
<u>ndhF</u>	<u>psbD</u>	<u>ycf2.1</u>	<u>rps19</u>		
<u>ndhG</u>	<u>psbE</u>	<u>ycf3</u>	<u>rps2</u>		
<u>ndhH</u>	<u>psbF</u>	<u>ycf4</u>	<u>rps3</u>		
<u>ndhI</u>	<u>psbH</u>	<u>ycf5</u>	<u>rps4</u>		
<u>ndhJ</u>					

Hybridization of the cDNA with the chloroplast macroarray filters

Before hybridization, the filters were incubated at 65 °C for 1 hour in 10 ml Church buffer (0.25M Na₂HPO₄ pH 7.2, 7% SDS). The [α -³²P] dCTP labeled cDNAs were synthesized at 50°C for 1h from 20 μ g of total RNA (Roche, Mannheim, Germany) using the SuperScriptTM III RNase H⁻ Reverse Transcriptase (Invitrogen, Karlsruhe, Germany). After inactivation of the enzyme at 70°C for 20 min, the labeled cDNAs were incubated at 37°C for 20 min with RNase H (Invitrogen, Karlsruhe, Germany) to remove RNA. The labelled cDNAs were purified using MicroSpinTM G-25 columns (Amersham Pharmacia Biotech, Freiburg, Germany). The cDNA probes were incubated for at least 12 h at 65°C in Church buffer. The filters were washed separately at 65°C for 20 min sequentially in three different washing buffers (2 X SSC, 0.1% SDS; 1.0 X SSC, 0.1% SDS ; 0.5 X SSC, 0.1% SDS).

Data normalization

Each macroarray filter contained 94 plastid genes (see the list in Table 2-2). To increase the accuracy of the arrays, a total of 6 spots per gene (3 different DNA concentrations in duplicate) were spotted on the filters. The washed filters were exposed to a phosphor image plate for at least 3 days. The radioactive images were scanned with a FLA-3000 phosphorimager (Fuji, Tokyo, Japan) and the obtained signals were imported to the AIDA Image Analyzer (3.25) software for background correction and normalization. The background noise was corrected after alignment and integration of the spots. For background subtraction, the mean value of three selected background dots was calculated. These dots were selected within a sub-grid where six spots of a gene were located together. Their intensity values were averaged and then used as a background value to all spots of the sub-grid. Afterwards, all spots in a filter were used to calculate the normalization constant by averaging the corrected background intensity value of all the genes. Following background correction and normalization, the intensity values of the spots corresponding to a particular gene were compared between wt and the mutant using the software AIDA Array Compare 3.25 (raytest Isotopenmeßgeräte GmbH, Straubenhardt, Germany). Changes in gene expression between wt and the mutant were determined by plotting the normalized values of the mutant against wt.

2.6 Protein techniques*

2.6.1 Isolation of total proteins

Seedlings grown on agar plates (~50 seedlings) were collected after freezing them in liquid nitrogen and a fine powder was obtained by grinding them with the help of a mortar and pestle. The powder was transferred to an Eppendorf tube and 500 µl of homogenization buffer were added (0.0625 M Tris-HCl pH 6.8; 1% (w/v) sodium dodecyl sulfate (SDS); 10% (v/v) glycerin, 0.01% (v/v) 2-mercaptoethanol). The samples were incubated for 10 min at 70°C. After centrifugation for 10 min at maximum speed, the supernatant containing the total protein fraction, was transferred to a fresh Eppendorf tube. The protein concentration was estimated using the colorimetric BCA protein assay (Pierce Biotechnology, Socochim SA, Lausanne, Switzerland).

* Unless mentioned, all reagents and equipment used were from Bio-Rad (Reinach, Switzerland)

2.6.2 Separation of proteins by SDS-PAGE

SDS-polyacrylamide gel electrophoresis of proteins was carried out according to Laemmli (1970). Gels were prepared with an acrylamide/bisacrylamide (37.5:1) solution to a final concentration of 12%. Protein samples were prepared with 25 µg of total protein supplemented with an 1:1 Laemmli sample buffer. After protein denaturation at 70°C for 5 min, the samples were loaded onto the gel. Low-range molecular weight standards were added to one well of the gel. Electrophoresis was performed using the Mini Protean 3™ system at a constant voltage of 150 V during 1 hour.

Gel staining

Proteins separated in the gel were stained with a solution containing 0.1% (w/v) Coomassie Brilliant Blue R-250, 20% (v/v) methanol and 20% (v/v) acetic acid by gently shaking during 45 min at room temperature. After washing the gel with water, the gel was de-stained in 20% (v/v) acetic acid until the bands appeared. The gels were dried in a Bio-Rad gel dryer at 80°C for 2 h.

2.6.3 Western analysis

Protein blotting to PVDF membrane

Proteins separated by SDS-PAGE were transferred onto an activated immuno-blot PVDF membrane using the Mini Trans-Blot Cell™ system. The transfer buffer contained 25 mM Tris pH 8.3, 192 mM glycine and 20% (v/v) methanol. The transfer was accomplished after 3 h at 250 mA. Proteins were stained by submerging the membrane into Ponceau S staining solution (0.2% (w/v) Ponceau, 3% (w/v) trichloroacetic acid and 3% (w/v) sulfosalicylic acid) for five minutes. After rinsing with water, the membrane was dried at room temperature.

Immunological detection

For immunodetection, the membrane was first incubated in the blocking buffer, that contains 5% (w/v) fat free milk powder in TBST (0.1 M Tris (pH 7.4), 150 mM NaCl and 0.2% (v/v) Tween-20) for 2 h at room temperature. Subsequently, the solution was discarded and a fresh blocking solution containing the first antibody (see the list of antibodies in Table 2-3) was added and incubated for one hour under the same conditions. After washing five times for 10 min with TBST a new aliquot of blocking solution containing the secondary antibody (dilution 1:3000) was added and incubated for one hour. As a secondary antibody, anti-chicken or anti-rabbit IgG coupled to peroxidase was used. The membrane was rinsed again five times with TBST before protein

detection. The colorimetric detection assay performed (Opti-4CN™) is based on the peroxidase-activated color development of 4CN.

Table 2-3: List of antibodies

Protein or protein complexes	Subunit	Dilution primary antibody	Secondary antibody	Source of the antibody
PSII	PsbA (D1)	1 : 3000	anti-chicken	Agrisera AB (Vännäs, Sweden)
		1 : 5000	anti-rabbit	Dr. J. Meurer (Botanical Institute, LMU, Munich, Germany)
	PsbD (D2)	1 : 3000	anti-rabbit	Dr. J. Meurer (Botanical Institute, LMU, Munich, Germany)
	PsbS	1 : 2000	anti-chicken	Agrisera AB (Vännäs, Sweden)
Rubisco	RbcL	1 : 2000	anti-chicken	Agrisera AB (Vännäs, Sweden)
LHCP	Lhca1	1 : 5000	anti-rabbit	Agrisera AB (Vännäs, Sweden)
ATP synthase	β	1 : 3000	anti-rabbit	Dr. J. Meurer (Botanical Institute, LMU, Munich, Germany)
	γ	1 : 3000	anti-rabbit	Dr. J. Meurer (Botanical Institute, LMU, Munich, Germany)
	δ	1 : 3000	anti-rabbit	Dr. J. Meurer (Botanical Institute, LMU, Munich, Germany)
Flu	Flu	1 : 3000	anti-rabbit	Dr. R. Meskauskiene

2.7 Mapping of the second-site mutation

2.7.1 Crude mapping

The *soldat8* locus was genetically mapped on chromosome II, using CAPS (cleaved amplified polymorphic sequence) or SSLP (simple sequence length polymorphism). These markers are listed in The Arabidopsis Information Resource database (TAIR, www.Arabidopsis.org).

Some markers were designed using the collection of predicted Arabidopsis single-nucleotide polymorphisms (SNP) and small insertions/deletions (INDELs) between the publicly available *Columbia* sequence and the *Landsberg erecta* sequence generated by Monsanto (<http://www.Arabidopsis.org/Cereon/>).

2.7.2 Fine mapping and sequencing

Part of the the region was sequenced in order to find the exact position of the gene within the 54.9 Kb genomic fragment flanked by the two closest markers which could be mapped. Overlapping primers covering the whole fragment were designed (Table 2-1) and PCR was performed on genomic DNA from *soldat8/flu* and *flu*, which was used as a control. The amplified products were purified and approx. 100 ng of DNA per sample were sent to Microsynth (Balgach, Switzerland) for sequencing. The sequences were compared to the sequenced Arabidopsis genome, using the SeqViewer tool from TAIR.

2.8 Complementation assay

2.8.1 Ligation of *SOLDAT8* genomic sequence into plasmid DNA

Amplification of SOLDAT8 genomic sequence

Specific primers flanking the *SOLDAT8* genomic sequence (including the promoter region) were designed (Prom(EcoRI).F + cDNA(BamHI).R), which contained at the end sequences of the restriction sites to be inserted into the fragment (*EcoRI* + forward and reverse + *BamHI*). For amplification, the Expand High Fidelity ^{PLUS} PCR System (Roche, Rotkreuz, Switzerland) was used. The DNA obtained was purified and quantified as described and approx. 0.5 µg were used for sequencing.

Digestion with restriction enzymes

A pCambia 3300 plasmid DNA (pCam, Fig. 2-1) isolated from *E.coli* cells as described, was purified and quantified. The pCam plasmid is a binary vector which is suitable for *Agrobacterium tumefaciens*-mediated Arabidopsis transformation. DNA fragments up to 5 Kb can be cloned into the pCam multiple cloning site. It contains two selectable markers, the neomycin phosphotransferase gene (*NPTII*) under the control of the nopaline synthase promoter, which confers resistance to kanamycin in bacteria, and the *BAR* gene, that confers resistance to the herbicide Basta (also known as glufosinate).

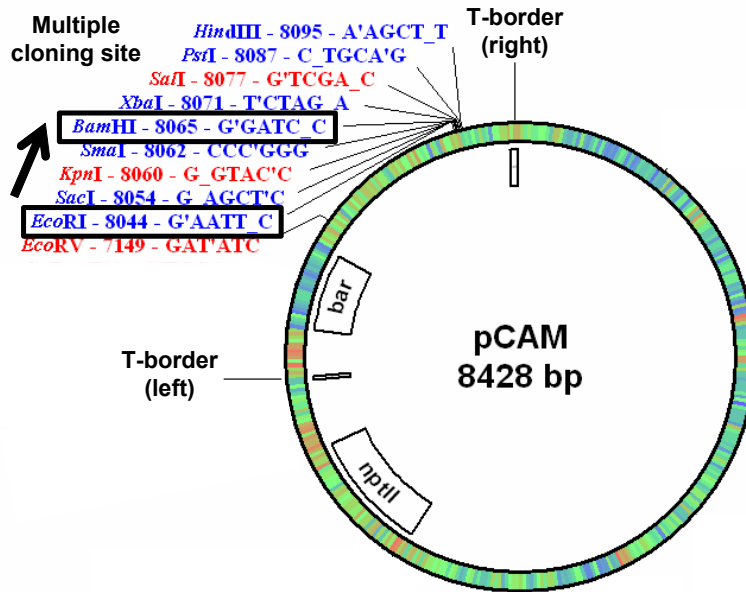


Fig. 2-1: Schematic presentation of pCAM 3300 vector used for complementation. The DNA fragment was cloned into the multiple cloning site of a pCam3300 vector. The restriction enzymes used for cloning are highlighted in black boxes within the multiple cloning site. The arrow represents the position and orientation of the DNA fragment inserted. Location of the T-DNA borders is also shown. *bar*, Basta-resistance gene; *nptII*, kanamycine-resistance gene.

One μg (this I have to check in the lab) of the purified *SOLDAT8* DNA and 5 μg of plasmid DNA were double-digested overnight at 37°C with *EcoRI* and *BamHI* enzymes (New England BioLabs, Ipswich, USA). The lengths of the fragments obtained were controlled on agarose gels. Bands with the correct size were purified using the QUIAEX[®] II agarose gel extraction protocol (Qiagen GmbH, Hilden, Germany) and the DNA amount was quantified.

Ligation

The DNA fragment and the plasmid DNA were mixed in the reaction tube in a ratio of 1:3.5 and 400 units of T4 DNA (New England BioLabs, Ipswich, USA) were added. The ligation was carried out at RT for 2 h and the enzyme was inactivated at 65°C for 10 min.

2.8.2 Transformation techniques

Transformation of Escherichia coli by heat shock

Preparation of competent *E.coli* cells

An LB-agar plate was streaked with *E.coli* DH5 α and incubated at 37°C overnight. One isolated colony was used to inoculate 2 ml of SOB medium (0.5% yeast extract, 2% tryptone, 10 mM NaCl, 2.5 mM KCl, 10 mM MgCl₂, 10 mM MgSO₄) and grown overnight at 37°C shaker (250 rpm). The culture was transferred to 250 ml of fresh SOB and grown in the same conditions until an OD₆₀₀ of 0.6 was reached. The bacteria were then sedimented by centrifugation at 2,500 rpm for 10 min at 4°C (Sorvall RC-5B) and resuspended in 80 ml of TB medium (10 mM Pipes, 15 mM CaCl₂, 250 mM KCl, 55 mM MnCl₂, pH 6.7 with KOH). After 10 min incubation on ice the bacterial suspension was again centrifuged as mentioned. The pellet was gently resuspended in 20 ml of TB and DMSO was added to a final concentration of 7%. The cells were aliquoted, immediately frozen in liquid nitrogen and stored at -80°C.

Transformation of *E.coli* DH5 α competent cells with the *SOLDAT8:pCambia* construct

An aliquot of *E.coli* DH5 α competent cells was defrosted on ice. Fifty μ l of competent cells were mixed with 10 μ l of the ligation product. After 10 min of incubation on ice, a heat shock was applied (40 s at 42°C). The tube was transferred back to ice and 400 μ l of LB + kanamycin (100 μ g/ml) were added. After 1 h of incubation at 37°C in the shaker (200-250 rpm), the liquid culture was spread on LB-agar plates containing kanamycin. As a positive control, cells transformed with the empty pCambia vector were used. Colonies appeared after overnight incubation at 37°C.

Verification of the transformation

To confirm the insertion of the transgene in *E.coli*, a Bakto-PCR was performed. The PCR mix was prepared as mentioned and inoculated with bacteria of an overnight culture on plate. The primers used correspond to pCambia sequences flanking the inserted gene (Table 2-1).

Amplification of the construct copies

A positive colony (containing the insert) was used to inoculate 3 ml LB-Kanamycin culture and the bacteria were grown overnight in the shaker at 37°C. The plasmid was isolated using the QIAprep® Spin Miniprep Kit as mentioned above and stored at -20°C until transformation.

Transformation of Agrobacterium tumefaciens by electroporation

Preparation of *Agrobacterium* electrocompetent cells

A stock culture of *Agrobacterium* C58C1 was defrosted on ice and 10 µl were used to inoculate 2 ml of LB containing 100 µg/ml Ampicillin and 100 µg/ml Rifampicin. After overnight culture in a shaker (200 rpm) at 28°C, the cells were transferred to 500 ml of fresh LB medium containing the antibiotics and were grown to an OD₆₀₀ of 0.5. To harvest, the culture was centrifuged for 15 min at 4°C and 5,000 rpm (Sorvall RC-5B) and the pellet was resuspended in 500 ml of 1 mM Hepes buffer pH 7.4. The cells were again centrifuged as mentioned above and the pellet was resuspended in 500 ml of the same buffer. After one more centrifugation step the pelleted cells were resuspended in 10 ml of 1 mM Hepes buffer pH 7.4 and centrifuged again. The pellet was finally resuspended in 2 ml ice-cold 10% glycerol and aliquoted. This bacterial stock was immediately frozen on liquid nitrogen and stored at -80°C.

Transformation of *Agrobacterium* with the SOLDAT8:pCambia construct by electroporation

An 80 µl aliquot of the electrocompetent *Agrobacterium* stock was thawed on ice and approx. 1 µg of the construct was added. After incubation for 3 min on ice, the mix was transferred to a precooled electroporation cuvette (0.2 cm electrode gap) and the following electroporation conditions were set on the Gene Pulser (Bio-Rad, AG, Reinach, Switzerland): 2.4 kV, 400 Ω and 30 µF. After electroporation the cuvette was immediately removed from the chamber and 1 ml of LB media was added. The suspension was transferred to an Eppendorf tube and incubated 2 h in a shaker at 28°C. The culture was spread on selective Ampicillin-Rifampicin LB-agar plates and after 48 h at 28°C colonies started to appear.

Verification of the transformation

A Bakto-PCR was performed to check the presence of the transgene in *Agrobacterium*, following the same method mentioned for the transformed *E.coli* cells. The colonies containing the construct were subcultured on liquid media and aliquots were stored at -80°C stock.

Agrobacterium-mediated transformation of Arabidopsis by floral dip (modified from Clough and Bent, 1998)

Plant growth

Arabidopsis was grown on soil under continuous light for five weeks or until bolting. The first emerging bolt was cut back to allow the proliferation of many secondary bolts. Four to six days after clipping, the plants were ready for transformation.

Agrobacterium growth

After 24 h growing in the shaker (200 rpm) at 28°C, the liquid preculture was transferred to 50 ml of the LB-medium containing antibiotics and incubated for 12 h under the same conditions. For the last subculture step, the 50 ml bacterial culture was pored on 1 l of the selective LB medium and grown until an OD₆₀₀ of 2. After 10 min of centrifugation at 5,000 rpm and 4°C, the supernatant was discarded. The pellet was resuspended in infiltration medium (4.9 g of MS with vitamins; 10% sucrose; 4 µl of 6-benzylaminopurine (10 mg/ml) and adjusted to an OD₆₀₀ of 0.8 (approx. 2 l of medium).

Transformation of Arabidopsis by floral dip

The *Agrobacterium* infiltration solution was supplemented with 500 µl of the detergent Silwet L-77 and the above-ground parts of Arabidopsis were dipped for 2-3 seconds with gentle agitation. The plants (T₀ plants) were then placed under a transparent plastic wrap film for 24 h to maintain high humidity. The T₁ seeds were collected after approx. 10 weeks.

Selection of positive transformants

T₁ seeds (seeds from T₀ plants) were vernalized and sown on MS plates supplemented with 25 µg/ml of Basta. The seedlings were grown for 10 days under continuous light and resistant seedlings were selected and transferred to soil for seed collection. Vernalized T₂ seeds were sown as described above and the percentage of resistance on MS-Basta medium per transgenic line was calculated (lines with 75% of resistant plants correspond to 1 copy of the transgene inserted). In the T₃ generation, homozygous lines with 100% resistance in MS-Basta could be selected.

2.9 *In vivo* measurements of photosynthetic activity

2.9.1 Principles of chlorophyll a fluorescence measurements

Upon illumination, chlorophyll molecules absorb light energy and transfer it to alternative pathways, leading to photochemistry, heat dissipation or the emission of fluorescence. Since these three processes occur in competition, any increase in the yield of one process will result in a decrease of the efficiency of the other two. Therefore, the yield of chlorophyll fluorescence reflects changes in photochemical efficiency and heat dissipation processes.

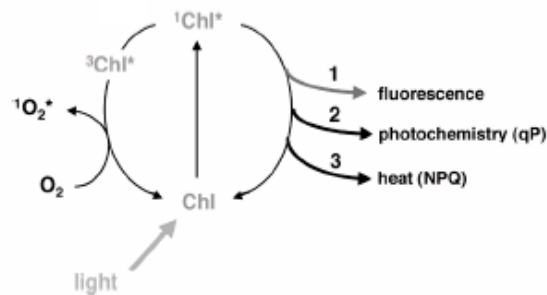


Fig. 2-2: Possible fates of excited chlorophyll (modified from Muller et al. 2001). Upon illumination chlorophyll is excited ($^1\text{Chl}^*$). From its singlet excited state it can relax back to the ground state in different ways: reemitting the light as red fluorescence (1), using the energy to drive photosynthetic reactions (2) or dissipating it as heat (3).

Fluorometers measure the kinetics of chlorophyll fluorescence changes, providing a non-invasive technique to monitor photosynthetic processes in plants.

PSII kinetics

A typical measurement is the quenching analysis of modulated fluorescence by the saturation pulse method, which provides information about the activity of Photosystem II (PSII) reaction centers *in vivo*. To study the fluorescence kinetics of PSII in *soldat8* mutants in comparison to wt, the FluorCam system (Photon Systems Instruments, Brno, Czech Republic) was used, designed for kinetically resolved fluorescence imaging of leaves and small plants. This fluorometer is equipped with a sample chamber containing a CCD video camera and an irradiation system. The data were automatically processed by a personal computer containing the FluorCam software.

The standard quenching analysis protocol provided by the FluorCam calculated automatically several fluorescence parameters as the maximum quantum efficiency of PSII and non-photochemical and photochemical quenching. The conditions of the saturation pulse method used

are shown in Fig. 2-3. Seedlings grown under continuous light were dark-adapted prior to the measurement to set all “open” (uninhibited) PSII centers into a relaxed (reduced) state. An initial illumination period with a weak and modulated measuring beam allowed measuring the ground state of fluorescence (F_0), where no electron transport occurs. Upon the application of a saturating flash, the fluorescence rises to its maximum value (F_m), which indicates the full reduction of the plastoquinone pool and Q_A , the first electron acceptor of PSII. This measurement allows the determination of the maximum quantum efficiency of PSII primary photochemistry, given by F_v / F_m . This parameter is very useful to determine the state of PSII and to estimate the extent of photoinhibition. Values lower than 0,8 indicate that a proportion of PSII reaction centers are damaged, a phenomenon often observed in plants under stress conditions

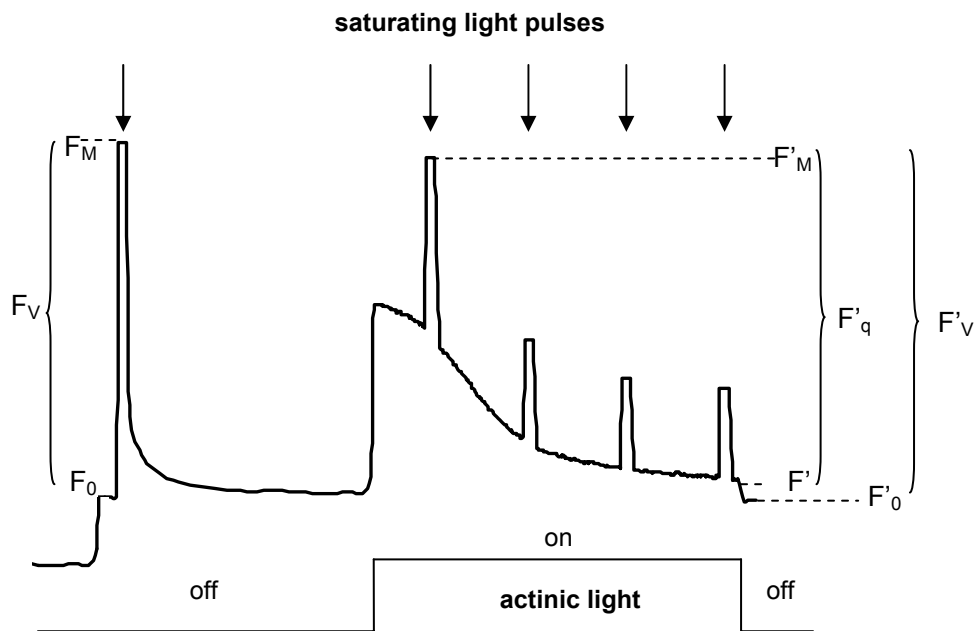


Fig. 2-3: Schematic view of a quenching analysis of modulated fluorescence by the saturation pulse method. To study the kinetics of chlorophyll fluorescence in PSII a quenching analysis was performed. The seedlings were first dark-adapted for 15 min. After applying for 2 s a weak measuring beam for 2 s to obtain the dark level of fluorescence (F_0), a first saturating pulse (0.8 s , $2000 \mu\text{mol m}^{-2} \text{ s}^{-1}$) raised the fluorescence to its maximum value (F_m). After 1 min dark relaxation, constant actinic light ($350 \mu\text{mol m}^{-2} \text{ s}^{-1}$ at 50% of intensity) was switched on and saturating pulses were applied during 1 min at intervals of 10 s. Afterwards the actinic light was switched off and the levels of fluorescence relaxed to steady-state values (F_0').

Upon the subsequent application of constant photosynthetically active illumination (actinic light), the photosynthetic apparatus passes through different transitory stages, constituting the so-called photosynthetic induction. This is accompanied by changes in chlorophyll fluorescence

yield (Kautsky and Hirsch, 1931). First a transient rise in fluorescence yield is observed, due to the lag phase between the start of electron transport, which occurs in milliseconds, and the process of carbon fixation, that has to be first activated by light. The yield of photosynthesis will increase progressively during this period until it reaches a steady state value (F').

The maximum fluorescence in the light-adapted state (F_m') can be obtained by applying saturating flashes in the presence of actinic light. This value is necessary to calculate the coefficients of photochemical (q_P) and non-photochemical (NPQ) quenching of chlorophyll fluorescence during illumination.

The parameter q_P indicates the proportion of excitation energy that is used to fuel photosynthesis and can be obtained using the following formula:

$$q_P = F_q' / F_v'$$

The NPQ value is indicative of the level of energy that can be de-excited by thermal dissipation processes. NPQ occurs at almost every light intensity and helps to regulate and protect photosynthesis when the absorbed light energy exceeds the capacity of light processing of chloroplasts. It can be formulated as follows:

$$NPQ = (F_m / F_m') - 1$$

Collectively these parameters, obtained by measuring chlorophyll fluorescence kinetics, provide considerable information about the function of the photosynthetic apparatus.

2.9.2 Light-induced changes in the PSI redox state

A pulse amplitude–modulated fluorometer (PAM101; Walz, Effeltrich, Germany) equipped with a dual wavelength emitter-detector unit, a data acquisition system (PDA-100; Walz) and a personal computer using Wincontrol version 1.72 software (Walz, Effeltrich, Germany) for data collection were used to measure and analyze *in vivo* kinetics of PSI fluorescence. Changes in PSI redox state in response to light were recorded as absorbance changes at 830 nm.

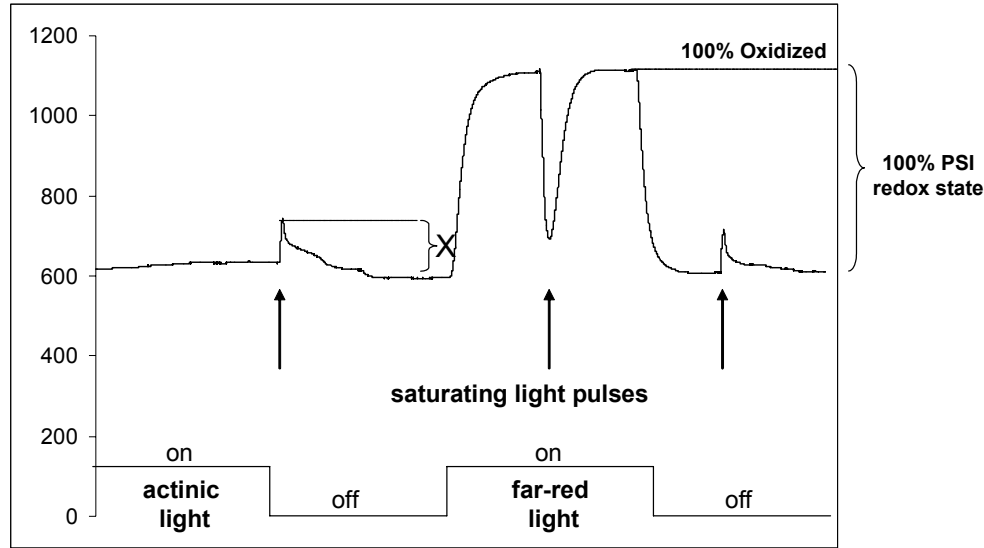


Fig. 2-4: Kinetics of a PSI *in vivo* chlorophyll fluorescence induction analysis. Under actinic illumination wt PSI is almost reduced but can be completely oxidized by far-red light. Light induced absorbance changes are indicative of PSI activity. On the y-axis fluorescence relative units are shown.

In Fig. 2-4 the procedure used for measuring PSI kinetics with PAM is shown. Actinic light ($20 \mu\text{mol m}^{-2} \text{s}^{-1}$) was first switched on for two minutes, until the fluorescence had reached a stable value. The actinic light was switched off after applying a first saturating pulse ($4000 \mu\text{mol m}^{-2} \text{s}^{-1}$). Changes in fluorescence between actinic lights on and off (X in Fig. 2-4) reflect the redox state of PSI. A value considered normal for healthy leaves is 20% of the maximum oxidation (100% redox state). The maximum oxidation state of PSI can be observed after switching on the far-red light, that specifically activates this photosystem. Once the far-red light has been turned off, fluorescence returns to a ground state level, indicating that PSI is again fully reduced. The ratio between X and the 100% oxidation value reflects the functionality of PSI.

Seedlings of *soldat8* and wt were grown under continuous light and kinetics of PSI activity changes were measured daily from the 3rd until the 10th day of development. These measurements were done in the group of Dr. J. Meurer at the Botanical Institute of the Ludwig-Maximilians University of Munich.

2.10 Other techniques

2.10.1 Microscopy techniques

Blue-light microscope

Etiolated seedlings from wt, *flu* and *soldat8/flu* were illuminated with blue light and examined under the Leica MZ12 fluorescence microscope with a Leica FM blue 10446146 filter (Leica Microsystems AG, Wetzlar, Germany). The bright red fluorescence emitted by the mutant is caused by the excitation of free Pchl_a.

Electron microscopy

Electron microscopy was performed by Dr. Martin Müller at the Electron Microscopy Center of the ETH Zürich (EMEZ).

2.10.2 The protoplast assay

To detect and characterize cell death, protoplasts from wt, *flu* and *soldat8/flu* seedlings were isolated from seedlings grown for five days under continuous light as described in Danon et al. (2005).

2.10.3 Pchl_a detection by HPLC

Wt, *flu* and *soldat8/flu* seedlings were grown for five days under continuous light. After a 15-hour dark period, thirty seedlings per sample were mechanically homogenized with a polytron (Ultra-Turrax T25, IKA Labortechnik, Staufen i. Br., Germany) in 700 µl of 90% acetone (Spectralanal; Riedel-de Haën, Seelze, Germany) containing 0.1% NH₃ (32% stock solution). After 10 min of centrifugation at maximum speed (~13,000 rpm) and 4°C, the supernatant was transferred to a fresh tube and kept at 4°C. To detect Pchl_a, a gradient high performance liquid chromatography (HPLC) system was used, equipped with a fluorescence detector (Spectra System FL3000), a degasser (Spectra System SCM400) and a quaternary gradient pump (Spectra System P4000) from Thermo Separation Products (Allschwil, Switzerland) and a reverse phase column 25C18-25QK (Interchrom, Montluçon, France). Eighty µl of sample were injected into the 50 µl-loop of the HPLC system. The following gradient was applied: 5 min 60% acetone, 20 min gradient from 60 to 100% acetone, 5 min gradient from 100 to 60% acetone. Running solutions (60% and 100% acetone) were supplemented with 50 µg/l of acetic acid. The fluorescence was measured at 630 nm using an excitation wavelength of 430 nm and Pchl_a

was quantified based on peak heights and areas calculated by a ChromJet computing integrator (Spectra-Physics, Fremont, USA).

3 Results

3.1 Characterization of the *soldat8/flu* mutant

3.1.1 Generation of second-site mutants

The homozygous *flu* mutant overaccumulates Pchl_{ide} in the dark (Meskauskiene et al., 2001). Upon transfer to light this photosensitizer reacts with molecular oxygen and gives rise to singlet oxygen. The accumulation of this reactive oxygen species triggers a signalling pathway leading to different stress phenotypes depending on the developmental stage of the plant (op den Camp et al., 2003).

In order to genetically characterize the pathway activated after the release of singlet oxygen, second-site mutants obtained by chemical mutagenesis of *flu* seeds were identified, which still overaccumulate Pchl_{ide} in the dark but no longer die after a dark-to-light shift. Two different groups could be clearly distinguished: *executer1/flu*, which behaves like wt at both the seedling and the mature plant stage (Wagner et al., 2004), and the *soldat/flu* group, in which seedling lethality is suppressed but not growth inhibition of mature plants.

After screening the phenotype of several *soldat/flu* mutants, *soldat8/flu* was chosen based on the clear suppression of cell death of seedlings that were kept under dark/light cycles.

3.1.2 The phenotype of mature *soldat8/flu* plants

Wt, *flu* and *soldat8/flu* plants were grown under continuous light until they reached the rosette leave stage. After transferring the plants to long-day conditions (16h light/8h dark) both *flu* and *soldat8/flu* stopped growing (Fig. 3-1) and developed similar necrotic lesions on the rosette leaves.

Remarkably, the growth inhibition in the *soldat8/flu* plants led to a somewhat different phenotype than in *flu*. The *flu* mutant had a characteristic bushy phenotype that was not present in the double mutant.



Fig. 3-1: Growth inhibition of *soldat8/flu* mutants. *flu* plants grown until the rosette leaf stage under continuous light, stop growing and develop necrotic lesions when they are transferred to dark/light cycles. *soldat8/flu* plants showed the same phenotype

3.1.2 The phenotype of *soldat8/flu* seedlings

The cotyledon-specific pale-green phenotype of soldat8/flu

Three- to four-day-old homozygous *soldat8/flu* mutants have pale-green cotyledons. This defect is progressively restored and cotyledons of 6-day-old seedlings are green as wt (Fig. 3-2). The two first true leaves also emerge pale-green but turn normally green within one day. Subsequently formed true leaves develop normally and are indistinguishable from wt leaves.

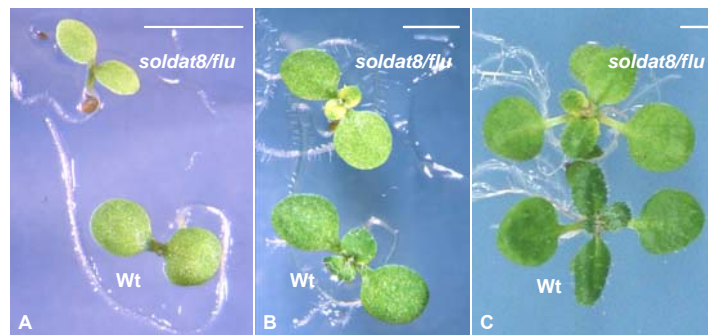


Fig. 3-2: Seedling development of *soldat8/flu* mutants. *soldat8/flu* has a defect in early development. Cotyledons emerge pale and expand slower than in wt (A). The first leaves also show a chlorophyll deficiency (B), that is later on restored (C).

Since the *flu* mutant grown under continuous light has the same phenotype as wt, we assumed that the pale-cotyledon phenotype of the double mutant is due to the *soldat8* mutation.

Accumulation of Pchlde in the dark

To test in a qualitative manner the accumulation of Pchlde, *soldat8/flu* seedlings were grown in the dark for three days. The double mutant showed similar levels of red fluorescence as *flu*, when observed under blue-light (Fig.3-3). Wt was used as a negative control that accumulated minor amounts of Pchlde in the dark, which were bound to the POR protein and upon blue light exposure did not fluoresce.



Fig. 3-3: Overaccumulation of Pchlde in *soldat8/flu*. Etiolated mutant and wt seedlings were exposed to blue light (400–450 nm), and the emitted fluorescence was imaged. Excitation of the free Pchlde present in the mutants results in the emission of bright red fluorescence.

As a quantitative approach to detect Pchlde, high performance liquid chromatography (HPLC) with a fluorescence detector was used. Pchlde was extracted and quantified by HPLC in *wt*, *flu* and *soldat8/flu* seedlings kept in the dark for 15h. The graph (Fig.3-4) shows the amounts of Pchlde. As previously reported, under these conditions *flu* accumulates 10 times more Pchlde than the *wt*. The double mutant contained approximately 60% of the Pchlde present in *flu*.

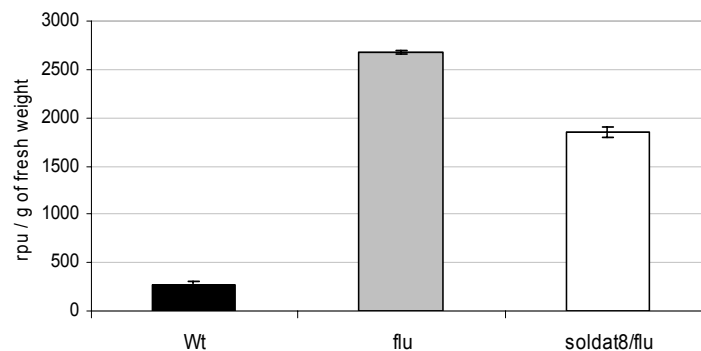


Fig. 3-4: Quantification of Pchlde content Wt, *flu* and *soldat8/flu* plants grown for 5 days under continuous light. After 15 h dark Pchlde was extracted and quantified by liquid chromatography. Pchlde is shown as relative Pchlde units (rpu) per g of fresh weight. *soldat8/flu* accumulated 6 times more Pchlde than the *wt*.

Suppression of the death response under non-permissive light/dark conditions

Seedlings of *wt*, *flu* and *soldat8/flu* were grown under dark/light cycles for five days. As shown in Fig.3-5, under these conditions *flu* seedlings collapsed and stopped growing, whereas in *soldat8/flu* the seedlings develop almost normally, except that they grow slower (more slowly?) than *wt* seedlings.

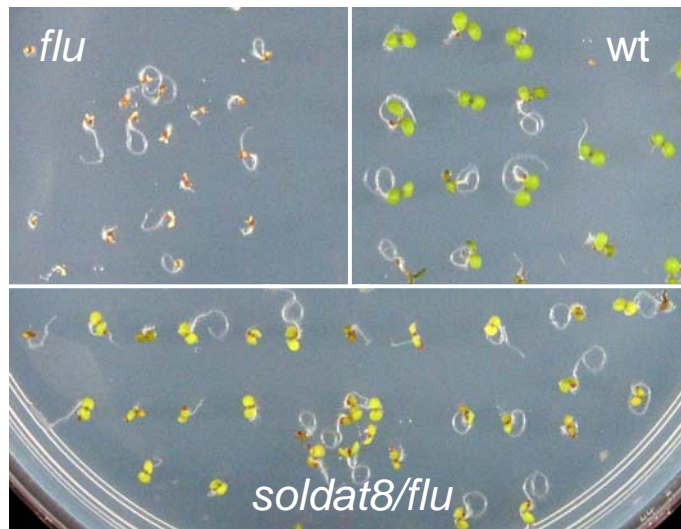


Fig. 3-5: The suppression of cell death in *soldat8/flu* seedlings grown under non-permissive long-day conditions. *Wt*, *flu* and *soldat8/flu* seedlings were grown under dark/light cycles for 5 days. The effect of the dark/light cycles on seedlings is shown in the picture: *flu* seedlings were bleached and collapsed, whereas *soldat8/flu* seedlings survived the stress.

Cell death induction was quantified by using the protoplast system as previously described (Danon et al., 2005). Protoplasts of *wt*, *flu* and *soldat8/flu* were isolated from seedlings grown for five days under continuous light after a 15-h dark period, and the percentage of dead cells was calculated 4, 8 and 24 h after reillumination (Fig. 3-6).

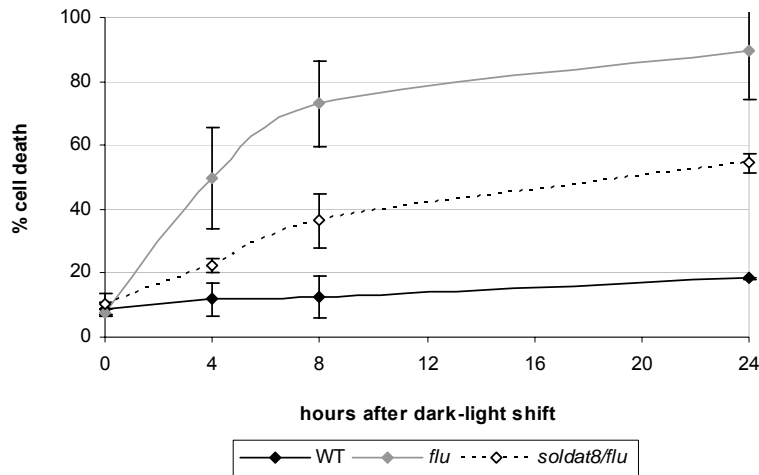


Fig. 3-6: The kinetics of cell death in protoplasts after a dark-to-light shift. Protoplasts were isolated from *wt*, *flu* and *soldat8/flu* seedlings and percentage of cell death was calculated 4, 8 and 24 hours after reillumination. *soldat8/flu* mutants show a significant decrease in cell death after reexposure to light when compared to the *flu*. The values represent the mean and standard deviations of three experiments with protoplasts extracted from approximately 500 seedlings each. A minimum of 100 protoplasts were counted per sample.

The number of dead protoplasts in *flu* increased rapidly during the first 4 hours until they reached roughly 50% of the total population. After 24 h of continuous light exposure, 80% of the *flu* protoplasts were dead. In contrast to protoplasts of *flu*, those obtained from *soldat8/flu* exhibited a significant suppression of cell death. The number of dead protoplasts of *wt* remained at a constant low level, and reflects the basal level of protoplast damage that occurs during incubation.

Singlet oxygen-mediated changes in gene expression

In previous work, genes activated after the release of singlet oxygen were identified using Affimetrix gene chips (op den Camp et al., 2003). At the rosette leaf stage, the expression of approximately 5% of the total genome changed after 30 min of reillumination (op den Camp et al., 2003). Most of these genes were similarly affected at the seedling stage (Danon et al., 2005). A set of them was used to monitor indirectly the level of activation of the signalling cascade induced by singlet oxygen in the *soldat8/flu* mutant.

Ethylene-Responsive element-binding Factors (ERFs) constitute a plant-specific class of transcription factors involved in the regulation of many developmental processes by ethylene (Riechmann and Meyerowitz 1998). *ERF5* (At5g47230) and *ERF6* (At4g17490) transcripts have been shown to peak 1 h after the dark/light shift in the *flu* mutant (Danon et al., 2005). A member of the AAA (ATPase Associated Activities) superfamily of ATPases, At3g28580, belongs also to

the group of genes induced selectively by the release of singlet oxygen in *flu* (op den Camp et al., 2003).

To assess the level of induction of these genes in the double mutant *soldat8/flu*, seedlings were first transferred to the dark for 15 h and then reexposed to light. After 1 h of illumination total RNA was extracted. Changes in transcript levels of *ERF5*, *ERF6* and *AAA ATPase* were quantified using real-time PCR (Fig. 3-7). These measurements confirmed the results of the previous work done with *flu*. The marker genes were also drastically upregulated in *soldat8/flu* but to a slightly lesser extent than in *flu*.

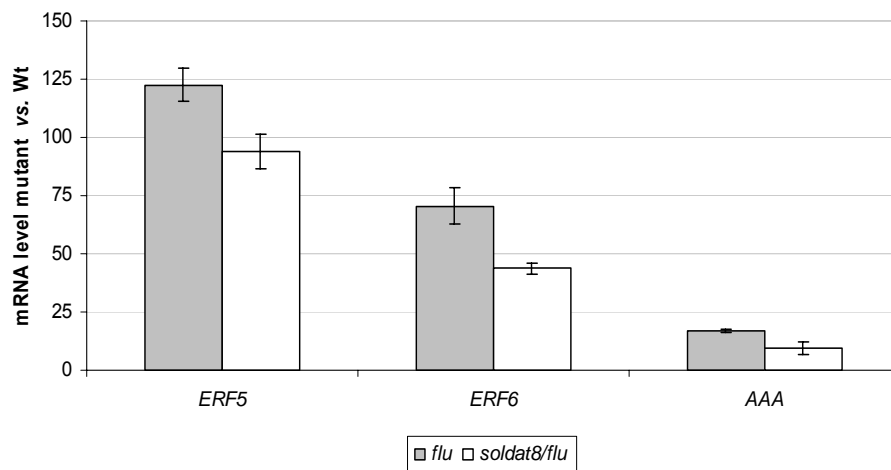


Fig. 3-7: The activation of stress genes in *soldat8/flu*. Activation of *ERF5*, *ERF6* and *AAA ATPase* mRNA accumulation occurred in *soldat8/flu* to a similar level as in the *flu* mutant. RNA from wt, *flu* and *soldat8/flu* seedlings was harvested 0 and 60 min after a dark-to-light shift. The expression levels of these genes in *flu* and *soldat8/flu* versus wt were determined by quantitative real-time PCR using the comparative delta-Ct method and normalization to the corresponding *ACTIN2* (At3g18780) levels. The values represent mean and standard deviations of two independent experiments.

3.2 Mapping of the *soldat8* locus

The *SOLDAT8* gene was identified by positional cloning. With this technique the interval containing the mutation is narrowed down by successively excluding all other parts of the genome. For this purpose genetic markers were used that are based on natural polymorphisms between different ecotypes. Once the position of these markers is determined in the genome they provide the information necessary to determine whether they are genetically linked with the mutation or not.

3.2.1 Establishment of a mapping population

In order to obtain a mapping population the *soldat8/flu* mutant ecotype *Landsberg* (Ler) was crossed with *flu* plants in *Columbia* (Col) background. The *flu* (Col) population used was obtained by backcrossing five times the original *flu* (Ler) with wild type Col.

F1 plants containing the *soldat8* mutation were allowed to self-pollinate resulting in a F2 population with a constant *flu* background and a 1:3 segregation for the mutation in the *SOLDAT8* gene.

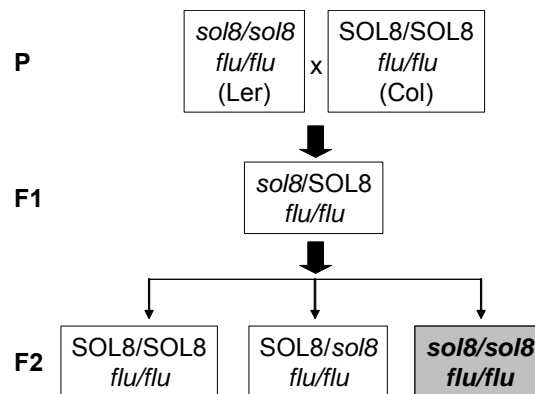


Fig. 3-8: The isolation and identification of F2 plants used for the mapping of *soldat8*. *soldat8/flu* double mutant in a Landsberg background, obtained by EMS mutagenesis in *flu* and the homozygous *flu* mutant in the Columbia background were used as parents in a cross (P). In the next generation (F1) plants were allowed to self-pollinate to obtain segregation for the *soldat8* character in the F2 generation. Double homozygous *soldat8/flu* mutants were selected and used for the mapping.

Homozygous *soldat8* F2 individuals were selected phenotypically. For the selection of double homozygous mutants (*soldat8/flu*), F2 plants were grown from the very beginning under long-day conditions. After five dark/light cycles only those plants containing the homozygous *soldat8* mutation (~25%) survived. After ten days they were transferred to soil and used for DNA extraction and seed production. In this way, a mapping population of 470 individuals was established.

3.2.2 Crude mapping

Since the cross Ler x Col is the most commonly used combination for mapping, many polymorphic markers are known that facilitate the localization of a gene of interest. For the crude mapping two types of genetic markers were used that had been previously identified and tested in our group. These were SSLP (simple sequence length polymorphism) and CAPS (cleaved

amplified polymorphic sequences) markers. The SSLP markers exploit the variability of short repetitive sequences that differ in length between the two accessions and with the CAPS markers the two ecotypes can be distinguished based on the presence or absence of polymorphic restriction sites.

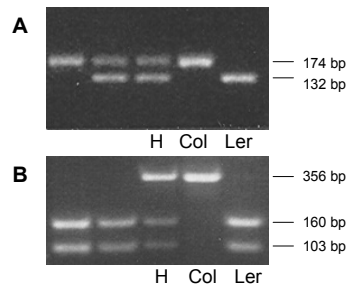


Fig. 3-9: The identification of different ecotypes. (A) Amplification with SSLP marker nga280 resulted in a fragment of 174 bp in Col and 132 bp in Ler. In heterozygotes (H) both fragments were visible. (B) Identification of Ler and Col ecotypes using the CAPS marker T2N18Trul2. After amplification the PCR products were digested with *Trul*. In Col the product remain uncut, while in Ler two bands appear. Heterozygous plants have the three fragments. The bands were resolved in a 3% (A) or 2% (B) agarose gel.

Fig.3-9 (A) shows an example of how to use SSLP markers. The difference in length of the repetitive element amplified results in a band 42 bp longer in Col than in Ler. In the heterozygous individuals both bands could be amplified. In the case of CAPS markers (Fig. 3-9 B), the fragments were cut with the restriction enzyme *Trul* after amplification. Only Ler contained the restriction site, therefore the fragment was cut into smaller fragments of 160 and 103 bp. DNA fragments from Col plants kept the original size (356 bp), since they could not be digested. In heterozygous plants a mixture of cut and uncut fragments resulted in a three-band pattern.

The following formula was used to calculate the genetic distance between each particular marker and the *SOLDAT8* gene:

$$\text{genetic distance (in cM)} = \frac{2 \times (\text{number of individuals with non-linked signal}) + \text{number of individuals with heterozygous signal}}{2 \times \text{total number of plants tested}} \times 100$$

The standard unit for genetic distances is the centimorgan (cM), which corresponds to a 1% probability of recombination between two loci. A set of chromosome-specific markers were

tested. A first round of crude mapping with a population of 120 plants placed the mutation on chromosome II, linked to the marker AthBio2b (Table 3-1). To increase the resolution of the mapping, the population was enlarged to 470 individuals and more chromosome II-specific markers were tested, which are available in The Arabidopsis Information Resource database (TAIR, www.Arabidopsis.org). T1J8 and F16M14 were the last markers that included a recombination with the mutated locus. To further increase the resolution of mapping, new primers had to be designed within the area defined by these two markers.

Table 3-1: Crude mapping: marker distances to the *SOLDAT8* locus. The genetic distance between the mutation and each marker was calculated. On a first round of mapping, a mapping population of 120 individuals was used. Later the size of the population was enlarged to 470 individuals to increase the resolution of mapping.

	Marker	calculated distance to <i>soldat8</i> locus (cM)	Chromosome
First round (120 plants)	nga63	52	I
	F19B11	40	II
	nga6	50	III
	T10P11	54	IV
	ap22	61	IV
	AthBio2b	6	II
Second round (470 plants)	nga361	4.58	II
	AlwNI	2.5	II
	T1J8	0.8	II
	F3G5	0	II
	F16M14	0.8	II
	F12L6	1.67	II
	AthBio2b	5.82	II

3.2.3 Fine mapping

A databank with all the polymorphisms found between the sequenced genomes of *Columbia* and *Landsberg* has been made publicly available by Monsanto (www.arabidopsis.org/Cereon). Based on this collection, new SSLP and CAPS markers covering the genome area containing the mutation could be identified. For this purpose, forward and reverse primers encompassing a particular polymorphism were designed (Table 3-2, sequences in Material and methods). With these markers the mapping region was reduced to a fragment of 54.9 Kb, flanked by the markers CEREON1 and T1J8 *Tru2*.

Table 3-2: Fine mapping: marker positions and distances to the *SOLDAT8* locus.

Marker	number of heterozygous plants	calculated distance to <i>soldat8</i> locus (cM)	Physical distance on CII (bp)
T1J8 (3)	2	0,2	15.492.161
CEREON1	2	0,2	15.496.911
T1J8	0	0	15.515.731
T1J8(MnlI)	0	0	15.518.081
T1J8(CaII)	0	0	15.522.540
T1J8(NlaIII2)	0	0	15.539.277
CEREON2	0	0	15.541.474
T1J8(StyI)	0	0	15.546.219
T1J8(MnlI2)	0	0	15.547.819
T1J8(TruI12)	0	0	15.551.812
T2N18(Tru1I.2)	1	0,1	15.600.486
T2N18 (4)	1	0,1	15.618.535
T2N18 (2)	1	0,1	15.631.830
T2N18 (3)	1	0,1	15.631.830
F13M22	1	0,1	15.680.913

3.2.4 Sequencing

Due to the relative small size of the genetically defined interval, a straightforward sequencing approach was carried out to identify the mutated gene. The 54.9 Kb region encompassed 13 open reading frames (ORF), according to the annotated Arabidopsis sequence available at the NCBI database (<http://ncbi.nlm.nih.gov>) (Fig.3-10).

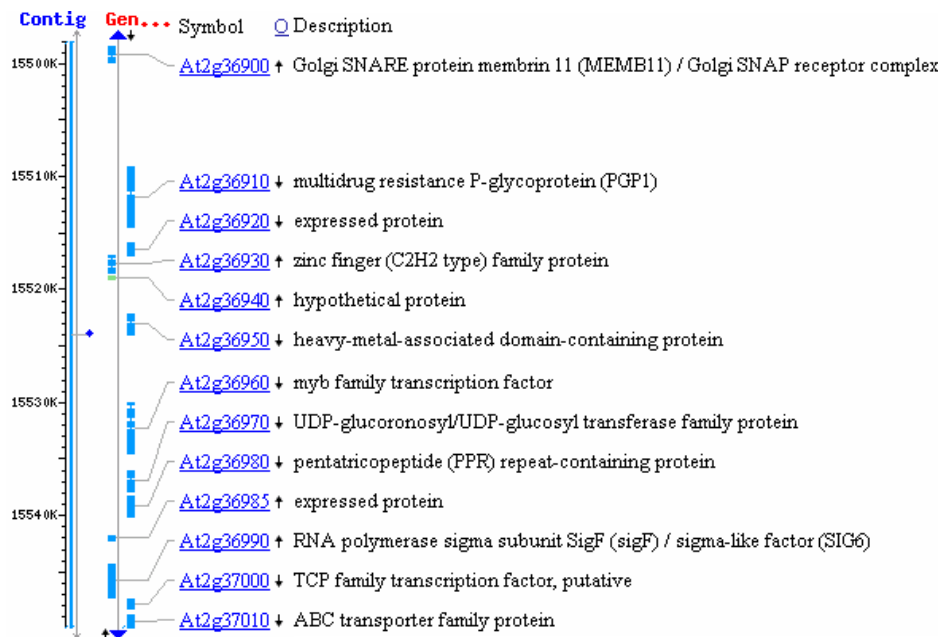


Fig. 3-10: Map Viewer display of the predicted genes in the region defined by the two last flanking markers. TAIR's Map Viewer is an integrated graphic display of each Arabidopsis chromosome that integrates genetic, physical and sequence maps.

Overlapping primers covering the full length of each predicted gene in this genomic region were designed (sequences in Material and methods). Genomic DNA of *Landsberg* and the *soldat8/flu* mutant was isolated and PCR amplification products were obtained for the selected genomic fragments. The sequences of wt and the mutant were compared after sequencing. The only nucleotide exchange in *soldat8* leading to an amino acid point mutation was found in the gene At2g36990, which encodes a chloroplast sigma factor, SIG6.

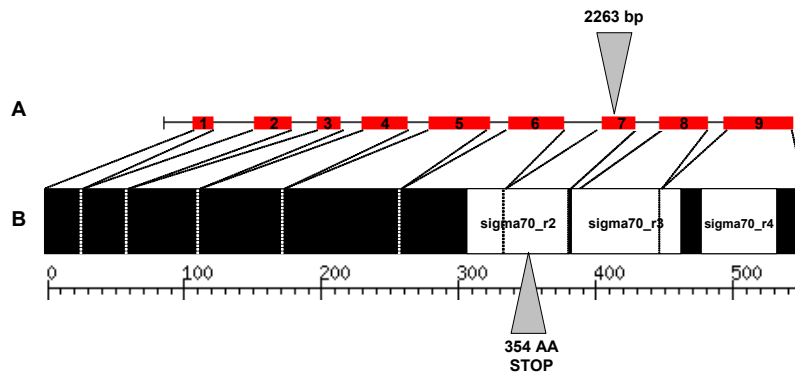


Fig. 3-11: Graphic representation of the *SOLDAT8* (*SIG6*) gene and the corresponding predicted *SIG6* protein. Arrowheads indicate the site of the nucleotide exchange in *soldat8/flu* mutant, at the seventh exon of *SOLDAT8* gene (top) and the corresponding amino acid exchange in a predicted conserved domain of the protein.

The mutant contained a thymine instead of a cytosine in the base pair number 2263 of the gene sequence, located in the seventh exon of the gene. The position corresponded to a stop codon in the amino acid position 354, which lies in the center of the sigma 70-like r2 conserved domain (Fujiwara et al., 2000), essential for the correct function of sigma factors (Ishizaki et al., 2005). Therefore we can expect that *soldat8* is a loss-of-function mutant.

3.3 Complementation

To confirm that the mutated *SOLDAT8* gene was responsible for the *soldat8/flu* phenotype a complementation assay was performed. The full-length sequence of the *SOLDAT8* gene was obtained by PCR-amplification of genomic DNA from wt plants. This genomic fragment contained the complete sequence of the gene including its native promoter. It was cloned into a pCambia vector. This binary vector confers kanamycin resistance to bacteria and Basta resistance to the plants containing it. *E. coli* competent cells were transformed with pCam:*SOLDAT8* construct and grown under optimal conditions.

To perform *Agrobacterium*-mediated transformation of *Arabidopsis*, *Agrobacterium* competent cells were electroporated and transformed with the pCam:*SOLDAT8* construct purified from the transformed *E. coli* cells. *Agrobacterium* cells carrying this construct were used to infect young flower buds of *soldat8/flu* plants.

Seeds from five *Agrobacterium*-infected plants (T₀₋₅) were plated on agar plates containing kanamycin. The seedlings resistant to the antibiotic (T₁₋₆) were transferred to soil and grown until the seeds (T₂) could be collected. The T₂ generations, coming from each of the six T₁ plants, were also tested on kanamycin. A 100%-kanamycin-resistant T₂ progeny indicated that the line was homozygous for the transgene.

Five *soldat8/flu* lines containing the wt copy of *SOLDAT8* gene were tested for complementation. Seedlings of each of these lines were grown under long-day conditions. In all of them the *flu* phenotype was restored (Fig. 3-12), the seedlings collapsed and died as the parental *flu* did. When grown under continuous light, they developed as wt and cotyledons were not pale.

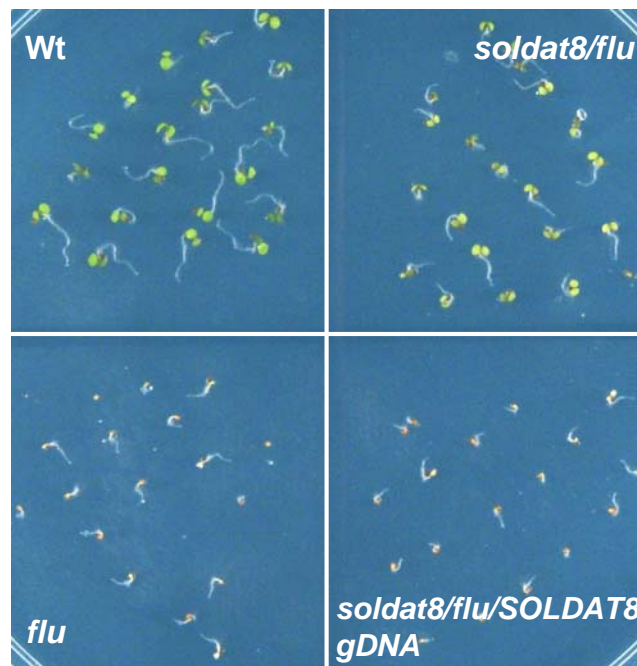


Fig. 3-12: Complementation assay. *flu* seedlings grown under dark/light cycles rapidly collapse while *soldat8/flu* survives. A wt copy of the *SOLDAT8* gene regained the original *flu* phenotype in the double mutant (I don't like it like this, I prefer as before "The double mutant containing a wt copy of the *SOLDAT8* gene rescued the original *flu* phenotype").

3.4 Characterization of the *soldat8* mutant*

3.4.1 Identification of the *soldat8* mutant

To better understand the role of SIG6 in the stress response developed by *flu* under non-permissive dark/light conditions, it was essential to identify Arabidopsis lines carrying a mutation exclusively in the *SOLDAT8* gene.

T-DNA insertional lines

According to the TAIR Germplasm Searching Engine there is no publicly available seed line with a mutation in the *SOLDAT8* gene. However, on the SIGnAL "T-DNA Express" Arabidopsis Gene Mapping Tool" (<http://signal.salk.edu/cgi-bin/tdnaexpress>), two T-DNA lines were predicted to have insertions located in the promoter region of the *SOLDAT8* gene (Fig. 3-13).

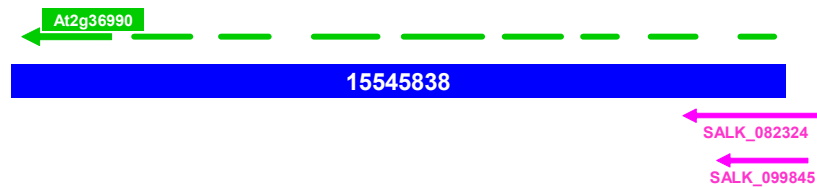


Fig. 3-13: SIGnAL graphical view of the available T-DNA insertion mutations of the *SOLDAT8* gene. Two insertional lines (in pink) were obtained from the Salk Institute Genome Analysis Laboratory (SIGnAL). In both lines the mutation was predicted to be in the promoter region. The *SOLDAT8* gene is shown in green and the two insertions are represented by pink arrows. On the blue bar the position on chromosome II is noted.

The lines were ordered from the ABRC (Arabidopsis Biological Resource Center) and analyzed to find individuals homozygous for the *SOLDAT8* T-DNA insertion. Plants containing a T-DNA insertion are kanamycin-resistant, a dominant trait. The two pools of seeds received (SALK_082324 18 seeds, SALK_099845 12 seeds) showed the 1:3 mendelian ratio (sensitive:resistant), which indicates the presence of at least one copy of the T-DNA cassette in the kanamycin-resistant plants. PCR screening revealed that none of the individuals resistant to kanamycin contained the T-DNA insertion in the *SOLDAT8* gene. This results indicated that the SALK mutant lines may have the T-DNA insertion somewhere else in the genome, but not in the *SOLDAT8* gene. Another line of evidence supporting this interpretation was the fact that

* *soldat8* designates *sigma6* mutants obtained from the backcross of *soldat8/flu* with wt. *soldat8* has two copies of the mutated form of *SOLDAT8* but they do not carry the *flu* mutation any longer.

seedlings selected on kanamycin were green as wt, whereas the homozygous *sig6* null mutant was shown to have pale-green cotyledons (Ishizaki et al., 2005).

Cross soldat8/flu x wt

As an alternative approach to find single *soldat8* mutants, the double mutant *soldat8/flu* was crossed with wt plants. The F1 progeny was grown until seed maturity and in the next generation (F2) segregation (Fig. 3-14) allowed the selection of homozygous *soldat8* individuals carrying two wt copies of the *FLU* gene (FF ss, bold in the figure).

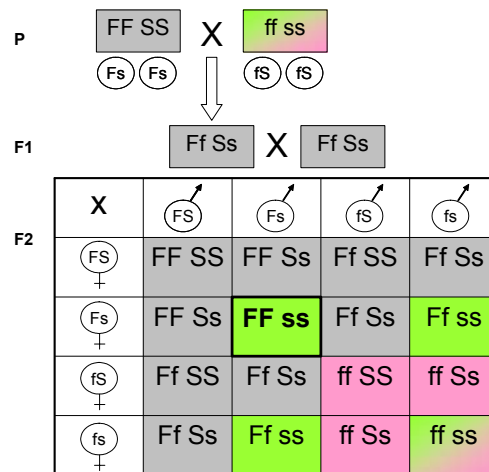


Fig. 3-14: The predicted segregation of *flu* (f) and *soldat8* (s) mutations. According to Mendel's law of independent assortment, two traits (*FLU/flu* and *SOLDAT8/soldat8*) will produce a 9:3:3:1 segregation in the F2 generation. F=wt *FLU* gene, f=mutant *Flu* gene, S=wt *SOLDAT8* gene, s=mutant *SOLDAT8* gene. Phenotypically it results in 9 wt plants (grey), 3 *flu* mutants (pink), 3 *soldat8* mutants (green) and 1 *soldat8/flu* double mutant (gradient).

To select single *soldat8* mutants without the *flu* background, the F2 generation was first phenotypically screened, selecting seedlings with pale-green cotyledons. PCR analysis was then used to confirm the presence of two mutated alleles in the *SOLDAT8* locus as well as to identify among the selected individuals those that carried two wt copies of the *FLU* gene. Point mutations in the *flu* and *soldat8* mutants can be identified by PCR if the last nucleotide (3' in the forward primer or 5' in the reverse) of one of the primers in the primer pair specific for the gene of interest corresponds to the nucleotide exchange in the mutant. Fig. 3-15 illustrates the approach used to identify homozygous *soldat8* individuals. Plants carrying two copies of the mutated *soldat8* gene could be clearly distinguished on an agarose gel, as only the primer pair containing the mutated reverse primer could amplify the specific region (Fig. 3-15 B, lane 2). All

plants preselected according to their pale-green phenotype carried the *soldat8* nucleotide exchange.

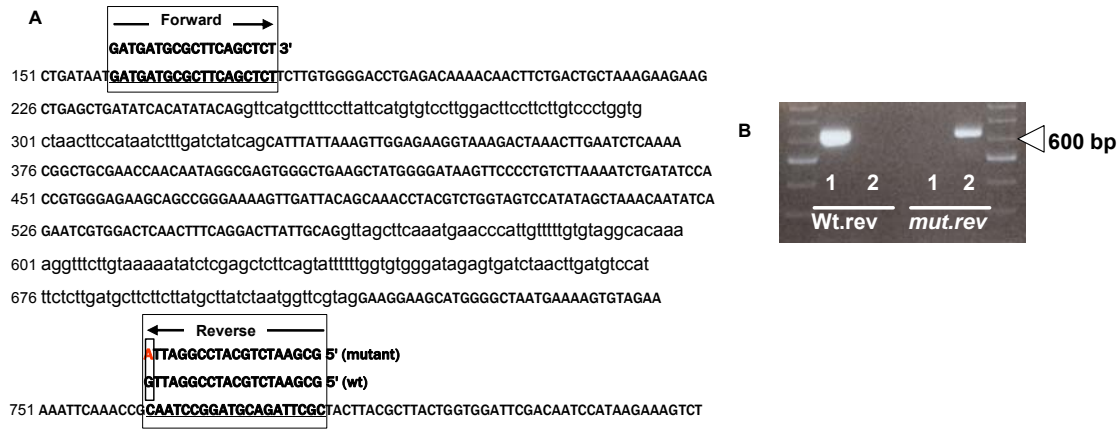


Fig. 3-15: The selection of homozygous *soldat8* single mutants by PCR analysis. In (A) the region of the *SOLDAT8* gene amplified by the specific primers is shown. To distinguish between mutant and wt plants, PCR was performed with two different primer combinations: forward + reverse (wt) or forward + reverse (mutant). The gel (B) revealed the identity of each individual tested: wt plants (1) generated a band of the expected size with the combination of forward + reverse (wt) primers, whereas no band appeared when the mutant version of the reverse primer was used. In the case of *soldat8* homozygous mutant (2) only the combination forward + reverse (mutant) produced a band on the gel. Heterozygous plants showed a band in both primer pair combinations.

Specific primers were designed in the same way for the *flu* mutation and a similar screen was performed among the F2 progeny to discard all individuals carrying a copy of the mutated *flu* gene.

All *soldat8* homozygous plants were grown until maturity and the seeds of each individual line were sown to select a homogeneous line with the clearest phenotype. This line (hereafter *soldat8*) was used to perform all the experiments characterizing the single *soldat8* mutant.

3.4.2 The *soldat8* phenotype

When grown under continuous light, *soldat8* mutants are indistinguishable from *soldat8/flu* mutants. They show the cotyledon-specific pale-green phenotype at the seedling stage but later, when they reach maturity, they become indistinguishable from wt. The growth and bolting (Fig. 3-16) were used to compare the development of the mutant and wt in a quantitative manner. For both parameters the mutant did not differ from the wt, indicating that the lack of SIG6 does not affect the development of mature plants.

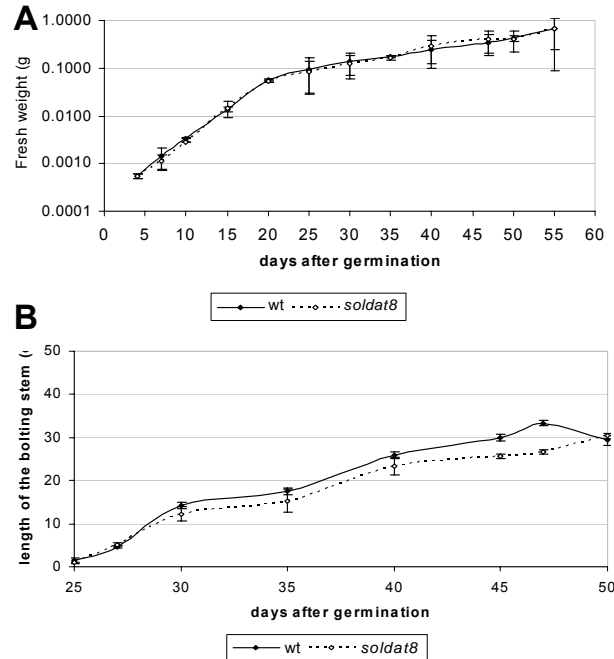


Fig. 3-16: Changes in the growth (A) and the length of the bolting stem (B) in the *soldat8* mutant compared to wt. Plants were grown on soil under continuous light conditions. Each value represents the mean and standard deviation from measurements taken on ten individuals. The growth was measured as fresh weight and the elongation of the primary caulinar stem was expressed in centimeters. Wt is shown as a solid line and the dashed line represents *soldat8*.

The main difference between *soldat8* mutant and *soldat8/flu* is that the former does not overaccumulate Pchl_a in the dark (Fig. 3-17), since the FLU protein is functional, acting as a negative regulator of chlorophyll biosynthesis in the dark.

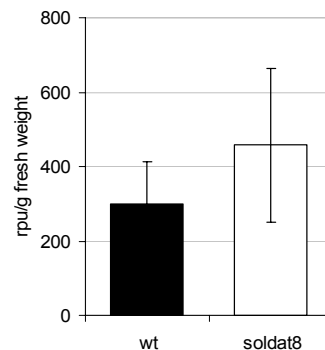


Fig. 3-17: Pchl_a accumulation in wt and *soldat8* seedlings after a 15 h dark period. Pchl_a is shown as relative Pchl_a units (rpu) per g of fresh weight. There is no significant difference in the amount of Pchl_a between the mutant and the wt.

Chloroplast development

Electron micrographs of chloroplasts from wt and *soldat8* were compared to investigate, whether the cotyledon pale phenotype was related to a defect in chloroplast development (Fig. 3-18). Indeed, cotyledons of 4-day-old light-grown seedlings of *soldat8* contained smaller plastids with markedly reduced thylakoid membranes than the wt. The size and membrane appearance of wt plastids, however, was restored in 10-day old-seedlings of the mutant. The number of chloroplasts was not affected by the *soldat8* mutation.

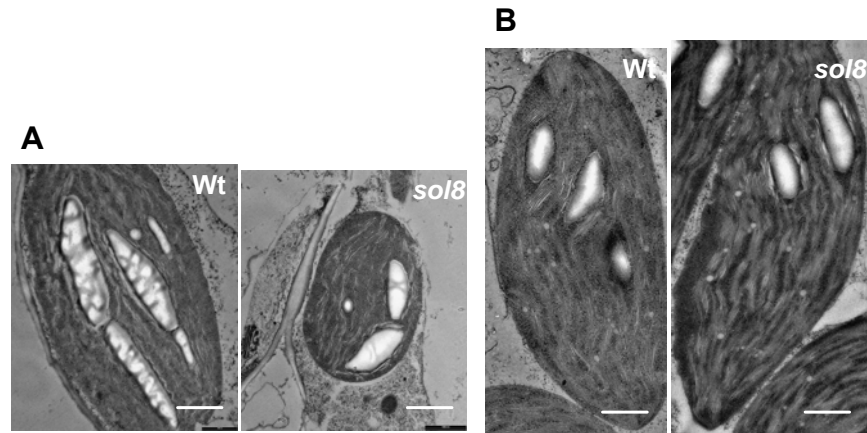


Fig. 3-18: Electron microscopy of plastids in *soldat8* and wt. The two images on the left (A) were obtained from 4-day-old seedlings. (B) shows the chloroplasts of 10-day-old seedlings. White bars represent 1 μ m.

3.4.3 Analysis of gene expression in the *soldat8* mutant

Expression of SOLDAT8

Analysis of *SOLDAT8* transcript levels by quantitative RT-PCR showed that the gene is not fully silent in the mutant. Different primer pairs were tested that correspond to different regions of the gene (see sequencing primers in Material and methods), and both the mutant and wt were found to accumulate transcripts of *SOLDAT8*. The amounts of transcripts accumulated by *soldat8* were in all cases significantly reduced relative to wt plants. With all the primer combinations similar values were obtained, thus Fig. 3-19 depicts only the results of one of them.

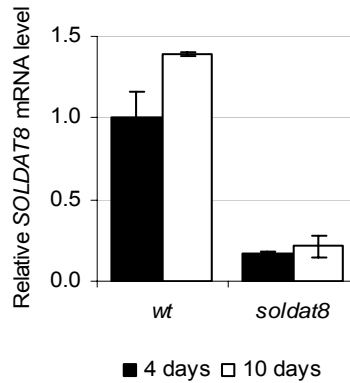


Fig. 3-19: The level of expression of the *SOLDAT8* gene in *soldat8* and *wt* in 4- and 10-day-old seedlings. RT-real time-PCR was performed with a primer pair amplifying a fragment of 600 bp, which included the point mutation.

In principle, a single nucleotide exchange, as is the case in *soldat8*, does not necessarily affect the length or amount of mRNA that accumulates. Nevertheless, it has been shown that particular genes mutated with EMS accumulated lower transcript levels than the *wt* (Li and Chory, 1997; Davis et al., 1999), but the mechanisms underlying this regulation are still unknown.

In order to analyze the kinetics of *SOLDAT8* expression during the development of Arabidopsis wild type, RNA obtained from plants at different developmental stages was reverse transcribed and quantitative PCR was performed. Fig. 3-20 shows that *SOLDAT8* is expressed already 24h after sowing, when germination had started. A low level of expression is maintained during the second day of development but in 3-day-old seedlings an increase in transcript level is observed, coinciding with the greening of cotyledons. *SOLDAT8* transcript levels reach a peak during the following 24 h (4-day-old), while the cotyledons expand. Later on, the amounts of *SOLDAT8* transcripts decrease again and the levels remain constant during the rosette-leave stage before (15 d) or after (25 d) bolting.

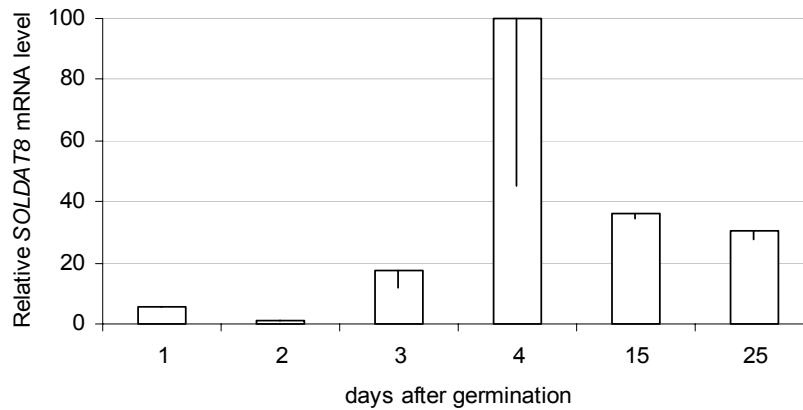


Fig. 3-20: The level of expression of the *SOLDAT8* gene during seedling development. RNA was extracted from 1- to 4-day-old wt seedlings and from 15- and 25-day-old rosette leaf plants. RT-real time-PCR was performed with *SOLDAT8*-specific primers. The level of expression is measured as the ratio between detected *SOLDAT8* transcripts and total amount of extracted RNA.

Expression of other sigma factors in the soldat8 mutant

SIG6 belongs to a family of sigma 70-like factors in plants with 6 members in Arabidopsis (AtSIG1-6) (Isono et al., 1997; Tanaka et al., 1997; Fujiwara et al., 2000; Hakimi et al., 2000). Sigma factors are nuclear-encoded proteins proposed to regulate promoter selectivity of the plastid-encoded polymerase in the chloroplasts of higher plants (Allison, 2000) in response to different developmental and environmental cues. SIG6 has been shown to act as a major general sigma factor in chloroplasts during early plant development (Ishizaki et al., 2005).

Both the T-DNA insertional mutant *sig6* (Ishizaki et al., 2005) and *soldat8*, which was obtained by EMS mutagenesis, are impaired in early cotyledon development due to the lack of the SIG6 protein, but restore a wt-like phenotype in older seedlings. In order to exclude the possibility that another sigma factor took over the function of SIG6 in the later stage, the transcript levels of the different Arabidopsis sigma factors were quantified by real-time PCR in 4- and 10-day-old seedlings.

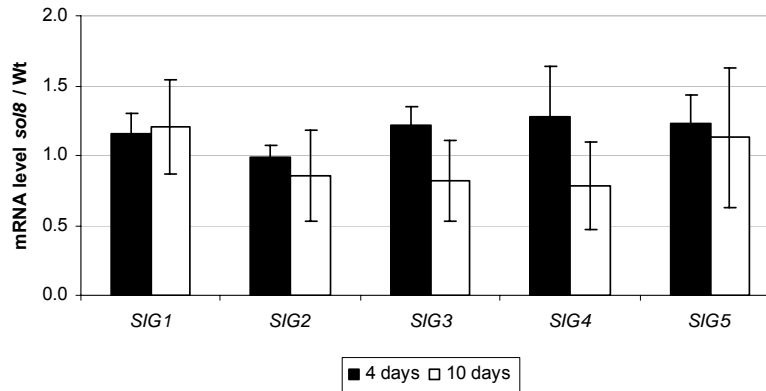


Fig. 3-21: The expression level of 5 SIG genes in *soldat8* versus wt. Genes encoding the different sigma factors 1 to 5 in Arabidopsis were transcribed to similar levels in seedlings from *soldat8* and wt. The cDNA obtained from 4- and 10-day-old seedlings was amplified by quantitative PCR using specific primers for the various SIG genes. The chart shows the levels of expression for each SIG gene in *soldat8* relative to that in wt at two different stages of seedling development.

As shown in Fig. 3-21, a transcriptional upregulation of any of the members of the SIG family does not occur during the transition to the wt phenotype. This could suggest the involvement of additional regulatory mechanisms in this recovery process that might compensate for the absence of SIG6.

Chloroplast gene expression

Chloroplast array

To analyze the effects of the lack of SIG6 on global plastid gene expression, a DNA array containing 94 genes encoded by the chloroplast genome of Arabidopsis was used. RNA was extracted from 4- and 10-day-old seedlings of *soldat8* and wt. Labeled cDNA obtained by reverse transcription was hybridized against the nylon filter arrays and the radioactive signals were analyzed.

Three different dilutions of cDNAs from each of the genes analyzed were spotted on the filter in duplicates. The drawing on the right shows schematically the distribution of duplicates for a gene. Black circles represent the minimum dilution factor, grey circles intermediate dilution and white circles maximum dilution of cDNA from a particular gene spotted onto the membrane.

Triplicate cDNA samples corresponding to each of the four conditions analyzed were hybridized. Fig. 3-22 shows one of the hybridized arrays per condition (4-day-old and 10-day-old wt and

soldat8). The signal corresponding to each of the 94 plastid genes analyzed were clearly distinguishable on each membrane.

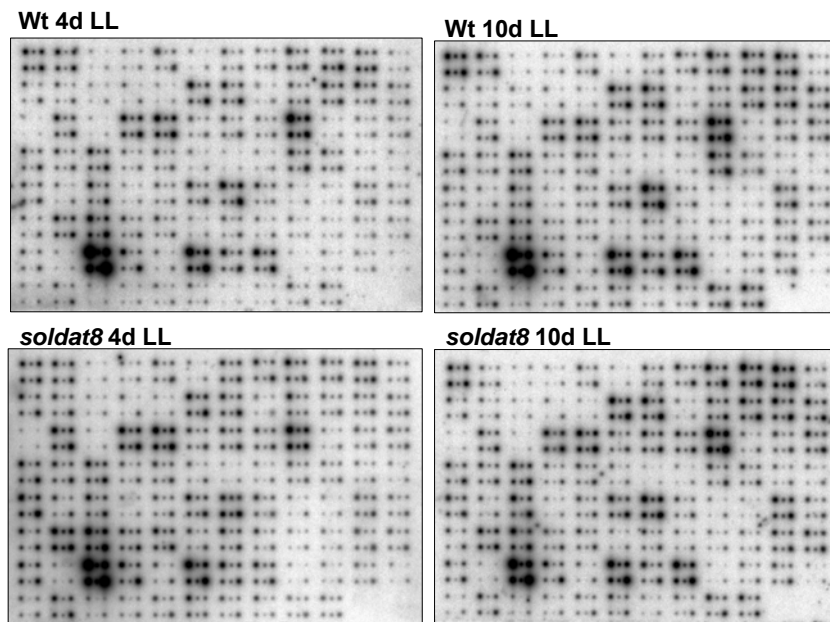


Fig. 3-22: Autorradiograms of chloroplast DNA arrays hybridized with *soldat8* and wt cDNA samples. RNA extracted from wt and *soldat8* seedlings (4- and 10-days-old) was reverse transcribed into cDNA, using radioactively labeled dCTP. The labeled cDNA was hybridized onto nylon membranes, which contained cDNAs corresponding to 94 plastid genes. The radioactive signals were detected using a phosphoimager.

Intensities of duplicate spots representing the same gene were averaged. The charts below show plastid gene expression of *soldat8* versus wt of 4- (Fig. 3-23 A) and 10-day old seedlings (Fig. 3-23 B). No dramatic differences in transcript levels could be observed in the mutant. Only three genes were significantly upregulated: *NDHC* ($2,75 \pm 0,06$) and *RPL20* ($2,72 \pm 0,05$) in 4-day-old seedlings and *TRNP* ($2,59 \pm 0,23$) in 10-day-old seedlings (description in Table 3-3).

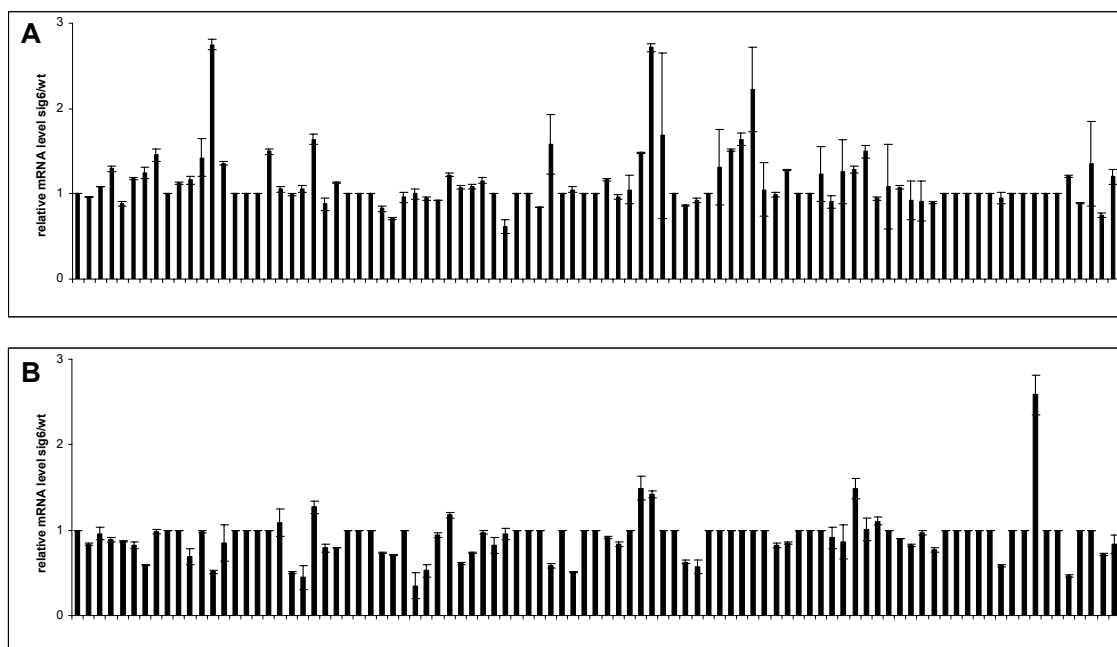


Fig. 3-23: The levels of expression of different chloroplast genes in *soldat8* relative to wt. A macroarray of the entire plastid chromosome was used to quantify the transcript steady-state of different plastid genes in seedlings of *soldat8* and wt at the 4th (A) and 10th (B) day of development. Intensities of duplicate spots representing the same gene were averaged and analyzed as percentages of the total signal on the array after subtracting the background. For normalization the transcription level of plastid 16S rRNA (*RRN16*) was used.

In order to exclude the possibility that a limit in sensitivity of the software used for quantification was the reason for such minor changes, an alternative approach was applied to assess the plastid transcription profile in the mutant in a more quantitative manner.

Table 3-3: Description of some relevant chloroplastic genes

ACCD	AtCG00500	carboxytransferase beta subunit
CLPP	AtCG00670	caseinolytic protease
NDHC	AtCG00440	NADH dehydrogenase D3 subunit of the chloroplast NAD(P)H dehydrogenase complex
RPL20	AtCG00660	chloroplast ribosomal protein L20, constituent of the large subunit of the ribosomal complex
RPOB	AtCG00190	Chloroplast DNA-dependent RNA polymerase B subunit
RPOC1	AtCG00180	RNA polymerase beta' subunit-1
TRNP	AtCG00620	Chloroplast-encoded proline-accepting tRNA.
YCF2.1	AtCG00860	hypothetical protein
YCF2.2	AtCG01280	hypothetical protein

Real-time PCR

The level of expression of 24 plastid genes previously analyzed with the chloroplast array were tested by real-time PCR using the same primers. Some of these genes had been previously shown to be up- or downregulated in the *sig6* mutant (Ishizaki et al., 2005). The results of the PCR analysis confirmed part of the array data (Fig. 3-24). Again, no gene showed a lower expression level in *soldat8* than the wt. Some genes that seemed to be slightly upregulated on the array (~2 fold) in 4-day-old mutant seedlings (*RPOB*, *RPOC*, *YCF2.1*) were clearly induced when analyzed by real-time PCR (2 to 8 fold, see Fig.3-24). Additional transcripts of two new genes, *ACCD* and *CLPP*, were detected in higher amounts in 4-day-old seedlings of *soldat8* but not in wt (description in Table 3-3).

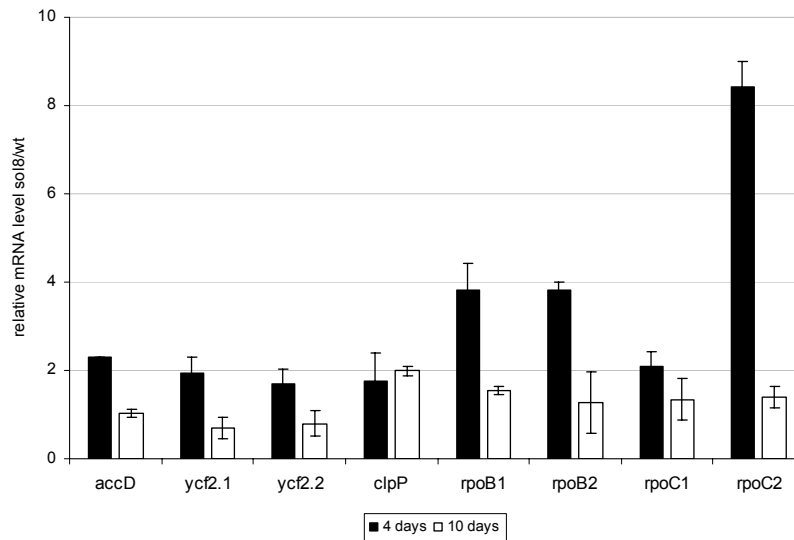


Fig. 3-24: Analysis of plastid gene expression by real-time PCR comparing *soldat8* and wt at two stages of seedling development. The same RNA samples used to perform the array experiment were used for the PCR analysis. Primers specific for 24 different chloroplast genes were used. Only those genes showing a clear difference in expression level between the mutant and wt are shown. A total of 8 genes were upregulated in *soldat8* 4-day-old seedlings (black bars) relative to wt. Older seedlings contained similar levels of transcript as the wt (white bars).

Interestingly, all the transcripts upregulated in the mutant in the early seedling stage represent genes transcribed by the nuclear-encoded polymerases (NEP). This pattern has been observed also in plastid encoded polymerase (PEP)-deficient mutants (Legen et al., 2002) and *sigma2* knockouts (Nagashima et al., 2004b).

3.4.4 Analysis of the protein content of the *soldat8* mutant

Total protein fractions were extracted from 4- and 10-day-old mutant and wt seedlings, respectively, and separated electrophoretically on an SDS-PAGE. Several of the plastid proteins in these samples were detected by western blot using a variety of specific antibodies. The proteins chosen for analysis represent different photosynthetic complexes located in the thylakoid membrane.

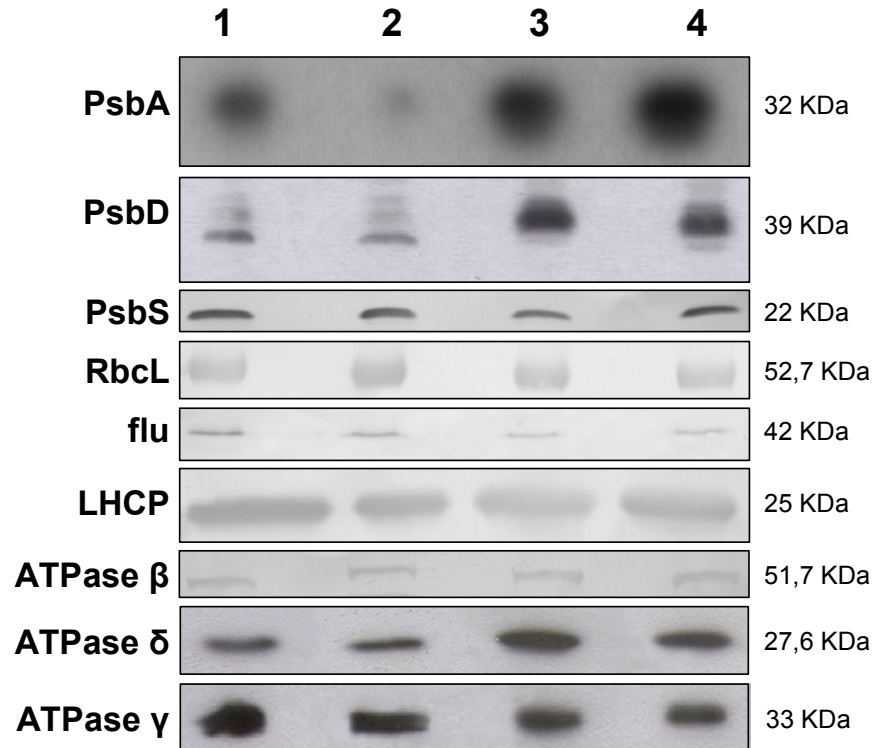


Fig. 3-25: Immunoblot analysis of chloroplast proteins. *soldat8* and wt seedlings were grown under continuous light for 4 days (1: wt, 2: *soldat8*) and 10 days (3: wt, 4: *soldat8*). Protein extracts were run on an SDS-PAGE gel and electroblotted onto a PVDF membrane. The proteins were incubated with specific antibodies and the immunoreactive bands could be detected with horseradish peroxidase or alkaline phosphatase.

The only protein that did not accumulate to similar amounts in *soldat8* and the wt was D1 (PsbA antibody, Fig. 3-25). The level of D1 was significantly reduced in 4-day-old mutant seedlings. In older *soldat8* seedlings no difference in D1 accumulation between mutant and wt was apparent. D1 is one of the core proteins of PSII core complex, important for photosynthetic electron transport and photoprotection.

3.4.5 *In vivo* measurements of photosynthetic activity

Effects of the soldat8 mutation on chlorophyll fluorescence induction

F_v / F_m

The kinetics of chlorophyll fluorescence induction were measured in wt and *soldat8* plants by performing a quenching analysis with an imaging fluorometer to assess *in vivo* the functional state of PSII in the mutant. Seedlings grown on agar plates under continuous light were used for the measurements at different developmental stages (3- to 7-days-old).

The ratio of variable to maximum fluorescence (F_v / F_m), indicative of the potential capacity of PSII, was reduced in 3-days-old *soldat8* seedlings to 0.54 ± 0.004 down from 0.86 ± 0.009 in wt (Fig. 3-26). This behavior is typical for mutants with an impairment in D1. However, a progressive increase of the value could be observed during the following days of development in the mutant. Five-day-old seedlings showed F_v / F_m near 0.8, suggesting that PSII could recover and reach functionality as the plants became more mature.

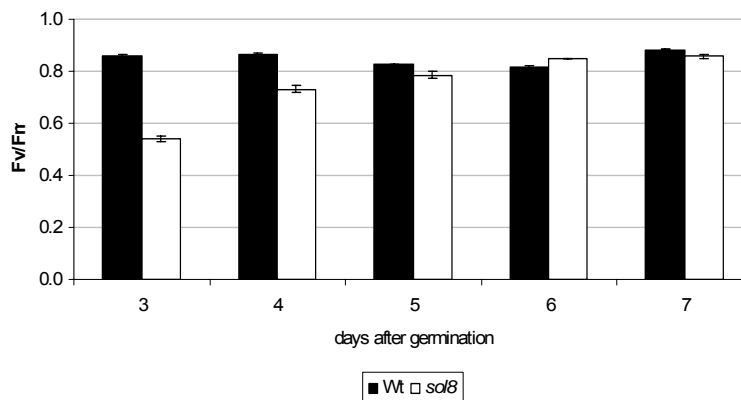


Fig. 3-26: Changes of F_v / F_m values during seedling development in *soldat8* and wt. A quenching analysis of modulated fluorescence by the saturation pulse method was performed with 3- to 7-day old seedlings. The software provided by the FluorCam calculated automatically the F_v / F_m values (relative fluorescence units). Black bars represent wt seedlings and open bars correspond to the mutant.

The charts showing the kinetics of fluorescence emission during the measurement (Fig. 3-27) enabled us to define more precisely reasons for the differences in F_v / F_m values between *soldat8* and wt at a very early seedling stage. Maximum fluorescence values (F_m) were similar in both the mutant and wt after a saturating pulse of light. The lower F_v / F_m value in the 3-days-old *soldat8* is caused by a higher ground fluorescence value (F_0) compared to the wt. F_0 , the so-

called “dark fluorescence” is a measure of the fluorescence excited by a weak beam that is not sufficient to reduce Q_A , the primary electron acceptor of PSII reaction center.

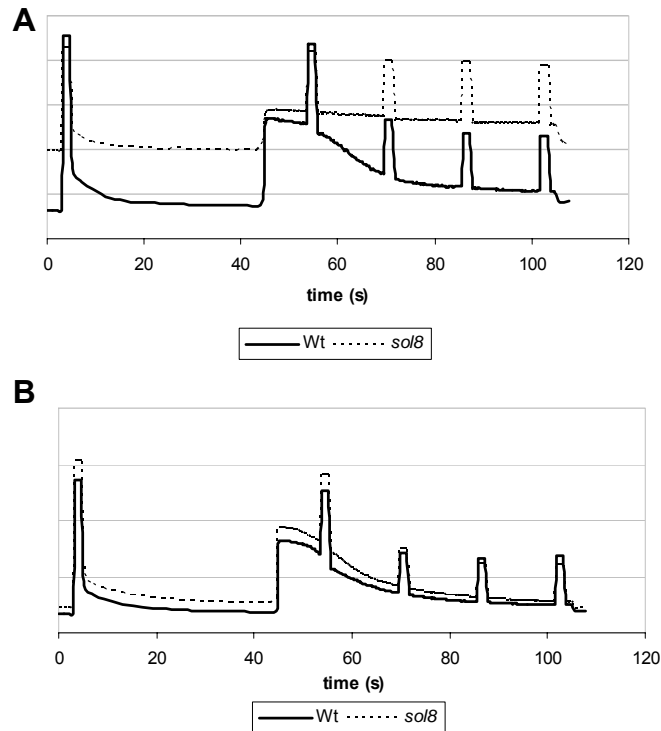


Fig. 3-27: Kinetics of the chlorophyll fluorescence induction during a saturation pulse analysis. The measurement was done with wt and *soldat8* seedlings grown under continuous light from the 3rd until the 7th day of development. The chart shows the kinetics at the 3rd (A) and 7th (B) day of development. Wt values are shown with a solid line and the dashed lines represent *soldat8* values. The y-axis represents relative fluorescence.

Higher F_0 values have been observed as a result of PSII damage in several plant species (Armond et al., 1980) and this could be the case also in *soldat8*, which has reduced amounts of D1 protein.

Photochemical and non-photochemical quenching

Photochemical quenching (qP) (Fig. 3-28 A) was slightly reduced in *soldat8* during the first days of development in comparison to wt, suggesting a lower electron flux directed to photochemistry in the mutant. Already at the 4th day the values were similar to those of the wt, indicative of a quick recovery to the normal yield of photosynthesis.

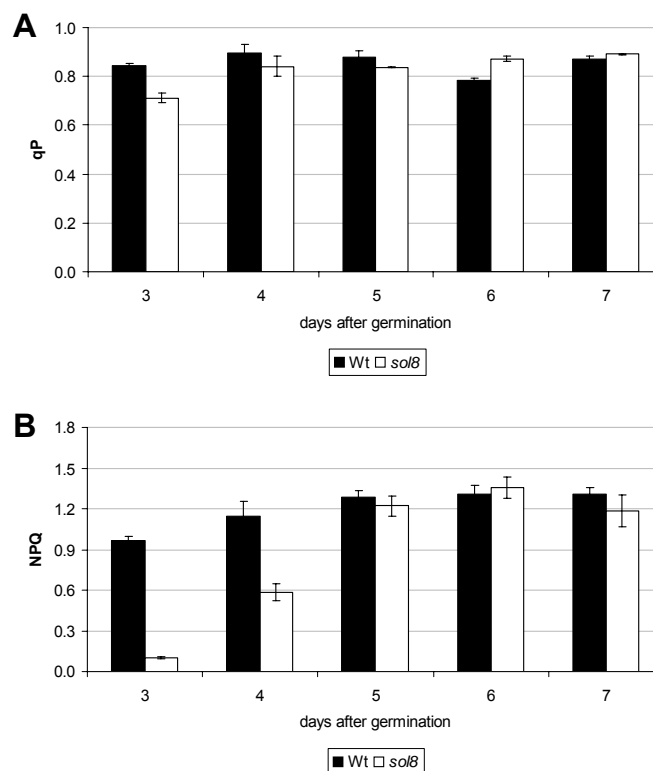


Fig. 3-28: Photochemical and non-photochemical quenching during seedling development in *sol8* and wt. (A) Photochemical (qP) and (B) non-photochemical (NPQ) coefficients calculated by the FluorCam software with data from the same quenching analysis shown in Fig. 3-26. Black bars represent wt seedlings and open bars correspond to the mutant.

NPQ was strongly impaired in 3- and 4-day-old seedlings of *sol8* (Fig. 3-28 B), but later reached wt levels. In the mutant, the lower NPQ is the result of an increased F_m' (Fig. 3-27), which is the maximum fluorescence value after a saturating pulse, when the actinic light is on. The series of saturating pulses applied during the light phase of the quenching analysis (see Fig. 2-3 in Material and Methods) represent an excess of excitation energy for the wt plants, that rapidly activate NPQ processes to dissipate the excess of light energy as heat. In wt this is observed as a progressive decrease of the ground fluorescence value (F') in the actinic light phase, that will finally reach a low standby value (Fig. 3-27). Conversely, 4-day-old mutant seedlings exhibited diminished suppression of the minimum fluorescence yield in the light (F'), suggesting an altered threshold of the response to light stress in the mutant.

The effect of light on the PSI redox state in young seedlings of soldat8

The previous measurements indicated a defect in the photosynthetic electron transport at PSII in *soldat8*. Further fluorescence analysis was performed to determine, whether the mutation affected also photosynthesis at Photosystem I (PSI). PSI catalyzes the light-induced charge translocation process initiated at PSII. Light-induced changes of the PSI redox state were recorded by absorbance changes at 830 nm using a pulse amplitude–modulated fluorometer.

Absorbance changes of PSI at 830 nm after light/dark switches during the induction by far-red light or after application of strong white light pulses in a far-red light background were close to the limit of detection in 4-day-old mutant seedlings, even when the measuring unit was adjusted to its highest sensitivity (Fig. 3-29). This indicated that PSI complexes were either not functional or missing in *soldat8* at this early stage. Ten-day-old mutant seedlings, however, had similar PSI kinetics as the wt, indicating a recovery of the activity of the photosynthetic electron chain.

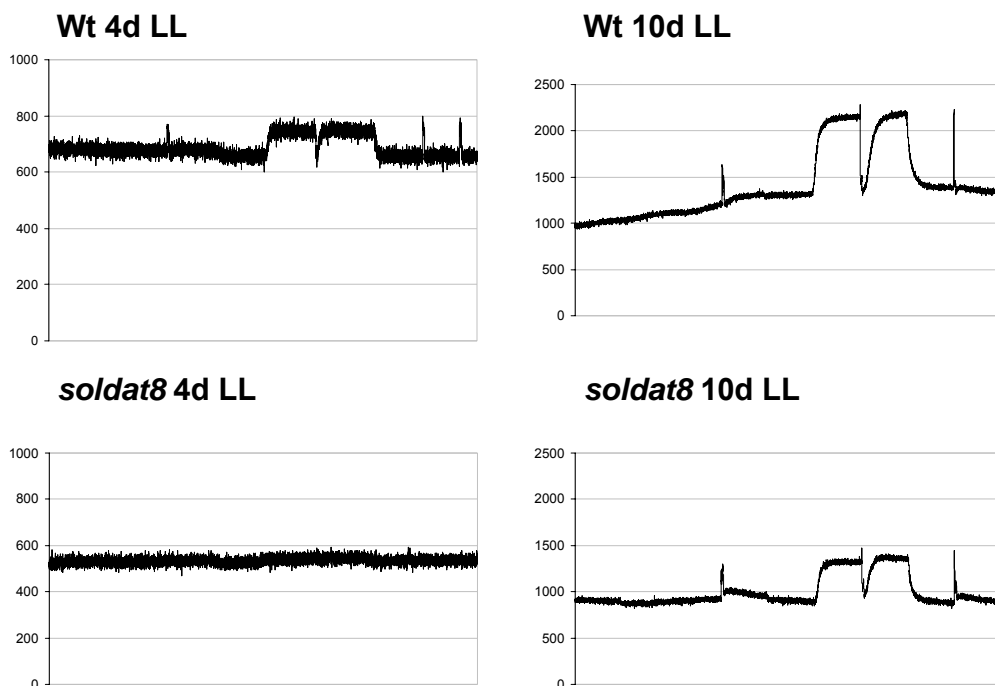


Fig. 3-29: PSI redox kinetics of *soldat8* and wt plants. Under illumination, wt PSI was almost fully reduced, but could be completely oxidized by far-red light. The low signal-to-noise ratio in the 4-day-old *soldat8* did not allow the quantification of PSI redox kinetics. The effect of PSI redox changes in older mutant seedlings were detectable, reaching redox values similar to those of wt. The y-axis represents relative fluorescence units.

3.4.6 The effect of high light stress

Singlet oxygen is produced during photosynthesis in plants and PSII is thought to be the main production site (Krieger-Liszkay, 2005). Even though this non-radical reactive oxygen species has been shown to be produced already under conditions, of no apparent stress (Keren et al., 1995), certain stress situations are known to enhance significantly the production of singlet oxygen. In addition to using the *flu* system (op den Camp et al., 2003), also high light stress has been shown to set off singlet oxygen generation in leaves (Hideg et al., 1998; Fryer et al., 2002). To gain insight into the role of SIG6 in the singlet-oxygen-induced signalling pathway, the effect of the *soldat8* mutation was tested under high light conditions.

Above a certain threshold, the toxic effects of singlet oxygen mask its signalling role in the cell, causing irreversible damages that can lead to necrosis (Wagner et al., 2004). Therefore, conditions had to be optimized to analyze the genetically determined cell death and to avoid necrosis caused by the cytotoxicity of singlet oxygen. High light induced a rapid non-necrotic cell death response in wt seedlings, similar to the cell death in young *flu* seedlings after a dark-to-light shift. In Fig. 3-30 the experimental set-up is shown. After growing the plants for six days under continuous low light ($10 \mu\text{mol m}^{-2} \text{s}^{-1}$) at 21°C , light was switched off and the chamber was cooled down to 4°C for 4 h, in order to maximize the sensitivity of seedlings to the following light stress. Afterwards, light was switched on that had been adjusted to $250 \mu\text{mol m}^{-2} \text{s}^{-1}$ (hereafter named high light) and the temperature was kept low, to ensure photoinhibition. It is well documented that decreased temperatures intensify photoinhibition in higher plants (Aro et al., 1990; Greer, 1990; Foyer et al., 1994; Long et al., 1994) due to a reduced rate, at which the quenching of PSII develops.

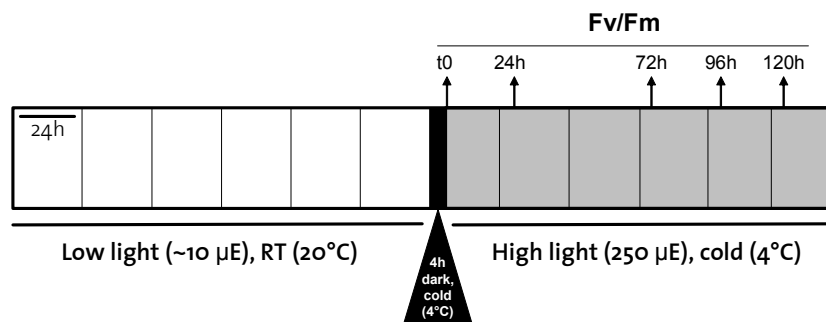


Fig. 3-30: Experimental design of the high light stress experiment. Seedlings were grown for six days under low light and after 4h of dark at 4°C the light intensity was increased 10 fold relative to the initial light intensity. Fluorescence measurements were done at different time points (F_v / F_m) during the photoinhibitory stress period.

The reactions ranging from F_v / F_m values of 0.8 to 0.9 for non-stressed plants down to 0 for fully bleached seedlings were divided into seven subgroups (Fig. 3-31 B). At the beginning of the combined low temperature/high light stress, both mutant and wt seedlings, not stressed yet, were placed in the categories of 0.75 to 0.85 and 0.85 to 0.95, with the mutants being slightly shifted towards the group of 0.75 to 0.85. After 24 h of stress all plants suffered from severe photoinhibition. Wt seedlings however, were clearly more affected than mutant plants. This higher susceptibility of wt to stress became even more obvious after 72 and 96 h of light stress. After 96 h almost all of the wt seedlings were bleached, whereas mutant seedlings were still green and maintained F_v / F_m values similar to those after 24 h of light stress (Fig. 3-31 A). This difference could be due to the activation of an acclimatory response in the mutant, if light acts as a stress factor for *soldat8* mutants. Indeed, the mutant shows higher F_v / F_m values (0.75-0.85) when grown under low light. As shown previously (Fig. 3-26) normal light conditions ($80-100 \mu\text{mol m}^{-2} \text{s}^{-1}$) seem to have detrimental effects on the mutant, as indicated by the very low F_v / F_m values (0.45-0.55) in comparison to wt.

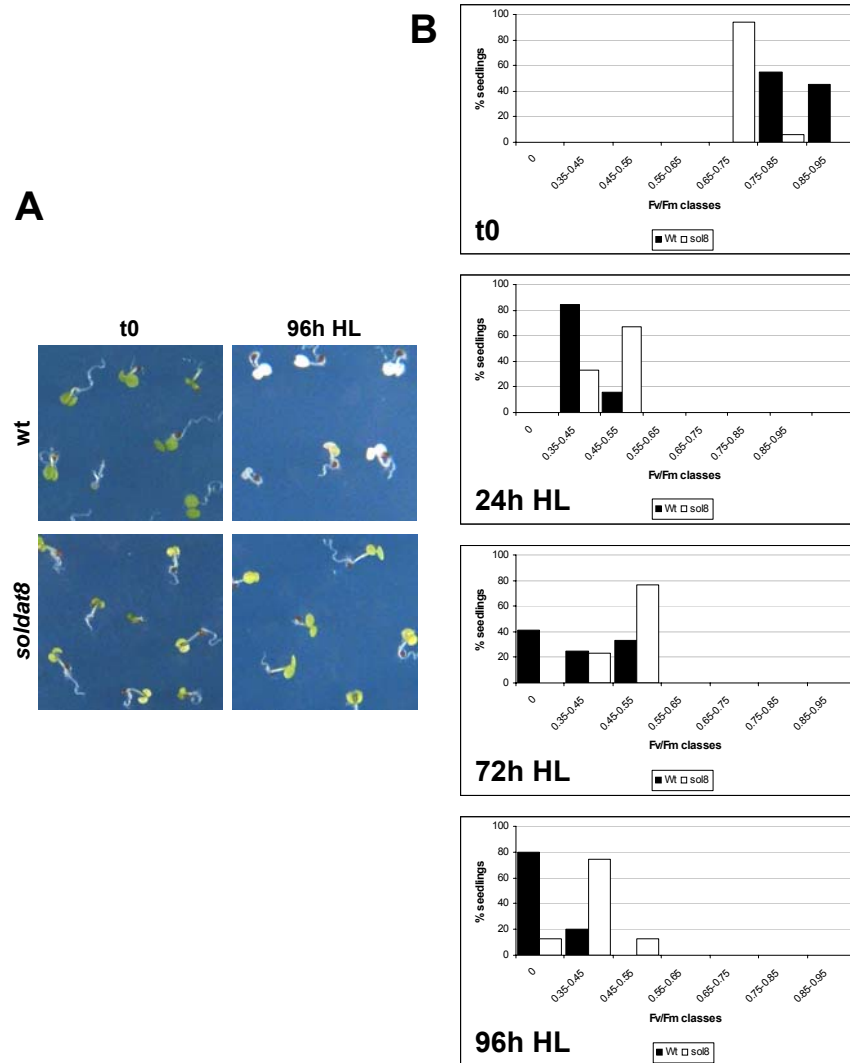


Fig. 3-31: The effects of high light stress and cold on wt and *soldat8* seedlings. Wt seedlings started to bleach 72 h after the beginning of the stress program and at 96 h all of them were bleached (A). In contrast, *soldat8* seedlings remained green in spite of the harsh stress conditions. The histograms in (B) shows the changes of F_v / F_m during the stress period. Each chart corresponds to one time point (0 to 96 hours) and the values shown by the individuals analyzed are grouped into 7 different F_v / F_m classes. Black bars correspond to wt and open bars to the mutant. “0” represents bleached seedlings. The equipment has a limit of detection of 0.35, which is indicative of photoinhibition. *soldat8* plants were longer photosynthetically active than the wt, as shown by the delay in reaching photoinhibitory F_v / F_m values.

Effects of acclimation to high light

The fact that light may represent a stress factor for *soldat8* mutants suggested a possible involvement of acclimatory processes in the resistance of *soldat8* to high light. The most plausible cause for this enhanced resistance could be the activation of acclimation pathways during early development in the mutant, when seedlings are first exposed to the light (preliminary stress), that would subsequently enhance resistance of plants against further stress.

To test this possibility, a modified stress program was used: half of the plants were preexposed to $250 \mu\text{mol m}^{-2} \text{s}^{-1}$ instead of $20 \mu\text{mol m}^{-2} \text{s}^{-1}$ for six hours (Fig. 3-32), while the other half was grown continuously under low light (Fig. 3-30).

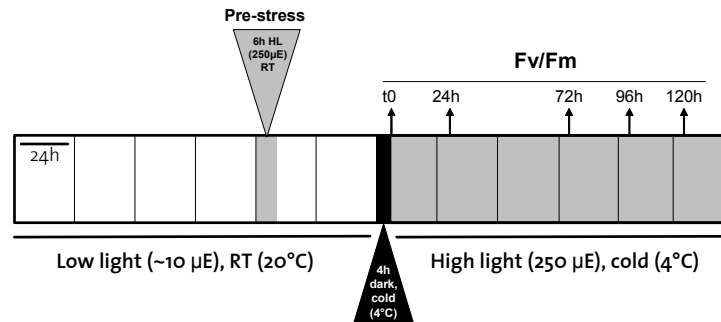


Fig. 3-32: Experimental design for the analysis of acclimation to high light stress. The same conditions as mentioned above (Fig. 3-30) were used except for the stress pretreatment that was applied to the plants. The pool of seedlings tested for acclimation were subjected to a short period of high light during the 5th day of growth under low light.

High light prestress had a beneficial effect on wt seedlings in that it delayed the bleaching process: after 96 h only a few seedlings were bleached (Fig. 3-33 A). The advantageous effects of acclimation were also evident in the fluorescence measurements (Fig. 3-33 B). Plants showed already higher F_v / F_m before the light stress. During the first 24 h of high light treatment, the fluorescence decreased to the same levels shown by non-pretreated plants, but later on the values remained slightly higher in prestressed plants and 72 h after the beginning of the stress program none of the seedlings was bleached.

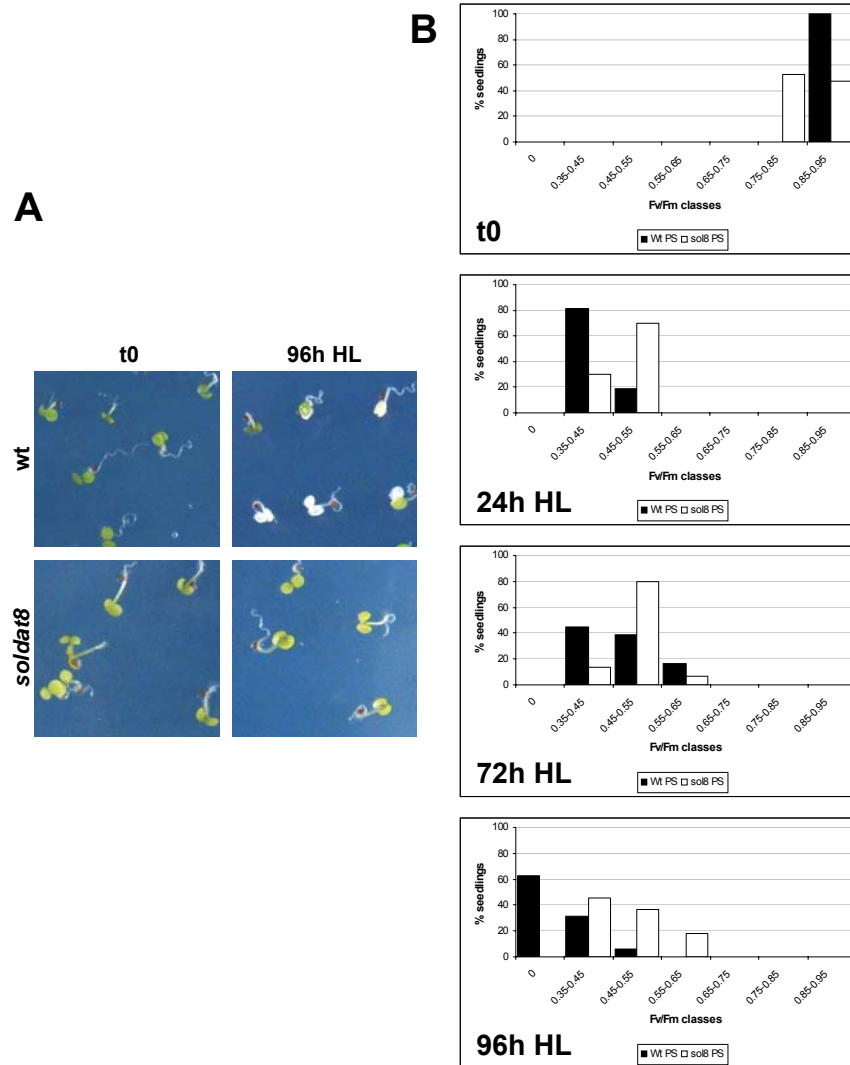


Fig. 3-33: The effects of acclimation to high light on photoinhibitory stress. Wt seedlings that had been subjected to high light prior to the stress program were more resistant than non-prestressed seedlings, resulting in a delay of bleaching. After 96 h of stress some wt seedlings were still green (Fig. 3-31 A). *soldat8* seedlings did not bleach. (B) F_v/F_m values in prestressed seedlings were in general higher than in non-prestressed seedlings (Fig. 3-31 B). High light pretreatment had a beneficial effect for both the mutant and wt, but PSII maximum quantum efficiency was again higher in *soldat8* than wt.

Also in *soldat8* plants the treatment had a clear beneficial effect. As illustrated in Fig. 3-33 B, at the end of the stress period (96 h), the mutant showed higher F_v / F_m values than those in non-prestressed *soldat8* seedlings (Fig. 3.-31 B). From this experiment it cannot be directly concluded that in the *soldat8* mutant the pathways leading to high light acclimation is already activated before the stress. The acclimatory treatment had a similar effect on the mutant as in the wt resulting in a slight increase of PSII maximum efficiency.

4 Discussion

4.1 Oxidative stress signalling

Activation of molecular oxygen to form ROS is an unavoidable consequence of aerobic metabolism. Since ROS can damage the cell, aerobic organisms use an array of ROS-scavenging mechanisms to cope with this constant source of stress. More than 2 billion years of evolution resulted in a finely tuned control of ROS that enabled most organisms to minimize their toxic effects and to use them as signalling molecules (Ledford and Niyogi, 2005).

Particularly hazardous is the process of photosynthesis, which requires light as the reducing force and produces O₂. In plants, the role of ROS as signalling molecules is commonly accepted. They have been shown to be involved in many essential processes like stress, growth and development (reviewed in Vranova et al., 2002; Apel and Hirt, 2004; Laloi et al., 2004; Mittler et al., 2004). Therefore, the concept of “oxidative stress” is being substituted by “oxidative signalling”, which comprehends “the mechanisms by which plant cells sense the environment and make appropriate adjustments to gene expression metabolism and physiology” (Foyer and Noctor, 2005).

It is still a matter of debate what exactly determines the specificity of the response in the context of oxidative signalling. The fact that ROS are central components of a signalling network where several signalling pathways interfere (Vranova et al., 2002) makes it extremely difficult to distinguish specific ROS signatures. Additionally, secondary cytotoxic effects derived from the high reactivity of these molecules usually obscure their direct downstream signalling targets. A further complication is the difficulty of detecting certain ROS, due to their reactivity and/or short half-life. The site of production of a given ROS within the cell also contributes to that complexity, since the spatial pattern of a signalling cascade may be essential for evoking a particular stress response (Neill et al., 2002).

All these factors have hindered the study of oxidative signalling in the past. Besides the relatively well described regulatory role of hydrogen peroxide (Neill et al., 2002; Laloi et al., 2004), very little is known about the signalling role of other ROS like superoxide (Jabs et al., 1996) or singlet oxygen (Leisinger et al., 2001; op den Camp et al., 2003).

4.2 Generation of singlet oxygen results in the activation of different stress responses in the *flu* system

Identification of the *flu* mutant (Meskauskiene et al., 2001) provided a unique opportunity to study the effects of chloroplast-generated singlet oxygen *in planta*. Generation of singlet oxygen rapidly occurs in the chloroplasts of the *flu* mutant after a dark-to-light shift, due to the overaccumulation of the photosensitizer Pchl_a in the dark (op den Camp et al., 2003). This causes visible stress responses in the mutant, when grown under non-permissive dark/light conditions: mature plants stop growing and seedlings collapse within a few hours and die (op den Camp et al., 2003). Massive changes in gene expression were shown to occur in *flu* shortly after the release of singlet oxygen. Among the genes induced by singlet oxygen, a group of 70 were specifically upregulated (op den Camp et al., 2003). In addition, singlet oxygen produced in *flu* protoplasts was shown to trigger cell death-activating pathways controlled by salicylic acid, ethylene and oxylipins (Danon et al., 2005). These results strongly suggest the existence of a genetically controlled signalling network activated by the release of singlet oxygen.

The possibility to isolate second-site mutants of *flu*, in which the stress phenotypes were no longer evident, further underscored this idea. As shown recently in our group, inactivation of a single gene, *EXECUTER1* (*EX1*), suppresses both the growth inhibition and seedling lethality of *flu* (Wagner et al., 2004). Interestingly, *ex1* mutants were more resistant to DCMU than wt plants, a herbicide that also stimulates the release of singlet oxygen in chloroplasts. Although the precise site of production of singlet oxygen within the chloroplast may differ between DCMU-treated wt and *flu*, in both cases an apoptosis-like cell death takes place after the release of singlet oxygen, highlighting the signalling role of this active form of oxygen.

A second group of mutants was identified during this molecular genetic screen that was termed *soldat* (Singlet Oxygen-Linked Death ActivaTor). These mutants are able to partially suppress cell death in seedlings. In contrast to *ex1/flu*, mature *soldat/flu* plants stop growing, when transferred from continuous light to long-day conditions, similar to *flu* (Fig. 3-1). Isolation of these two distinct groups of mutants, *soldat/flu* and *ex1/flu*, offered the possibility to genetically dissect the two different signalling pathways, and to identify a common branch point from which these stress response pathways may diverge.

4.3 A mutation in *SOLDAT8* suppresses cell death in *flu* seedlings

The *soldat8/flu* double mutant was chosen among the 18 different *soldat/flu* lines initially identified in the *flu* suppressor screen, because of three notable traits that made it of special interest: (I) accumulation of high amounts of Pchl_{ide} in the dark (Fig. 3-3), (II) suppression of cell death at the seedling stage of *flu* (Fig. 3-5) and (III) a cotyledon-specific pale-green phenotype (Fig. 3-2). Whereas the first trait is linked to the *flu* mutation, the second and third appeared to be a consequence of the mutation in the *SOLDAT8* gene, specifically affecting the seedling stage.

In the dark, the *soldat8/flu* mutant overaccumulates Pchl_{ide}. Although the levels of Pchl_{ide} in *soldat8/flu* are lower than in the *flu* mutant (60%) (Fig. 3-4), they seem to be sufficient to induce the generation of singlet oxygen after illumination. In agreement with this idea is the fact that *flu* stress marker genes are also induced in *soldat8/flu* after the dark/light shift (Fig. 3-7). Excess of Pchl_{ide} has been shown to accumulate in *flu* in its free form, since it exceeds the binding capacity of the POR enzyme. The six-fold higher bulk of free Pchl_{ide} accumulated in the dark by *soldat8/flu*, when compared to wt, transfers the energy of light directly to molecular oxygen to form singlet oxygen.

soldat8/flu plants grown to maturity under continuous light immediately stop growing and develop necrotic lesions after being transferred to dark/light conditions (Fig. 3-1). At this stage, growth inhibition can be reversed by returning the plants to continuous light. Inhibition of growth is a general stress tolerance strategy adopted by plants, which are exposed to adverse environmental conditions (Netting, 2000). Growth inhibition occurs to a similar extent in both *soldat8/flu* and *flu*, although the characteristic bushy phenotype of *flu* grown under these conditions can not be observed in the double mutant. The reduced growth together with the enhanced shoot formation and development of crinkled leaves cause the bushy phenotype in *flu*, that might indicate a higher degree of stress in this mutant than in *soldat8/flu*.

Only at the cotyledon stage, the *soldat8* mutation suppresses the *flu* phenotype, indicating the existence of independent singlet oxygen-triggered pathways depending on the developmental stage of the plant. *flu* seedlings grown under long-day conditions cannot develop properly and after four light-dark cycles are completely collapsed (Fig. 3-5). Under these conditions, 4-day-old *soldat8/flu* seedlings open and expand the cotyledons similar to the wt. In order to quantify precisely the cell death induction response after a dark-to-light shift, the protoplast assay was used. This system has been previously established in our group and successfully used to characterize the *flu* mutant (Danon et al., 2005). Protoplasts extracted after a 15 h-dark

incubation of 5-day-old light-grown seedlings were used to quantify the cell death induction after reillumination. Significant suppression of cell death 24 h after reexposure to continuous light was observed in *soldat8/flu* protoplasts, when compared to *flu* (Fig. 3-6). The fact that in *soldat8/flu* the percentage of cell death is higher than in wt may be due to the unavoidable damage directly inflicted by the cytotoxicity of singlet oxygen. Singlet oxygen is a highly reactive molecule and only some of its multiple potential targets might act as downstream components in the signal transduction pathway leading to the stress response. Physicochemical damage may arise in the cell, when singlet oxygen unspecifically oxidizes other cellular components. Indeed, the cell death observed in the *flu* mutant after a dark-to-light shift combines typical features from both programmed cell death and necrosis, pointing to a simultaneous dual action of singlet oxygen within the cell (Danon et al., in preparation).

Intriguingly, analysis of several *flu* marker genes (those specifically induced in the mutant shortly after the release of singlet oxygen (op den Camp et al., 2003) reveals significant upregulation in *soldat8/flu* seedlings compared to wt after reillumination, reaching values close to 70% of the level of the *flu* mutant (Fig. 3-7). The genes investigated include two ethylene responsive factors (*ERF5* and *ERF6*) known to be induced by a number of stress elicitors like salicylic acid, jasmonic acid, salt and drought (Wang et al., 2002). The upregulation of these genes in *soldat8/flu* indicates that the stress pathway activated in *flu* after the release of singlet oxygen is also triggered in the double mutant, even though in an attenuated manner, as shown by the lower expression level of stress genes, when compared to *flu*.

4.4 The *SOLDAT8* locus encodes a chloroplast sigma factor, SIG6

A map-based cloning strategy was used to identify the *SOLDAT8* gene. With an initial mapping population of 120 plants the mutation was linked to the lower arm of chromosome II. Due to the relatively high recombination frequency in the vicinity of *SOLDAT8*, a second round of mapping using a population of 470 plants allowed us to localize the gene on a chromosomal region of approximately 55 Kb (Fig. 3-10). Sequencing of the 13 ORF found in this genomic area revealed a nucleotide exchange in the locus At2g36990 that encodes a chloroplast sigma factor, SIG6 (Fig. 3-11). The single nucleotide exchange in the mutant leads to a stop codon in the sigma 70-like r2 domain. This domain is conserved throughout the sigma factors, from bacteria to higher plants. In bacteria this domain mediates the binding of RNA polymerase to DNA (Gruber and Gross, 2003) and most likely it is also essential for this function in higher plants (Ishizaki et al.,

2005). In the case of *soldat8* mutants a truncated protein might be formed which lacks all its conserved domains.

The complementation assay (Fig. 3-12) unequivocally showed that the mutation in *SOLDAT8* was the cause of cell death suppression in *soldat8/flu* mutants and the cotyledon-specific pale phenotype. Transgenic *soldat8/flu* seedlings expressing a wt copy of the *SOLDAT8* gene do no longer survive under long-day conditions similar to the parental *flu* line. When grown under continuous light, the cotyledons are green as in wt.

4.5 Involvement of *SIG6* in the recognition of the plastid-encoded polymerase of young cotyledons

4.5.1 The nuclear-encoded plastid sigma factors

It is widely accepted that plastids evolved from a cyanobacterial endosymbiont. During evolution, most of the genes of the plastid ancestor were lost or transferred to the nucleus (Bock and Khan, 2004). Nevertheless, plastids have retained a small circular genome containing approx. 120 genes, which encode 4 rRNAs, 30 tRNAs and approx. 80 proteins involved in transcription, translation and photosynthesis (Sugita and Sugiura, 1996). These genes are transcribed by at least three types of RNA polymerases: an eubacterial-type multi-subunit RNA polymerase, named PEP (Plastid-Encoded RNA Polymerase) and at least two phage-type monomeric RNA polymerases or NEPs (Nuclear-Encoded RNA Polymerases) (reviewed in Hess and Borner, 1999).

NEPs transcribe predominantly housekeeping genes in non-photosynthetic chloroplasts (Hedtke et al., 1997). NEPs can potentially perform basal transcription of most plastid genes, but in photosynthetically active tissues the dominant enzyme is PEP, which is responsible for transcription of photosynthesis-related genes (De Santis-Maclossek et al., 1999). A switch in RNA polymerase usage occurs during plastid development. Glutamyl-tRNA might play a key role in the shift from predominant NEPs during early chloroplast development to predominant PEP during light-dependent chloroplast maturation (Hanaoka et al., 2005). This process, which involves repression of NEPs' activity and activation of PEP, seems to be a key event in early plant growth (Bisanz-Seyer et al., 1989; Baumgartner et al., 1993).

In eubacteria, the PEP homolog is composed of a multisubunit core enzyme with catalytic activity of RNA synthesis and a sigma factor, which binds to the RNA polymerase and initiates transcription. Most bacterial genomes encode exchangeable sigma factors with different

promoter specificities (Ishihama, 2000). Two groups of sigma factors exist in bacteria, the alternative sigma 54 factors and the essential sigma 70 factors (Wosten, 1998). Sigma 70 factors are responsible for the transcription of housekeeping genes, and sigma 54 factors regulate the transcription of specific sets of genes in response to environmental changes (Gruber and Gross, 2003).

The plastid genome carries the *RPO* genes, which are homologous to the core complex subunits of eubacteria and encode a functional polymerase (Hu and Bogorad, 1990; Hu et al., 1991). Sigma factors present in chloroplasts are not encoded by the plastome. A gene encoding a chloroplast sigma factor was first detected in the nuclear genome of a red alga, *Cyanidium caldarium* (Liu and Troxler, 1996; Tanaka et al., 1996). Nuclear genes encoding orthologous sigma factors have been also identified in higher plants (Allison, 2000). In mustard plastids they were shown to facilitate the binding of a bacterial RNA polymerase to plastid gene promoters and to enhance its transcription activity, but binding to DNA was not observed (Tiller et al., 1991; Tiller and Link, 1993). Fig. 4-1 shows the conserved regions known to mediate the binding of sigma 70 to DNA and RNA polymerases in bacteria (Gruber and Gross, 2003). The genomic sequences of plastid sigma factors contain regions homologous to the conserved domains in sigma 70.



Fig. 4-1: The conserved regions of eubacterial sigma factors and their functional assignment in sigma 70. The function of region 1 is still unknown and it is the most variable part of plant sigma factors. Region 2 encompasses 4 sub-regions: 2.1 binds to the core of RNA polymerase; 2.2 present a hydrophobic core; 2.3 is involved in promoter melting; 2.4 recognizes the -10 promoter regions. Region 3 also binds to the RNA polymerase core and region 4 recognizes the -35 promoter regions.

In *Arabidopsis*, a family of six sigma factors has been identified (*AtSIG1-6*) (Isono et al., 1997; Tanaka et al., 1997; Fujiwara et al., 2000) that have been extensively characterized. SIG2 participates in the transcription of some chloroplast tRNA genes. Mutants lacking the SIG2 factor had a pale-green phenotype and showed reduced accumulation of chlorophyll (Chl) and photosynthesis-related proteins (Shirano et al., 2000; Kanamaru et al., 2001; Privat et al., 2003). The levels of expression of some tRNAs were significantly reduced in these mutants whilst specific NEP-dependent genes were highly transcribed (Kanamaru et al., 2001). It has been

suggested that diminished amounts of tRNA-Glu in *sig2* knockouts may directly affect the Chl biosynthesis pathway, resulting in the observed Chl deficit (Kanamaru and Tanaka, 2004). The same authors proposed SIG2 as a translational regulator of photosynthesis-related proteins. Some plastid tRNAs become a limiting factor for the massive protein synthesis that occurs during light-dependent chloroplast development. Therefore, a transcriptional downregulation of these tRNAs would have a direct impact on protein synthesis.

SIG4 has been shown to control the amount of a plastidial NDH (NADH-plastoquinone-oxidoreductase) complex via the transcriptional regulation of NDHF, a gene coding for a subunit of the complex (Favory et al., 2005). The NDH complex participates in an electron transport chain around photosystem I known as chlororespiration that regulates the redox state of transporters to optimize the rate of cyclic electron transport (Casano et al., 2000). Interestingly, this enzyme is also involved in several stress responses (photooxidative stress, drought) (Horvath et al., 2000; Casano et al., 2001) and senescence (Zapata et al., 2005). Through transcriptional regulation of the NDH complex, SIG4 might specifically activate the response to certain stress conditions where an excess of excitation energy endangers the chloroplast.

SIG5 acts as a mediator of blue-light signalling in chloroplasts. Low-intensity blue light specifically induces *SIG5* expression (Tsunoyama et al., 2002) and transcription initiation at the blue-light responsive promoter of *PSBD* and possibly *PSBA* (respectively D2 and D1, core proteins in PSII) is dependent on this sigma factor (Tsunoyama et al., 2004). *SIG5* is also induced under various stress conditions and *sig5* knockout mutants show delayed recovery to high light stress (Nagashima et al., 2004a). Based on these observations it has been recently suggested that SIG5 is a stress-responsive factor, and may be involved in plant protection via an enhanced repair of PSII (Kanamaru and Tanaka, 2004).

4.5.2 Characterization of SIG6

A study analyzing the function of SIG6 based on the characterization of a *sig6* null mutant line has been published recently (Ishizaki et al., 2005). Some of the approaches performed and the results obtained coincide or overlap with those obtained in the present work. However, in our study special emphasis has been placed on understanding how the lack of SIG6 is able to suppress cell death in *flu* seedlings and to assess a possible role of this factor in singlet oxygen signalling.

Since no insertional lines carrying a mutation in the *SOLDAT8* gene were publicly available, an alternative approach was undertaken in order to obtain *sig6* mutants. The double mutant *soldat8/flu* was crossed with wt plants and *soldat8* single mutants were selected from the segregating F2 population (Fig. 3-14). *soldat8* mutants show the characteristic pale-green cotyledon phenotype but no longer overaccumulate Pchlide in the dark. Thus, these two phenotypical traits can be separated genetically and linked to different mutations in *SOLDAT8* and *FLU*, respectively: *soldat8* plants no longer carry the *flu* mutation but contain the nucleotide exchange in *SOLDAT8* leading to the stop codon mentioned previously. Hereafter, we will refer to *soldat8* as the mutant obtained by a backcross, as mentioned above, whereas *sig6* designates the T-DNA insertional line used by Ishizaki et al. (2005). Both *soldat8* and *sig6* mutants carry a mutation in the same *SOLDAT8* gene, but since our results slightly differ from those obtained with the *sig6* T-DNA insertional mutant we opted to keep the original name used in our screen.

In contrast to the T-DNA *sig6* mutant, that lacks an intact *SOLDAT8* gene, in *soldat8* the transcription of *SOLDAT8* still occurs, although the levels of RNA are 6 times lower in the mutant than in wt (Fig. 3-19). Downregulation of the transcription levels in genes mutated by EMS has been previously reported (Li and Chory, 1997; Davis et al., 1999) and has been attributed to the “nonsense-mediated mRNA decay” (NMD). NMD is used by eukaryotes to avoid the production of truncated and potentially harmful proteins. This surveillance pathway ensures the degradation of mRNAs containing premature translation termination codons (reviewed in Conti and Izaurralde, 2005). Recent evidences suggest that the plant-specific NMD may considerably differ from that found in other organisms (Hori and Watanabe, 2005). In *soldat8* an aberrant mRNA is produced, which encodes a truncated SIG6 that is shorter by one third than in wt, lacking most of its functional domains. Targeting of this mRNA by NMD in *soldat8* could explain the lower levels of *SOLDAT8* mRNA observed in the mutant.

Young seedlings of *soldat8* showed a cotyledon-specific pale phenotype caused by reduced amounts of Chl (data not shown). With increasing age of the seedlings, cotyledons of *soldat8* turned progressively green. The first true leaves emerged also pale, but turned green after one day. Ten-day-old *soldat8* seedlings were indistinguishable from wt, with a similar growth behavior as wt. In young seedlings of *soldat8* the effects of the mutation were also apparent at the microscopic level: cotyledons contained plastids that were reduced in size and in membrane content, when compared to wt (Fig. 3-18). Chloroplast morphology was totally restored in 10-day-old mutant seedlings. These observations strongly suggest a specific role for SIG6 in early

seedling development. Although *SOLDAT8* is constitutively expressed in the light, a peak of expression was observed in four-day-old seedlings, which reflects the proposed essential role of this factor in cotyledons (Fig. 3-20).

In older seedlings (~1 week) another sigma factor apparently could partially take over the role of SIG6, since at this stage the wt phenotype was restored in *soldat8* seedlings. However, at the transcriptional level, no other sigma factor gene was found to be upregulated in the mutant (Fig. 3-21), indicating that in case an alternative sigma factor would substitute for SIG6 in the course of seedling development, this switch might be controlled at a post-transcriptional level.

In mustard (Pfannschmidt and Link, 1997; Homann and Link, 2003) and wheat (Sato et al., 1999), similar mechanisms underlying chloroplast maturation have been observed. These species possess two different types of PEP, which are predominant in either developing or mature chloroplasts and have different promoter preferences. Based on sequence analysis, it has been proposed that sigma factors might confer promoter specificity through selective binding to the polymerase present in young chloroplasts or to the one existing in mature plastids. Each polymerase may only be able to bind a set of sigma factors with specific DNA binding properties that would define the transcription initiation point.

Arabidopsis possesses only one type of PEP, but a large family of sigma factors compared to other higher plants. According to sequence similarity, the six *Arabidopsis* sigma factors (SIG1-6) can be classified into groups with different promoter specificity, which raises the possibility that chloroplast maturation in *Arabidopsis* may be driven by changes in PEP sigma-binding affinity. Alternatively, the recently identified plastid sigma factor-associated proteins (Morikawa et al., 2002) could directly regulate the activity of the sigma proteins in chloroplasts, similarly to the sigma factor binding proteins of bacteria (Hughes and Mathee, 1998; Ishihama, 2000).

In order to shed light on the role of SIG6 in plastid gene expression, the transcript levels of most genes encoded by the plastome in *Arabidopsis* were compared between *soldat8* and wt at different developmental stages of seedlings. As a general approach, plastid array data were analyzed. Very minor changes between wt and *soldat8* were observed and unexpectedly no plastid gene was found to be significantly downregulated in the mutant (Fig. 3-23). To overcome possible sensitivity limitations of the method used to analyze the array data, quantitative PCR was subsequently used. Again, no gene known to be predominantly transcribed by PEP was downregulated. However, real-time PCR revealed that NEP-dependent transcripts accumulated in higher amounts in 4-day-old *soldat8* seedlings as compared to wt (Fig. 3-24). Upregulation of these genes has been previously observed in PEP-deficient mutants (Legen et al., 2002) and

sig2 knockout mutants (Nagashima et al., 2004a), which also show a pale phenotype. This could indicate that in cases where PEP can not function properly, NEP partially takes over the role of PEP in an attempt to compensate the reduced expression of genes which can potentially be transcribed by both polymerases. Indeed, mutants with an impaired PEP activity are viable, suggesting that their chloroplasts may be, at least partially, functional and this could be due to NEP activity. Since PEP function is needed for chloroplast maturation, the fact that *soldat8* chloroplasts can finally reach a mature stage is in agreement with the proposed specific role of SIG6 during early development of chloroplasts. According to the model proposed by Shiina et al. (2005) plastids may contain another general sigma factor functioning together with SIG6 at a later stage.

In *soldat8* the pattern of gene expression partly diverges from that reported for *sig6* (Ishizaki et al., 2005). The authors showed that most PEP-dependent transcripts are downregulated in the mutant. The discrepancy of results could be due to the difference in ecotypes, *i.e.* *soldat8* (Ler) and *sig6* T-DNA insertional mutant (Col) and methodological differences such as the use of different primers and techniques to analyze gene expression.

The analysis of a large set of photosynthesis-related proteins showed that *soldat8* contained markedly reduced amounts of D1 protein in 4-day-old seedlings, when compared with wt (Fig. 3-25). Six days later, *soldat8* produced similar amounts of D1 as wt. All other proteins tested reached similar levels in the mutant as in wt. D1 is one of the core proteins of the reaction center of PSII and it plays a key role in the photoinhibition-repair cycle of PSII (Andersson and Aro, 2001). Photoinhibition is a result of photoinduced damages caused by the harmful effect of ROS on PSII. Such photodamage occurs at all light intensities (Tyystjarvi and Aro, 1996; Anderson et al., 1997) and the D1 protein, which shows the highest turnover rate among all thylakoid proteins (Mattoo et al., 1984), seems to act as a ROS scavenger (Aro et al., 1993). However, only at high light intensities irreversible damage becomes evident *in vivo*, when oxidative damage exceeds the repair capacity of the system (Aro et al., 1993). Singlet oxygen is the main ROS produced in PSII during photoinhibitory conditions (Vass et al., 1992) and it is thought to react directly with D1. Degradation of damaged D1 protein may be a security mechanism to prevent uncontrolled damage of PSII. D1 degradation could act as a singlet oxygen detoxification mechanism at the site of production of this ROS, as proposed by Krieger-Liszakay (2005). *In vitro* experiments with rose bengal as a photosensitizer have shown that singlet oxygen not only induces D1 degradation, but also inhibits PSII repair at the step of D1 synthesis (Nishiyama et al., 2004).

The fact that *soldat8* contains less D1 protein than wt could be explained by an increased degradation or a diminished synthesis of the protein. In either case it would indicate an enhanced sensitivity of the mutant to light. Thus *soldat8* may suffer from photo-oxidative stress even under normal light conditions. It is tempting to speculate that underdeveloped chloroplasts of *soldat8* are not able to process the light properly, and that a higher level of excess excitation energy enhances the formation of ROS and the subsequent damage of PSII, in particular of D1.

To test the extent of damage in PSII and its consequences at the physiological level, *in vivo* fluorescence measurements using wt and *soldat8* seedlings were performed. The maximum quantum efficiency of PSII (F_v / F_m) was 30% lower in the mutant than in 3-day-old wt seedlings (Fig. 3-26). During the following days of development, the mutant gradually restored F_v / F_m to wt levels. The reduced F_v / F_m values of young *soldat8* seedlings indicate a partial inhibition of photosynthesis that correlates with the decreased amounts of the D1 protein.

The analysis of chlorophyll fluorescence induction kinetics revealed higher levels of fluorescence in the mutant than in wt, indicating a reduced capacity to use the light energy for photochemistry in *soldat8* (Fig. 3-27). The mutant shows the same maximum fluorescence as wt after applying a saturating pulse (F_m), but the basal level of fluorescence is higher (F_0) resulting in lower F_v / F_m values. An increase of F_0 has been interpreted as a reduction of the rate constant of energy trapping by PSII centers (Havaux, 1993). This can be the result of either physical dissociation of light harvesting complexes from the PSII core or a damaged PSII core. Dissociation of the antenna from the core complex has been observed for instance as a result of heat stress in several plant species, which resulted in impairment of PSII, as evidenced by a higher F_0 (Armond et al., 1980). In case the PSII core is damaged it cannot transfer properly the energy from light to Q_A , the next electron carrier in the photosynthetic electron chain. As a consequence Q_B can not efficiently accept the electrons from Q_A resulting in an increased F_0 fluorescence yield, even under low light intensity. The lower amount of D1 protein in *soldat8* indicates that a damaged PSII core rather than a dissociation between the antenna and the core, might be the cause of a higher F_0 in the mutant, when compared to wt. In agreement with these results, photochemical and non-photochemical quenching were reduced in the mutant supporting the idea of an impaired electron transport chain in *soldat8* (Fig. 3-28). Taken together, these results strongly suggest that light *per se* is a constant stress factor for *soldat8* during the very first days of development.

To test whether the dysfunction of photosynthesis in young *soldat8* seedlings is specific for PSII or also affects PSI, a PSI redox kinetic analysis was carried out. Young *soldat8* seedlings did not

show any light-induced redox changes of PSI (Fig. 3-29). The PSI redox pattern characteristic of wt appeared later in the mutant. The lack of this signal in *soldat8* 4-day-old seedlings could be due to the insufficient sensitivity of the equipment used. Collectively, the results obtained thus far suggest that in *soldat8* seedlings the photosynthetic electron transport chain is partially impaired during very early stages of development. Later on, most probably concurrent with the appearance of mature chloroplasts, photosynthesis proceeds normally as in wt.

4.6 Enhanced tolerance of photo-oxidative stress in *soldat8* seedlings

The effect of the *soldat8* mutation on singlet oxygen-mediated stress responses was assessed by transferring the seedlings to high light and cold temperatures. High light has been shown to induce the production of singlet oxygen (Hideg et al., 1998; Fryer et al., 2002) and photoinhibition is enhanced further, when high light is combined with low temperatures (Aro et al., 1990; Greer, 1990; Foyer et al., 1994; Long et al., 1994).

Fluorescence analysis (Fig. 3-31) showed that after 24 h of a combined high light/cold stress treatment all seedlings suffered from severe photoinhibition, but the effects were clearly less harsh in the mutant than in wt. At the end of the stress treatment (96 h), the entire wt population was bleached, whereas the mutant seedlings were still green and did not show substantial changes in F_v / F_m values.

Characterization of *soldat8* revealed some possible mechanisms that could explain, why this mutant has an enhanced tolerance to photo-oxidative stress. The mutant is able to withstand high light treatment better than wt and it shows a partially suppressed singlet oxygen-mediated stress responses in the *flu* background.

There are at least two different interpretations to explain the phenotype of *soldat8* in relation to photo-oxidative stress: (1) undifferentiated chloroplasts that are unable to transmit a singlet oxygen-mediated plastid signal to the nucleus, or (2) acclimation to photo-oxidative stress.

(1) The fact that in *soldat8* chloroplast development is delayed and chloroplasts are smaller with not fully developed thylakoid membranes could support the idea that the mutant may be impaired in plastid-to-nucleus signalling. This would certainly alter the signalling pathway and the subsequent stress response induced after the release of singlet oxygen in plastids of seedlings exposed to high light. *soldat8* seedlings would simply not show a stress response because its immature plastids could not release the proper signal activating the expression of

nuclear-encoded stress-related genes. However, this seems not to be the case in *soldat8*. In the *flu* background, the *soldat8* mutation does not interfere with the plastid-to-nucleus communication activated after the release of singlet oxygen, as indicated by the pronounced induction of *flu* marker genes in the double mutant (Fig. 3-7).

Plastids of young *soldat8* seedlings contain lower amounts of Chl than wt, as reflected by the pale-green cotyledons of the mutant. However, the reduced Chl content seems not to be the cause of the mutant's stress tolerance as indicated by the F_v / F_m fluorescence measurements that were done to assess the activity of PSII. These do not show a lowering of the F_m value that would be expected if indeed the mutant had a lower PSII capacity than wt.

(2) *In vivo* fluorescence measurements of PSII activity suggested that during very early seedling development light *per se* is a stress factor in *soldat8*. The mutant shows a higher F_0 than wt, which is indicative of a damaged PSII (Armond et al., 1980). This could be confirmed by protein analysis, which revealed that among all PSII proteins analyzed, only D1 was present in reduced amounts in *soldat8*. We do not know, if the lower amount of D1 is a consequence of reduced protein synthesis or enhanced protein degradation in the mutant. One possibility could be that in *soldat8* seedlings the stress caused by light results in an increased turnover of D1, which might slow down D1 protein accumulation.

In *soldat8*, acclimatory adjustments seem to occur during very early seedling development, which could increase the mutant's tolerance to future stress. Acclimatory processes could be activated in *soldat8* early upon light exposure, so that when seedlings are exposed later to high light they can resist the stress longer than wt.

The importance of acclimation to light stress could be demonstrated in prestressed wt plants that tolerated high light stress better than non-prestressed ones (Fig. 3-33). Under these conditions, *soldat8* seedlings also performed better if prestressed, which indicates that constitutive minor stress in these mutants does not activate yet the maximum acclimatory capacity of these plants.

4.7 Conclusions and future prospects

In the present work the *SOLDAT8* locus has been mapped as part of a detailed analysis to study singlet oxygen-mediated signalling in *flu* after a dark-to-light shift. Two groups of second-site mutants that were identified in a *flu*-suppressor screen have been investigated: *ex1/flu* and *soldat/flu*. In these mutants, Pchl_{ide} overaccumulates to similar levels as in *flu*, but stress phenotypes are suppressed to different degrees. In *ex1/flu* mutants, both growth inhibition and seedling lethality, are suppressed, whereas *soldat* mutations in the *flu* background abrogate

death of seedlings but not growth inhibition of mature plants. The isolation of different second-site mutants that block the singlet oxygen-mediated pathway at different points, allowed the identification of candidate genes involved in singlet oxygen signalling.

soldat8 mutants carry a mutation in a gene, which encodes a chloroplast sigma factor. During very early stages of development these mutants have a cotyledon-specific phenotype, with pale-green cotyledons containing underdeveloped plastids. The phenotype of the wt is gradually restored and in one week-old seedlings the effects of the mutation are no longer evident. A complementation assay confirmed that a mutation in the *SOLDAT8* gene is the cause for the cotyledon-specific phenotype in *soldat8* mutants. The *flu* phenotype was restored in *soldat8/flu* plants complemented with a wt copy of the *SOLDAT8* gene.

Characterization of the *soldat8* mutant showed that SIG6 participates in the regulation of early chloroplast development in cotyledons. Young mutant seedlings contain small plastids with reduced thylakoid membranes. The lack of SIG6 does not dramatically affect chloroplast gene expression in *soldat8*. However, it has a specific impact on one of the chloroplast proteins, D1, a core protein of PSII. This protein has a high turnover and its synthesis and degradation are tightly regulated, since it has an essential role in photosynthesis and photoprotection. In the future it would be very interesting to study the cause of the decrease of D1 in the mutant, whether it is the result of a defect in its synthesis or of degradation or of both processes. In agreement with the lower D1 content is the reduced capacity of *soldat8* to use light energy for photochemistry as indicated by the *in vivo* analysis of photosynthetic activity.

Taken together, the results suggest that light is a stress factor for *soldat8* mutants at a very early stage of development. *soldat8* seedlings grown under low light show higher PSII activity than under normal light conditions. Moreover, these mutants show an enhanced tolerance of photoinhibitory conditions at the cotyledon stage, suggesting that in *soldat8* light may act as a trigger for the activation of an acclimatory response, setting up the mutant for future adverse situations. Suppression of the *flu* phenotype in *soldat8/flu* seedlings seems to be a consequence of this previous activation of acclimatory processes in the mutant upon light exposure.

References

- Allan AC, Fluhr R** (1997) Two distinct sources of elicited reactive oxygen species in tobacco epidermal cells. *Plant Cell* **9**: 1559-1572
- Allison LA** (2000) The role of sigma factors in plastid transcription. *Biochimie* **82**: 537-548
- Alscher RG, Donahue JH, Cramer CL** (1997) Reactive oxygen species and antioxidants: relationships in green cells. *Physiologia Plantarum* **100**: 224-233
- Alvarez ME, Pennell RI, Meijer PJ, Ishikawa A, Dixon RA, Lamb C** (1998) Reactive oxygen intermediates mediate a systemic signal network in the establishment of plant immunity. *Cell* **92**: 773-784
- Anderson JM, Park YI, Chow WS** (1997) Photoinactivation and photoprotection of photosystem II in nature. *Physiologia Plantarum* **100**: 214-223
- Andersson B, Aro E-M** (2001) Potodamage and D1 protein turnover in photosystem II. *In* E-M Aro, B Andersson, eds, *Regulation of photosynthesis*, Vol 11. Kluwer Academic Publishers, pp 377-393
- Apel K, Hirt H** (2004) Reactive oxygen species: metabolism, oxidative stress, and signal transduction. *Annual Review of Plant Biology* **55**: 373-399
- Apel K, Santel H-J, Redlinger TE, Falk H** (1980) The Protochlorophyllide Holochrome of Barley (*Hordeum vulgare* L.). Isolation and Characterization of the NADPH : Protochlorophyllide Oxidoreductase. *European Journal of Biochemistry* **111**: 251-258
- Apostol I, Heinsteinst PF, Low PS** (1989) Rapid stimulation of an oxidative burst during elicitation of cultured plant cells: role in defense and signal transduction. *Plant Physiology* **90**: 109-116
- Armond PA, Bjorkman O, Staehelin LA** (1980) Dissociation of supramolecular complexes in chloroplast membranes. A manifestation of heat damage to the photosynthetic apparatus. *Biochimica et Biophysica Acta* **601**: 433-443
- Aro EM, Hundal T, Carlberg I, Andersson B** (1990) *In vitro* Studies on Light-Induced Inhibition of Photosystem-II and D1-Protein Degradation at Low-Temperatures. *Biochimica et Biophysica Acta* **1019**: 269-275
- Aro EM, Virgin I, Andersson B** (1993) Photoinhibition of Photosystem II: Inactivation, Protein Damage and Turnover. *Biochimica et Biophysica Acta* **1143**: 113-134
- Asada K** (1999) THE WATER-WATER CYCLE IN CHLOROPLASTS: Scavenging of Active Oxygens and Dissipation of Excess Photons. *Annual Review of Plant Physiology and Plant Molecular Biology* **50**: 601-639
- Baumgartner BJ, Rapp JC, Mullet JE** (1993) Plastid Genes Encoding the Transcription/Translation Apparatus Are Differentially Transcribed Early in Barley (*Hordeum vulgare*) Chloroplast Development (Evidence for Selective Stabilization of psbA mRNA). *Plant Physiology* **101**: 781-791
- Bisanz-Seyer C, Li Y-F, Seyer P, Mache Rg** (1989) The components of the plastid ribosome are not accumulated synchronously during the early development of spinach plants. *Plant Molecular Biology* **12**: 201-211
- Bock R, Khan MS** (2004) Taming plastids for a green future. *Trends in Biotechnology* **22**: 311-318

- Bolwell GP, Bindschedler LV, Blee KA, Butt VS, Davies DR, Gardner SL, Gerrish C, Minibayeva F** (2002) The apoplastic oxidative burst in response to biotic stress in plants: a three-component system. *Journal of Experimental Botany* **53**: 1367-1376
- Boo YC, Lee KP, Jung J** (2000) Rice plants with a high protochlorophyllide accumulation show oxidative stress in low light that mimics water stress. *Journal of Plant Physiology* **157**: 405-411
- Bowler C, Montagu MV, Inzé D** (1992) Superoxide dismutases and stress tolerance. *Annual Review of Plant Physiology and Plant Molecular Biology* **43**: 83-116
- Boyer J** (1982) Plant productivity and environment. *Science* **218**: 443-448
- Bradley DJ, Kjellbom P, Lamb CJ** (1992) Elicitor- and wound-induced oxidative cross-linking of a proline-rich plant cell wall protein: A novel, rapid defense response. *Cell* **70**: 21-30
- Casano LM, Martin M, Sabater B** (2001) Hydrogen peroxide mediates the induction of chloroplastic Ndh complex under photooxidative stress in barley. *Plant Physiology* **125**: 1450-1458
- Casano LM, Zapata JM, Martin M, Sabater B** (2000) Chlororespiration and poisoning of cyclic electron transport. Plastoquinone as electron transporter between thylakoid NADH dehydrogenase and peroxidase. *Journal of Biological Chemistry* **275**: 942-948
- Charles SA, Halliwell B** (1980) Effect of hydrogen peroxide on spinach (*Spinacia oleracea*) chloroplast fructose biphosphatase. *Biochemical Journal* **189**: 373-376
- Chen Z, Silva H, Klessig DF** (1993) Active oxygen species in the induction of plant systemic acquired resistance by salicylic acid. *Science* **262**: 1883-1886
- Clough SJ, Bent AF** (1998) Floral dip: a simplified method for *Agrobacterium*-mediated transformation of *Arabidopsis thaliana*. *Plant Journal* **16**: 735-743
- Conti E, Izaurralde E** (2005) Nonsense-mediated mRNA decay: molecular insights and mechanistic variations across species. *Current Opinion in Cell Biology* **17**: 316-325
- Danon A, Miersch O, Felix G, Camp RG, Apel K** (2005) Concurrent activation of cell death-regulating signaling pathways by singlet oxygen in *Arabidopsis thaliana*. *Plant Journal* **41**: 68-80
- Dat J, Vandenabeele S, Vranova E, Van Montagu M, Inze D, Van Breusegem F** (2000) Dual action of the active oxygen species during plant stress responses. *Cellular and Molecular Life Sciences* **57**: 779-795
- Dat JF, Inze D, Van Breusegem F** (2001) Catalase-deficient tobacco plants: tools for in planta studies on the role of hydrogen peroxide. *Redox Report* **6**: 37-42
- Davies MJ** (2003) Singlet oxygen-mediated damage to proteins and its consequences. *Biochemical and Biophysical Research Communication* **305**: 761-770
- Davis SJ, Kurepa J, Vierstra RD** (1999) The *Arabidopsis thaliana* HY1 locus, required for phytochrome-chromophore biosynthesis, encodes a protein related to heme oxygenases. *Proceedings of the National Academy of Sciences of the United States of America* **96**: 6541-6546
- De Santis-Maclossek G, Kofer W, Bock A, Schoch S, Maier RM, Wanner G, Rudiger W, Koop HU, Herrmann RG** (1999) Targeted disruption of the plastid RNA polymerase genes rpoA, B and C1: molecular biology, biochemistry and ultrastructure. *Plant Journal* **18**: 477-489
- Delledonne M, Zeier J, Marocco A, Lamb C** (2001) Signal interactions between nitric oxide and reactive oxygen intermediates in the plant hypersensitive disease resistance response.

Proceedings of the National Academy of Sciences of the United States of America **98**: 13454-13459

Doke N (1983) Generation of superoxide anion by potato tuber protoplasts during the hypersensitive response to hyphal cell wall components of *Phytophthora infestans* and specific inhibition of the reaction by suppressors of hypersensitivity. *Physiological and Molecular Plant Pathology* **23**: 359-367

Favory JJ, Kobayashi M, Tanaka K, Peltier G, Kreis M, Valay JG, Lerbs-Mache S (2005) Specific function of a plastid sigma factor for ndhF gene transcription. *Nucleic Acids Research* **33**: 5991-5999

Foyer CH, Lelandais M, Kunert KJ (1994) Photooxidative stress in plants. *Physiologia Plantarum* **92**: 696-717

Foyer CH, Noctor G (2000) Oxygen processing in photosynthesis: regulation and signalling. *New Phytologist* **146**: 359-388

Foyer CH, Noctor G (2005) Oxidant and antioxidant signalling in plants: a re-evaluation of the concept of oxidative stress in a physiological context. *Plant Cell and Environment* **28**: 1056-1071

Fryer MJ, Oxborough K, Mullineaux PM, Baker NR (2002) Imaging of photo-oxidative stress responses in leaves. *Journal of Experimental Botany* **53**: 1249-1254

Fufezan C, Rutherford AW, Krieger-Liszkay A (2002) Singlet oxygen production in herbicide-treated photosystem II. *FEBS Letters* **532**: 407-410

Fujiwara M, Nagashima A, Kanamaru K, Tanaka K, Takahashi H (2000) Three new nuclear genes, sigD, sigE and sigF, encoding putative plastid RNA polymerase [sigma] factors in *Arabidopsis thaliana*. *FEBS Letters* **481**: 47-52

Girotti AW, Kriska T (2004) Role of lipid hydroperoxides in photo-oxidative stress signaling. *Antioxidants & Redox Signaling* **6**: 301-310

Glazebrook J (2001) Genes controlling expression of defense responses in *Arabidopsis*--2001 status. *Curr Opin Plant Biol* **4**: 301-308

Goslings D, Meskauskiene R, Kim C, Lee KP, Nater M, Apel K (2004) Concurrent interactions of heme and FLU with Glu tRNA reductase (HEMA1), the target of metabolic feedback inhibition of tetrapyrrole biosynthesis, in dark- and light-grown *Arabidopsis* plants. *Plant Journal* **40**: 957-967

Grant JJ, Loake GJ (2000) Role of reactive oxygen intermediates and cognate redox signaling in disease resistance. *Plant Physiology* **124**: 21-29

Greer DH (1990) The combined effects of chilling and light stress on photoinhibition of photosynthesis and its subsequent recovery. *Plant Physiology and Biochemistry* **28**: 447-455

Gruber TM, Gross CA (2003) Multiple sigma subunits and the partitioning of bacterial transcription space. *Annual Review of Microbiology* **57**: 441-466

Hakimi MA, Privat I, Valay JG, Lerbs-Mache S (2000) Evolutionary conservation of C-terminal domains of primary sigma(70)-type transcription factors between plants and bacteria. *Journal of Biological Chemistry* **275**: 9215-9221

Hammond-Kosack KE, Jones JD (1996) Resistance gene-dependent plant defense responses. *Plant Cell* **8**: 1773-1791

- Hanaoka M, Kanamaru K, Fujiwara M, Takahashi H, Tanaka K** (2005) Glutamyl-tRNA mediates a switch in RNA polymerase use during chloroplast biogenesis. *EMBO Reports* **6**: 545-550
- Havaux M** (1993) Characterisation of Thermal damage to the photosynthetic electron transport system in potato leaves. *Plant Science* **94**: 19-33
- Havaux M, Eymery F, Porfirova S, Rey P, Dormann P** (2005) Vitamin E Protects against Photoinhibition and Photooxidative Stress in *Arabidopsis thaliana*. *Plant Cell*
- Hedtke B, Borner T, Weihe A** (1997) Mitochondrial and chloroplast phage-type RNA polymerases in Arabidopsis. *Science* **277**: 809-811
- Hess WR, Borner T** (1999) Organellar RNA polymerases of higher plants. *International Review of Cytology* **190**: 1-59
- Hideg E, Kalai T, Hideg K, Vass I** (1998) Photoinhibition of photosynthesis in vivo results in singlet oxygen production detection via nitroxide-induced fluorescence quenching in broad bean leaves. *Biochemistry* **37**: 11405-11411
- Homann A, Link G** (2003) DNA-binding and transcription characteristics of three cloned sigma factors from mustard (*Sinapis alba* L.) suggest overlapping and distinct roles in plastid gene expression. *European Journal of Biochemistry / FEBS* **270**: 1288-1300
- Hori K, Watanabe Y** (2005) UPF3 suppresses aberrant spliced mRNA in Arabidopsis. *Plant Journal* **43**: 530-540
- Horton P, Ruban A** (2005) Molecular design of the photosystem II light-harvesting antenna: photosynthesis and photoprotection. *Journal of Experimental Botany* **56**: 365-373
- Horvath EM, Peter SO, Joet T, Rumeau D, Cournac L, Horvath GV, Kavanagh TA, Schafer C, Peltier G, Medgyesy P** (2000) Targeted inactivation of the plastid ndhB gene in tobacco results in an enhanced sensitivity of photosynthesis to moderate stomatal closure. *Plant Physiology* **123**: 1337-1350
- Hu J, Bogorad L** (1990) Maize chloroplast RNA polymerase: The 180-, 120-, and 38-kilodalton polypeptides are encoded in chloroplast genes. *Proceedings of the National Academy of Sciences of the United States of America* **87**: 1531-1535
- Hu J, Troxler RF, Bogorad L** (1991) Maize chloroplast RNA polymerase: The 78-kilodalton polypeptide is encoded by the plastid rpoC1 gene. *Nucleic Acids Research* **19**: 3431-3434
- Hughes KT, Mathee K** (1998) The anti-sigma factors. *Annual Review of Microbiology* **52**: 231-286
- Ishihama A** (2000) Functional modulation of *Escherichia coli* RNA polymerase. *Annual Review of Microbiology* **54**: 499-518
- Ishizaki Y, Tsunoyama Y, Hatano K, Ando K, Kato K, Shinmyo A, Kobori M, Takeba G, Nakahira Y, Shiina T** (2005) A nuclear-encoded sigma factor, Arabidopsis SIG6, recognizes sigma-70 type chloroplast promoters and regulates early chloroplast development in cotyledons. *Plant Journal* **42**: 133-144
- Isono K, Shimizu M, Yoshimoto K, Niwa Y, Satoh K, Yokota A, Kobayashi H** (1997) Leaf-specifically expressed genes for polypeptides destined for chloroplasts with domains of [sigma] factors of bacterial RNA polymerases in *Arabidopsis thaliana*. *Proceedings of the National Academy of Sciences of the United States of America* **94**: 14948-14953

- Jabs T, Dietrich RA, Dangl JL** (1996) Initiation of runaway cell death in an Arabidopsis mutant by extracellular superoxide. *Science* **273**: 1853-1856
- Kanamaru K, Nagashima A, Fujiwara M, Shimada H, Shirano Y, Nakabayashi K, Shibata D, Tanaka K, Takahashi H** (2001) An Arabidopsis sigma factor (SIG2)-dependent expression of plastid-encoded tRNAs in chloroplasts. *Plant & Cell Physiology* **42**: 1034-1043
- Kanamaru K, Tanaka K** (2004) Roles of chloroplast RNA polymerase sigma factors in chloroplast development and stress response in higher plants. *Bioscience, Biotechnology and Biochemistry* **68**: 2215-2223
- Karpinska B, Wingsle G, Karpinski S** (2000) Antagonistic effects of hydrogen peroxide and glutathione on acclimation to excess excitation energy in Arabidopsis. *International Union of Biochemistry and Molecular Biology: Life* **50**: 21-26
- Karpinski S, Gabrys H, Mateo A, Karpinska B, Mullineaux PM** (2003) Light perception in plant disease defence signalling. *Current Opinion in Plant Biology* **6**: 390-396
- Karpinski S, Reynolds H, Karpinska B, Wingsle G, Creissen G, Mullineaux PM** (1999) Systemic signalling and acclimation in response to excess excitation energy in Arabidopsis. *Science* **284**: 654-657
- Kautsky H, Hirsch A** (1931) Neue Versuche zur Kohlensäureassimilation. *Naturwissenschaften* **19**: 964
- Keren N, Gong H, Ohad I** (1995) Oscillations of reaction center II-D1 protein degradation in vivo induced by repetitive light flashes. Correlation between the level of RCII-QB- and protein degradation in low light. *Journal of Biological Chemistry* **270**: 806-814
- Klessig DF, Durner J, Noad R, Navarre DA, Wendehenne D, Kumar D, Zhou JM, Shah J, Zhang S, Kachroo P, Trifa Y, Pontier D, Lam E, Silva H** (2000) Nitric oxide and salicylic acid signaling in plant defense. *Proceedings of the National Academy of Sciences of the United States of America* **97**: 8849-8855
- Knight H, Knight MR** (2001) Abiotic stress signalling pathways: specificity and cross-talk. *Trends in Plant Science* **6**: 262-267
- Knox JP, Dodge AD** (1985) Singlet oxygen and plants. *Phytochemistry* **24**: 889-896
- Kochevar IE** (2004) Singlet oxygen signaling: from intimate to global. *Science STKE* **2004**: pe7
- Krieger-Liszkay A** (2005) Singlet oxygen production in photosynthesis. *Journal of Experimental Botany* **56**: 337-346
- Krieger-Liszkay A, Rutherford AW** (1998) Influence of Herbicide Binding on the Redox Potential of the Quinone Acceptor in Photosystem II: Relevance to Photodamage and Phytotoxicity. *Biochemistry* **37**: 17339-17344
- Kruk J, Holländer-Czytko H, Oettmeier W, Trebst A** (2005) Tocopherol as singlet oxygen scavenger in photosystem II. *Journal of Plant Physiology* **162**: 749-757
- Kulheim C, Agren J, Jansson S** (2002) Rapid regulation of light harvesting and plant fitness in the field. *Science* **297**: 91-93
- Laemmli UK** (1970) Cleavage of Structural Proteins during the Assembly of the Head of Bacteriophage T4. *Nature* **227**: 680-685
- Laloi C, Apel K, Danon A** (2004) Reactive oxygen signalling: the latest news. *Current Opinion in Plant Biology* **7**: 323-328

- Lamb C, Dixon RA** (1997) The oxidative burst in plant disease resistance. *Annual Review of Plant Physiology and Plant Molecular Biology* **48**: 251-275
- Ledford HK, Niyogi KK** (2005) Singlet oxygen and photo-oxidative stress management in plants and algae. *Plant, Cell and Environment* **28**: 1037-1045
- Legen J, Kemp S, Krause K, Profanter B, Herrmann RG, Maier RM** (2002) Comparative analysis of plastid transcription profiles of entire plastid chromosomes from tobacco attributed to wild-type and PEP-deficient transcription machineries. *Plant J* **31**: 171-188
- Leisinger U, Rufenacht K, Fischer B, Pesaro M, Spengler A, Zehnder AJ, Eggen RI** (2001) The glutathione peroxidase homologous gene from *Chlamydomonas reinhardtii* is transcriptionally up-regulated by singlet oxygen. *Plant Mol Biol* **46**: 395-408
- Levine A, Tenhaken R, Dixon R, Lamb C** (1994) H₂O₂ from the oxidative burst orchestrates the plant hypersensitive disease resistance response. *Cell* **79**: 583-593
- Li J, Chory J** (1997) A Putative Leucine-Rich Repeat Receptor Kinase Involved in Brassinosteroid Signal Transduction. *Cell* **90**: 929-938
- Liu B, Troxler RF** (1996) Molecular characterization of a positively photoregulated nuclear gene for a chloroplast RNA polymerase [sigma] factor in *Cyanidium caldarium*. *Proceedings of the National Academy of Sciences of the United States of America* **93**: 3313-3318
- Long SP, Humphries S, Falkowski PG** (1994) Photoinhibition of Photosynthesis in Nature. *Annual Review of Plant Physiology and Plant Molecular Biology* **45**: 633-662
- Macpherson A, Telfer A, Barber A, T.Truscot** (1993) Direct detection of singlet oxygen from isolated photosystem II reaction centers. *Biochimica et Biophysica Acta* **1143**: 301-309
- Malan C, Greyling MM, Gressel J** (1990) Correlation between CuZn superoxide dismutase and glutathione reductase and environmental and xenobiotic stress tolerance in maize inbreds. *Plant Science* **69**: 157-166
- Martin GB, Bogdanove AJ, Sessa G** (2003) Understanding the functions of plant disease resistance proteins. *Annu Rev Plant Biol* **54**: 23-61
- Martinez GR, Loureiro AP, Marques SA, Miyamoto S, Yamaguchi LF, Onuki J, Almeida EA, Garcia CC, Barbosa LF, Medeiros MH, Di Mascio P** (2003) Oxidative and alkylating damage in DNA. *Mutation Research* **544**: 115-127
- Marx JL** (1985) Oxygen free radicals linked to many diseases. *Science* **235**: 529-531
- Mattoo AK, Hoffman-Falk H, Marder JB, Edelman M** (1984) Regulation of Protein Metabolism: Coupling of Photosynthetic Electron Transport to in vivo Degradation of the Rapidly Metabolized 32-Kilodalton Protein of the Chloroplast Membranes. *Proceedings of the National Academy of Sciences of the United States of America* **81**: 1380-1384
- Meskauskiene R, Apel K** (2002) Interaction of FLU, a negative regulator of tetrapyrrole biosynthesis, with the glutamyl-tRNA reductase requires the tetratricopeptide repeat domain of FLU. *FEBS Letters* **532**: 27-30
- Meskauskiene R, Nater M, Goslings D, Kessler F, op den Camp R, Apel K** (2001) FLU: a negative regulator of chlorophyll biosynthesis in *Arabidopsis thaliana*. *Proceedings of the National Academy of Sciences of the United States of America* **98**: 12826-12831
- Mishra NP, Ghanotakis DF** (1994) Exposure of a photosystem II complex to chemically generated singlet oxygen results in D1 fragments similar to the ones observed during aerobic photoinhibition *Biochimica et Biophysica Acta* **1187**: 296-300

- Mittler R** (2002) Oxidative stress, antioxidants and stress tolerance. *Trends in Plant Science* **7**: 405-410
- Mittler R, Herr EH, Orvar BL, van Camp W, Willekens H, Inze D, Ellis BE** (1999) Transgenic tobacco plants with reduced capability to detoxify reactive oxygen intermediates are hyperresponsive to pathogen infection. *Proceedings of the National Academy of Sciences of the United States of America* **96**: 14165-14170
- Mittler R, Vanderauwera S, Gollery M, Breusegem FV** (2004) Reactive oxygen gene network of plants. *Trends in Plant Science* **9**: 490-497
- Moan J** (1990) On The Diffusion Length of Singlet Oxygen In Cells And Tissues. *Journal of Photochemistry and Photobiology B-Biology* **6**: 343-347
- Morikawa K, Shiina T, Murakami S, Toyoshima Y** (2002) Novel nuclear-encoded proteins interacting with a plastid sigma factor, Sig1, in *Arabidopsis thaliana*. *FEBS Letters* **514**: 300-304
- Muller P, Li X-P, Niyogi KK** (2001) Non-Photochemical Quenching. A Response to Excess Light Energy. *Plant Physiology*. **125**: 1558-1566
- Murashige T, Skoog F** (1962) A revised medium for rapid growth and bioassays with tobacco tissue cultures. *Physiologia Plantarum* **15**: 473-497
- Nagashima A, Hanaoka M, Motohashi R, Seki M, Shinozaki K, Kanamaru K, Takahashi H, Tanaka K** (2004a) DNA microarray analysis of plastid gene expression in an *Arabidopsis* mutant deficient in a plastid transcription factor sigma, SIG2. *Bioscience, Biotechnology and Biochemistry* **68**: 694-704
- Nagashima A, Hanaoka M, Shikanai T, Fujiwara M, Kanamaru K, Takahashi H, Tanaka K** (2004b) The multiple-stress responsive plastid sigma factor, SIG5, directs activation of the psbD blue light-responsive promoter (BLRP) in *Arabidopsis thaliana*. *Plant & Cell Physiology* **45**: 357-368
- Neill S, Desikan R, Hancock J** (2002) Hydrogen peroxide signalling. *Current Opinion in Plant Biology* **5**: 388-395
- Netting AG** (2000) pH, abscisic acid and the integration of metabolism in plants under stressed and non-stressed conditions: cellular responses to stress and their implication for plant water relations. *Journal of Experimental Botany* **51**: 147-158
- Nishiyama Y, Allakhverdiev SI, Yamamoto H, Hayashi H, Murata N** (2004) Singlet oxygen inhibits the repair of photosystem II by suppressing the translation elongation of the D1 protein in *Synechocystis* sp. PCC 6803. *Biochemistry* **43**: 11321-11330
- Niyogi KK** (2000) Safety valves for photosynthesis. *Current Opinion in Plant Biology* **3**: 455-460
- Noctor G, Foyer CH** (1998) ASCORBATE AND GLUTATHIONE: Keeping Active Oxygen Under Control. *Annual Review of Plant Physiology and Plant Molecular Biology* **49**: 249-279
- Noctor G, Veljovic-Jovanovic S, Driscoll S, Novitskaya L, Foyer CH** (2002) Drought and oxidative load in the leaves of C3 plants: a predominant role for photorespiration? *Annals of Botany* **89 Spec No**: 841-850
- op den Camp RG, Przybyla D, Ochsenbein C, Laloi C, Kim C, Danon A, Wagner D, Hideg E, Gobel C, Feussner I, Nater M, Apel K** (2003) Rapid induction of distinct stress responses after the release of singlet oxygen in *Arabidopsis*. *Plant Cell* **15**: 2320-2332
- Overmyer K, Brosche M, Kangasjarvi J** (2003) Reactive oxygen species and hormonal control of cell death. *Trends in Plant Science* **8**: 335-342

- Pfannschmidt T** (2003) Chloroplast redox signals: how photosynthesis controls its own genes. *Trends in Plant Science* **8**: 33-41
- Pfannschmidt T, Link G** (1997) The A and B forms of plastid DNA-dependent RNA polymerase from mustard (*Sinapis alba* L.) transcribe the same genes in a different developmental context. *Molecular & General Genetics* **257**: 35-44
- Polle A** (2001) Dissecting the superoxide dismutase-ascorbate-glutathione-pathway in chloroplasts by metabolic modeling. Computer simulations as a step towards flux analysis. *Plant Physiology* **126**: 445-462
- Prasad TK, Anderson MD, Martin BA, Stewart CR** (1994) Evidence for Chilling-Induced Oxidative Stress in Maize Seedlings and a Regulatory Role for Hydrogen Peroxide. *Plant Cell* **6**: 65-74
- Privat I, Hakimi M-A, Buhot L, Favory J-J, Mache-Lerbs S** (2003) Characterization of Arabidopsis plastid sigma-like transcription factors SIG1, SIG2 and SIG3. *Plant Molecular Biology* **51**: 385-399
- Rathjen JP, Moffett P** (2003) Early signal transduction events in specific plant disease resistance. *Current Opinion In Plant Biology* **6**: 300-306
- Riechmann JL, Meyerowitz EM** (1998) The AP2/EREBP family of plant transcription factors. *Biological Chemistry* **6**: 633-646
- Rizhsky L, Hallak-Herr E, Van Breusegem F, Rachmilevitch S, Barr JE, Rodermeil S, Inze D, Mittler R** (2002) Double antisense plants lacking ascorbate peroxidase and catalase are less sensitive to oxidative stress than single antisense plants lacking ascorbate peroxidase or catalase. *Plant Journal* **32**: 329-342
- Ryter SW, Tyrrell RM** (1998) Singlet molecular oxygen ($^1\text{O}_2$): a possible effector of eukaryotic gene expression. *Free Radical Biology & Medicine* **24**: 1520-1534
- Sambrook J, Fritsch EF, Maniatis T** (1989) *Molecular Cloning - A Laboratory Manual*, Ed 2nd. Cold Spring Harbor Press, Cold Spring Harbor, New York
- Satoh J, Baba K, Nakahira Y, Tsunoyama Y, Shiina T, Toyoshima Y** (1999) Developmental stage-specific multi-subunit plastid RNA polymerases (PEP) in wheat. *Plant Journal: For Cell And Molecular Biology* **18**: 407-415
- Schopfer P, Plachy C, Frahy G** (2001) Release of reactive oxygen intermediates (superoxide radicals, hydrogen peroxide, and hydroxyl radicals) and peroxidase in germinating radish seeds controlled by light, gibberellin, and abscisic acid. *Plant Physiology* **125**: 1591-1602
- Shiina T, Tsunoyama Y, Nakahira Y, Khan MS** (2005) Plastid RNA polymerases, promoters, and transcription regulators in higher plants. *International Review of Cytol* **244**: 1-68
- Shirano Y, Shimada H, Kanamaru K, Fujiwara M, Tanaka K, Takahashi H, Unno K, Sato S, Tabata S, Hayashi H** (2000) Chloroplast development in *Arabidopsis thaliana* requires the nuclear-encoded transcription factor Sigma B. *FEBS Letters* **485**: 178-182
- Singh K, Foley RC, Onate-Sanchez L** (2002) Transcription factors in plant defense and stress responses. *Current Opinion in Plant Biology* **5**: 430-436
- Sugita M, Sugiura M** (1996) Regulation of gene expression in chloroplasts of higher plants. *Plant Molecular Biology* **32**: 315-326
- Tanaka K, Oikawa K, Ohta N, Kuroiwa H, Kuroiwa T, Takahashi H** (1996) Nuclear encoding of a chloroplast RNA polymerase sigma subunit in a red alga. *Science* **272**: 1932-1935

- Tanaka K, Tozawa Y, Mochizuki N, Shinozaki K, Nagatani A, Wakasa K, Takahashi H** (1997) Characterization of three cDNA species encoding plastid RNA polymerase sigma factors in *Arabidopsis thaliana*: evidence for the sigma factor heterogeneity in higher plant plastids. *FEBS Letters* **413**: 309-313
- Tiller K, Eisermann A, Link G** (1991) The chloroplast transcription apparatus from mustard (*Sinapis alba L.*). Evidence for three different transcription factors which resemble bacterial sigma factors. *European Journal of Biochemistry / FEBS* **198**: 93-99
- Tiller K, Link G** (1993) Sigma-like transcription factors from mustard (*Sinapis alba L.*) etioplast are similar in size to, but functionally distinct from, their chloroplast counterparts. *Plant Molecular Biology* **21**: 503-513
- Trebst A, Depka B, Holländer-Czytko H** (2002) A specific role for tocopherol and of chemical singlet oxygen quenchers in the maintenance of photosystem II structure and function in *Chlamydomonas reinhardtii*. *FEBS Letters* **516**: 156-160
- Tsugane K, Kobayashi K, Niwa Y, Ohba Y, Wada K, Kobayashi H** (1999) A recessive *Arabidopsis* mutant that grows photoautotrophically under salt stress shows enhanced active oxygen detoxification. *Plant Cell* **11**: 1195-1206
- Tsunoyama Y, Ishizaki Y, Morikawa K, Kobori M, Nakahira Y, Takeba G, Toyoshima Y, Shiina T** (2004) Blue light-induced transcription of plastid-encoded psbD gene is mediated by a nuclear-encoded transcription initiation factor, AtSig5. *Proceedings of The National Academy of Sciences of The United States of America* **101**: 3304-3309
- Tsunoyama Y, Morikawa K, Shiina T, Toyoshima Y** (2002) Blue light specific and differential expression of a plastid [sigma] factor, Sig5 in *Arabidopsis thaliana*. *FEBS Letters* **516**: 225-228
- Tyystjarvi E, Aro EM** (1996) The rate constant of photoinhibition, measured in lincomycin-treated leaves, is directly proportional to light intensity. *Proceedings of the National Academy of Sciences of the United States of America* **93**: 2213-2218
- Vass I, Styring S, Hundal T, Koivuniemi A, Aro E, Andersson B** (1992) Reversible and Irreversible Intermediates during Photoinhibition of Photosystem II: Stable Reduced Q_A Species Promote Chlorophyll Triplet Formation. *Proceedings of the National Academy of Sciences of the United States of America* **89**: 1408-1412
- Vranova E, Inze D, Van Breusegem F** (2002) Signal transduction during oxidative stress. *Journal of Experimental Botany* **53**: 1227-1236
- Wagner D, Przybyla D, Op den Camp R, Kim C, Landgraf F, Lee KP, Wursch M, Laloi C, Nater M, Hideg E, Apel K** (2004) The genetic basis of singlet oxygen-induced stress responses of *Arabidopsis thaliana*. *Science* **306**: 1183-1185
- Wang KL, Li H, Ecker JR** (2002) Ethylene biosynthesis and signaling networks. *Plant Cell* **14 Suppl**: S131-151
- Wendehenne D, Durner J, Klessig DF** (2004) Nitric oxide: a new player in plant signalling and defence responses. *Current Opinion In Plant Biology* **7**: 449-455
- Willekens H, Chamnongpol S, Davey M, Schraudner M, Langebartels C, Van Montagu M, Inze D, Van Camp W** (1997) Catalase is a sink for H₂O₂ and is indispensable for stress defence in C3 plants. *Embo Journal* **16**: 4806-4816
- Wosten MM** (1998) Eubacterial sigma-factors. *FEMS Microbiology Reviews* **22**: 127-150

Zapata JM, Guera A, Esteban-Carrasco A, Martin M, Sabater B (2005) Chloroplasts regulate leaf senescence: delayed senescence in transgenic ndhF-defective tobacco. *Cell Death & Differentiation* **12**: 1277-1284

Zimmermann P, Zentgraf U (2005) The correlation between oxidative stress and leaf senescence during plant development. *Cellular and Molecular Biology Letters* **10**: 515-534

Acknowledgements

It is difficult to summarize in a few lines all those who have made this work possible. First of all I would like to thank Prof. Dr. Klaus Apel for giving me the opportunity to perform my PhD work in his laboratory in excellent working conditions and for reviewing this work. I am grateful to him for introducing me into the plant genetics field and giving me an exciting project, for his critical discussions and permanent support during these years.

I am thankful to Prof. Dr. Nikolaus Amrhein for officiating as a co-referent.

The Institute of Plant Sciences has been an optimal place to develop my work and to meet exceptional people. I will never forget the D31 people, the discussions which have been constantly going on in the lab (not always very scientific) that made life more colorful and exciting. Particular thanks to Dr. Antoine Danon for supervising my work, for his ideas and understanding and for reviewing this essay. To Jean-Charles and Chan for their help, interesting opinions about life and inexhaustible energy and sense of humor. To the great atmosphere of the lab have very much contributed Cristophe and Ais. Very special thanks to all the plant genetics group members, including the polish team (Dominika K., Emilia, Monika, Wiola, Magda and Dominika P.), Klára, Marco, Andre, Keun Pyo, Rasa, Geetanjali, Dani, Verónica, Hanno, Frank, Dieter and Mena. Thanks to Martha for being always helpful and for having always a good advice. I am grateful to all my friends in the group for the nice time we spent together in and outside the lab.

I would also like to thank Dr. Jörg Meurer and his group at the Botanical Institute of the Ludwig-Maximilians University of Munich, especially Won and Lina, who helped me a lot with the experiments. They all made my stay in Munich very pleasant and interesting.

To the initial Waidspital team Rachel, Marcos, Natasa, Fjodor, Marta and Valmir for the all the very good moments spent together.

Very especial thanks to Berta, Marian and Noe. For sharing with me every step in this path since already so many years. For their invaluable friendship and empathy over the distance.

Above all I would like to express my gratitude to my family for being always at my side. To my parents Ricardo y Montse and to my brother Ricard for their enormous patience, support and love. To Maria for giving me courage and side with my decisions. To Pit for his always original points of view, optimism, support and care.

My most sincere thanks to all of them.

Curriculum vitae

Name: Núria Sánchez Coll
Date of birth: December 14th, 1978
Place of birth: Barcelona, Spain

- 2002-2006 **Ph.D. thesis**, Prof. Dr. K. Apel
Institute of Plant Sciences, ETH Zurich
- 2001-2002 **M.sc. in Plant genomics**, Prof. Dr. P. Puigdomènech
Institute of Molecular Biology Barcelona, High Council of Scientific Investigation (IBMB-CSIC), Spain
Thesis: “*In silico* comparative analysis between *Cucumis melo* and *Arabidopsis thaliana*”
- 1999-2000 **Research assistant**, Plant Physiology and Molecular Biology
Plant Biology Department, University of Barcelona, Spain
- 2001-1996 **Degree in Biological Sciences** (Biotechnology)
University of Barcelona, Spain
- 1996 **Selectivity exam** (final exam in the high school, to enter a university)
- 1995-1996 **University orientation course**
FERT Batxillerat, Barcelona, Spain
- 1992-1995 **High school**
Col.legi Pare Manyanet, Barcelona, Spain
- 1984-1992 **Primary school**
Col.legi Pare Manyanet, Barcelona, Spain